

FMH606 Master's Thesis 2021

Energy and Environmental Technology, EET

Analysing Aqueous Pyrolysis Liquid as feed for Anaerobic Digestion

Dheeraj Raya

Faculty of Technology, Natural sciences and Maritime Sciences
Campus Porsgrunn

Course: FMH606 Master's Thesis, 2021

Title: Analysing Aqueous Pyrolysis Liquid as feed for anaerobic digestion

Number of pages: 81 pages

Keywords: Anaerobic digestion, Lignocellulosic biomass, Aqueous pyrolysis liquid, Phenol, Furfural, HMF, ADM1, inhibition, methane yield

Student:	Dheeraj Raya
Supervisor:	Assoc. Prof Wenche Hennie Bergland
Co-Supervisor:	Nirmal Ghimire
External partner:	Gudny Øyre Flatabø
Availability:	Open

Summary:

Lignocellulosic biomass contains cellulose and hemicellulose which makes it suitable for Anaerobic Digestion (AD) process. However, due to complexity of the lignocellulosic biomass, pretreatment methods should be used to make it more easily degradable. Pyrolysis, one of the pretreatment method, results in formation of Aqueous pyrolysis liquid (APL) as a product. APL are known to have high chemical oxygen demand. Thus, it shows potential to be used as feed for AD process to produce methane but it contains toxic compounds such as phenols, furfural, HMF, acetones, and many others, most of which are known to inhibit the AD process. In this thesis, APL obtained from Scanship AS, is evaluated by carrying batch experiment to understand its methane potential and to understand organic loads where it disturbs the AD process. Co-digestion of APL with hydrolyzed sludge (HS) was also carried out to test its potential to be used as co-substrate. Finally, ADM1 model was extended by addition of inhibitory compounds (phenol, furfural and HMF) to model the methane production rate which was observed during experiment.

The results show that by addition of APL in range of (5-20 % of COD) during co-digestion increased the methane yield by 8-23% and shows potential to be used as co-substrate during AD process. However, during batch test of APL, increasing the organic load resulted in decrease in methane yield. Organic load above 2 gCOD/L severely inhibited the AD process by showing very low methane production rate. In contrast, batch test of APL with low organic load showed good methane production rate.

Since, APL contains numerous compound, inoculum stored for 2 months showed decrease in methane yield for all the organic load tested. Thus, it is recommended to use fresh and diverse inoculum as possible.

Simulation performed with standard ADM1 models was not able to predict the methane production rate from APL. However, extended ADM1 model showed ability to handle APL for predicting behavior of APL and inhibition constant was the most sensitivity parameter which could effect the methane production rate. APL with low organic load was predicted well by extended ADM1 model. Use of low inhibition constant and low startup concentration of biomass during simulation of APL with higher organic load resulted in good fit with experimental results suggesting implementation of further compounds which could inhibit AD process would increase the model predictability.

Preface

This report was written on the topic of “Analysing Aqueous Pyrolysis Liquid as feed for Anaerobic digestion” to fulfill the partial requirement for Master study program in Energy and Environmental Technology at University of South-Eastern Norway, Faculty of Technology, Natural Science and Maritime Sciences.

The goal of the work was to evaluate APL as a feed for AD process and understanding the effect of APL at different organic load. In addition, ADM1 model was extended to simulate the APL.

I would like to express my sincere gratitude to my main supervisor Assoc. Prof. Wenche Hennie Bergland for her guidance, support, technical advice, and feedback throughout the thesis. In addition, I am grateful to my co-supervisor Nirmal Ghimire for his technical advice and assistance with the experimental planning. Finally, I would like to thank our external partner Gudny Øyre Flatabø for her suggestion, comments, and feedback.

I would also like to thank Hildegunn Haugen, Eshetu Janka Wakjera, Kadja Bless for their suggestion and guidance.

Finally, I would like to thank my fellow master student Sabin, Sandeep and Ashish for their comment and support during this semester. In addition, I would like to thank my family and my wife Dikshya for their continuous support and motivation throughout my stay in Porsgrunn.

Porsgrunn, 24.05.2021

Dheeraj Raya

Content

Preface	4
Content.....	5
Nomenclature	7
1 Introduction	9
2 Theory	11
2.1 Lignocellulosic biomass	11
2.1.1 <i>Biomass conversion pathway</i>	11
2.2 Pyrolysis of Biomass.....	12
2.3 Aqueous Pyrolysis Liquid.....	13
2.4 Anaerobic Digestion	14
2.4.1 <i>Anaerobic Digestion Assessment</i>	15
2.5 ADM1	16
2.5.1 <i>Growth kinetics</i>	16
2.5.2 <i>Inhibition</i>	17
2.6 Inhibitors in AD	18
2.6.1 <i>Inhibitory compounds from APL</i>	18
2.7 APL integrated AD process.....	19
2.8 Phenol.....	20
2.9 Furfural	20
2.10 HMF	21
2.11 Possible treatment of APL for reduced toxicity	22
3 Materials and Methods	23
3.1 Analytical Methods	23
3.2 Material Characterization	23
3.2.1 <i>Inoculum</i>	23
3.2.2 <i>APL</i>	24
3.2.3 <i>Food/sludge Co-substrate</i>	24
3.3 Experimental Approach.....	25
3.3.1 <i>AMPTS II Test</i>	25
3.3.2 <i>Syringe Test</i>	26
3.4 Modelling and Simulations.....	27
3.4.1 <i>Determination of Inhibition Constant (K_i)</i>	27
3.4.2 <i>Extended ADM1 model implementation</i>	28
3.4.3 <i>Simulation cases</i>	35
3.4.4 <i>Inputs for ADM1</i>	36
4 Results.....	38
4.1 Experimental results.....	38
4.1.1 <i>AMPTS II using fresh inoculum</i>	38
4.1.2 <i>Syringe Test</i>	40
4.1.3 <i>Inoculum</i>	41

4.1.4 AMPTS II using stored inoculum 41

4.2 Simulation result..... 43

4.2.1 Simulation of Inoculum (Sim-1) 43

4.2.2 Simulation of APL1.2..... 45

4.2.3 Simulation of APL2.4..... 50

4.2.4 Comparative simulation using Monod and Haldane growth kinetics 57

5 Discussion..... 59

5.1 Co-digestion of APL and HS 59

5.2 Effect of OL on methane yield from APL 59

5.2.1 Effect of higher OL in batch tests 59

5.2.2 Effect of lower OL on batch test..... 60

5.3 Effect of inoculum storage on methane yield during batch test of APL 60

5.4 Possible overcome of inhibition and microbial adaption..... 61

5.5 Comparison of Standard ADM1 model and Extended model..... 61

5.6 Necessity for properly defining the APL during simulation..... 61

5.7 Effect of inhibition constant (K_i)..... 62

5.8 Degradation of inhibitory compounds 63

5.9 Difference of using Monod and Haldane type growth kinetics 63

6 Conclusion 64

7 Suggestion for future works 65

References..... 66

Appendices..... 71

Nomenclature

Abbreviation	Description
AD	Anaerobic Digestion
ADM1	Anaerobic Digestion Model No. 1
APL	Aqueous Pyrolysis Liquid
APL1.2	APL at organic load of 1.2 gCOD/L using fresh inoculum
APL1.2-s	APL at organic load of 1.2 gCOD/L using stored inoculum
APL2.4	APL at organic load of 2.4 gCOD/L using fresh inoculum
APL2.4-s	APL at organic load of 1.2 gCOD/L using stored inoculum
Blank	Batch test with only inoculum
BMP	Biomethane Potential test
CH ₄	Methane
CO	Carbon Monoxide
CO ₂	Carbon dioxide
COD	Chemical Oxygen Demand
Control	Batch test with inoculum and HS as substrate
H ₂	Hydrogen gas
HBu	Butyric acid
HMF	5-hydroxymethylfurfural
HS	Hydrolysed Sludge
HVa	Valeric acid
IWA	International Water Association
LCFA	Long Chain Fatty Acid

Nomenclature

NH ₄	Ammonium
OL	Organic Load
pH	Potential of hydrogen
S _{ac}	Soluble Acetate
S _I	Soluble Inert
S _{IN}	Total inorganic nitrogen
sCOD	Soluble COD
TAN	Total Ammonium Nitrogen
tCOD	Total COD
X _C	Particulate Composite
X _{ch}	Particulate Carbohydrate
X _I	Particulate Inert
X _{li}	Particulate Lipids
X _{pr}	Particulate Protein

1 Introduction

With rapid increase in population and globalization, global energy demand is increasing rapidly. Fossil fuels are being used extensively to meet the energy demand, which accounts for 81.3% of total energy supply [1], and possesses major concern on its sustainability and greenhouse gas emission [2]. Alternative source to replace the use of fossil fuel has become the urgent need for human civilization and various renewable energy sources like solar, wind geothermal and biomass are being explored.

Biomass are abundant in nature and cheap compared to other renewable energy alternatives. Estimated about 2.2×10^{11} tons of dry lignocellulosic biomass are produced every year and around 10% of which are available on sustainable basis [3] and traditional used for heat and power generation only [2].

Conversion of biomass to energy can be carried out either by thermochemical process such as pyrolysis, gasification, combustion, and thermal liquefaction or biochemical process such as fermentation and digestion [2]. Lignocellulosic biomass is composed of three main building blocks: cellulose (40-60%), hemicellulose (20-40%) and lignin (10-25%) [5]. Cellulose and hemicellulose are protected by lignin and acts as barrier towards its degradation during anaerobic digestion [6] and presence of lignin in high concentration is also know to decrease the biomethane potential [7]. Slow degradation/decomposition under anaerobic condition is major hurdle for anaerobic digestion (AD) [8]. Thus, it requires pretreatment before use in AD [4].

Pyrolysis is one of preferred method for treating lignocellulosic biomass as it yields value added product such as syngas, biochar and biooil, most of which can be further used for various purposes. Aqueous pyrolysis liquid (APL) is a aqueous phase of biooil having high chemical oxygen demand (COD) produced during condensation of the gaseous matter, formed during the pyrolysis [9].

Biomass decompose to produce phenolic compounds, furans, ketones, weak acid and number of other compounds during the pyrolysis process, all of which are translated back into biooil during condensation process (Figure 1.1) [6].

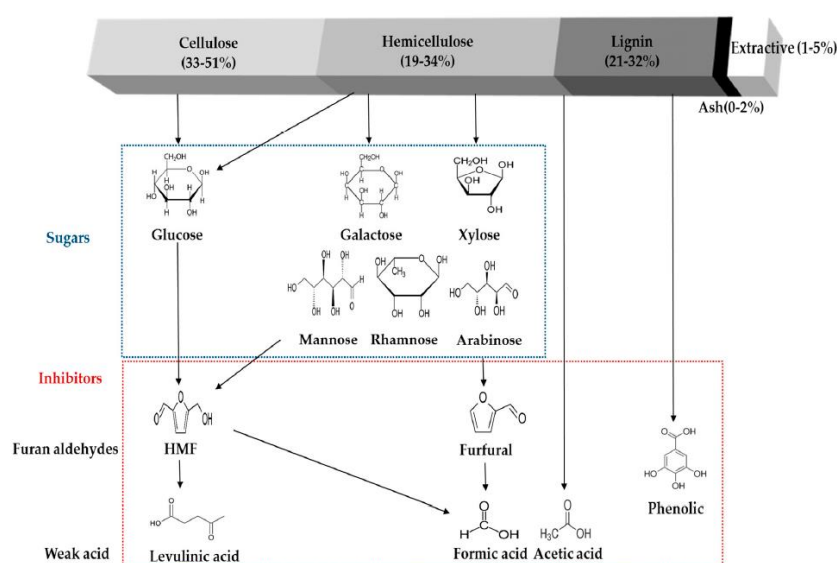


Figure 1.1 Brief scheme of main inhibitory compound formation during pyrolysis of lignocellulosic biomass.

Most of these are known to be toxic to the AD and causes inhibition [6]. It was reported that 2-3 gCOD/L of APL was toxic to AD [9]. Furthermore, current research also focuses on using APL as a co-substrate as it was found to increase the methane production [10].

Hence, this thesis would focus on evaluating APL as a feed for AD process to harness energy using fresh and stored inoculum. Furthermore, the content of APL such as COD, VFA, pH and the biogas potential of APL would be analyzed by using batch reactor. This thesis would also investigate the possibility of APL as a co-substrate.

Similarly, present ADM1 model can predict well for simple substrate [11] and has been extensively used by the scientific community to understand the AD process under different scenario. However, ADM1 model lacks ability to model and predict the behavior of substance like APL, containing number of compounds which are known to be toxic to AD process. Thus, ADM1 model would be further extended by addition of compounds (phenol, furfural and HMF) found in APL and would be evaluated based on experimental results. The model would be evaluated for simulating the APL as a feed for anaerobic digestion and would reflect the key parameter required for increasing the model accuracy for predicting the behavior of APL during AD process.

2 Theory

This chapter reflects the overview of pyrolysis process and its product, APL's content, and inhibition caused by constituent of APL during AD process. Furthermore, brief description regarding degradation of phenol, furfural and HMF is presented and introduces the ADM1 model which is modified in chapter 3.4.2.

2.1 Lignocellulosic biomass

Biomass refers to biological organisms as well as any organic matter derived from them. Lignocellulosic biomass are dry and non-edible plant matter [12] which includes agricultural residue, energy crops, forestry residue and yard trimmings. They are rich in carbohydrate and lacks proteins [13]. Lignocellulosic biomass mainly consists of cellulose, hemicellulose and lignin along with some extractives (tanins, resins and fatty acids) and inorganic salts [12].

Lignocellulosic biomass is mainly characterized by microstructure and the chemical compositions. They are made of fibrous elements, hollow fibrous cells, and interconnected with each other [2]. Depending upon these interconnecting cells, lignocellulosic biomass are divided in softwood and hardwood (having irregularly large fibrous elements) and its composition is listed in Table 2.1 [12].

Table 2.1 Chemical composition of softwood and hardwood

Biomass	Cellulose	Hemicellulose	Lignin
Hardwood	40-55	24-40	18-25
Softwood	45-50	25-35	25-35

Cellulose are the most important structural component of plant and contains D-glucose unit, a six-carbon ring[12]. These D-glucose unit can interact with each other giving crystalline unit which provides the strength and stability[14]. Hemicellulose are the branched polysaccharides surrounding cellulose which acts as a link between cellulose and lignin and improves the rigidity of lignocellulosic material. Hemicellulose contains different subunits of pentose such as xylose, and arabionase and hexoses such as mannose, galactose, and glucose. These monomers are linked together to form branched polysaccharides. Lignin are mainly crosslinked aromatic polymer giving the structural integrity and prevent against microbial attack [12].

2.1.1 Biomass conversion pathway

Biological fermentation of lignocellulose biomass is difficult due to presence of lignin. Lignin acts as barrier that prevents cellulosic enzyme to degrade the cellulose[7]. Physical treatment i.e milling, grinding etc. of lignocellulosic biomass to increase the accessibility of cellulosic material can be done however, low density of lignocellulosic biomass effects AD process by forming floating layer on surface of AD reactors [8]. Thus, pretreatment of lignocellulosic biomass is required to increase the availability of cellulose to the enzymes which converts carbohydrate to fermentable sugars [4].

Pretreatment can be mainly done by chemical and thermochemical process. Chemical process uses chemical to extract the cellulose. However, use of chemical treatment is expensive [5]. Thermochemical conversion process is preferred to treat biomass because of short process time

duration [15]. Under thermochemical conversion, organic matter are decomposed under high temperature and pressure resulting in solid, liquid and gas as byproducts [16]. Gasification, which produces gas and pyrolysis, mainly produces liquid are main processes under extensive research in thermochemical conversion process[5].

2.2 Pyrolysis of Biomass

Pyrolysis is mostly preferred over gasification as it yield liquid fuel which can be easily stored and transported [9]. Pyrolysis converts biomass into biochar, gas and liquid in absence of oxygen at temperature greater than 400°C [3]. Process parameter such as temperature and retention time effects the product formed. High bio-char yield is obtained during low temperature and higher retention time. Higher temperature and short retention time produce high yield of syngas whereas higher amount of bio-oil can be obtained from intermediate pyrolysis [8].

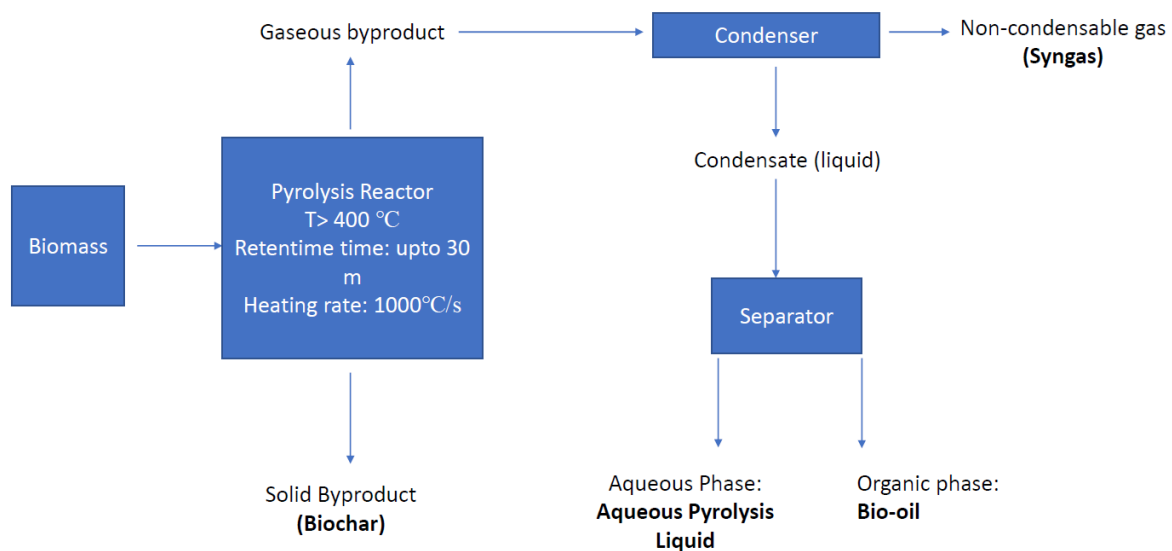


Figure 2.1 Products formed during pyrolysis of biomass.

Solid product, biochar is a beneficial solid amendment[19]. Gas product known as syngas is composed of carbon monoxide (CO), hydrogen (H₂) and methane (CH₄) that can be combusted alone or can be used in boiler, engines and other equipment [19]. Pyrolysis liquid mainly consist of acid and water [17] and can be separate into distinct phase: organic phase known as bio-oil and aqueous phase commonly known as Aqueous pyrolysis liquid (APL) [20] and contains hundreds of organic compounds[21]. Bio-oil can be upgraded to be used in typical combustion systems. However, APL cannot be upgraded into bio-fuels due to high content of water [9].

Components of lignocellulosic biomass decomposes at different temperatures during pyrolysis process. Cellulose degrades into levoglucosan, 5-Hydroxymethylfurfural (5-HMF), sugars, acids etc. 5-HMF and furfural are the major product of pyrolysis of hemicellulose and cellulose. Phenolic compounds are mainly formed by pyrolysis of lignin[22] which increases with increase in temperature [23].

2.3 Aqueous Pyrolysis Liquid

APL are dark-brown liquid with distinctive odor and consists of 85-90% water [24]. It is formed due to initial moisture present in feedstock [24] and consists of more than 400 compounds [21]. It was previously reported that APL contains mainly acids, esters, ketones, alcohols, aldehydes, furans, phenol and others (Figure 2.2)[25].

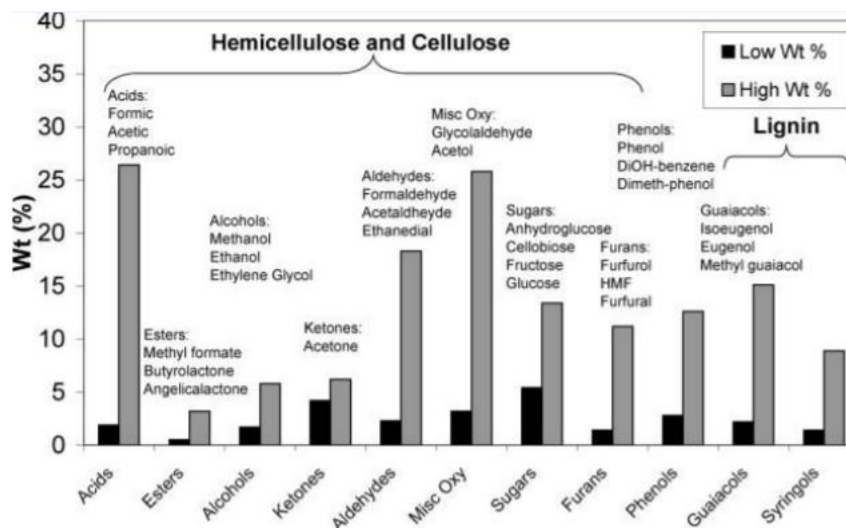


Figure 2.2 Chemical compounds present in APL from fast pyrolysis of plant biomass [25].

Presence of organic compounds in APL, make it suitable for anaerobic digestion to produce methane. The composition of APL previously reported has shown high COD concentration ranging from 30-500 g/L [26]. Various compounds present in APL during pyrolysis at different temperature is presented in Table 2.2.

Table 2.2 Chemical Characterization of APL produced from different biomass and at different temperature

Biomass	Temperature	acetic acid	propionic acid	Phenolic compounds	HMF	furfural	COD	References
Birch Bark	500	105g/L	12g/L	24.4g/L			499g/L	[26]
Corn Stalk pallet	400	26 g/kg	1.6 g/kg	17 g/kg				[16]
Corn stover	500	28.98g/L	13.33g/L				486g/L	[27]
Digeste d	530	4.6g/L	0.6g/L	203mg/L	0.6mg/L	69mg/L	48.5g/L	[21]

Compound present in APL highly depends upon the type of biomass used during the pyrolysis. Use of biomass containing higher concentration of nitrogen such as digestate release nitrogenated compounds. Similarly, use of softwood during pyrolysis results in formation of higher phenolic compounds. Furthermore, APL obtained from pyrolysis at higher temperature showed increase in phenolic compounds and were found to be toxic then APL obtained from pyrolysis at lower temperature [28].

2.4 Anaerobic Digestion

Anaerobic digestion, oldest known process, is the biological breakdown of the organic matter to obtain biogas containing mainly methane and carbon dioxide. Consortium of microorganism digest complex organic matter in absence of oxygen. There are mainly four biochemical reactions during anaerobic digestion: hydrolysis, acidogenesis, acetogenesis and methanogenesis (Figure 2.3) [29].

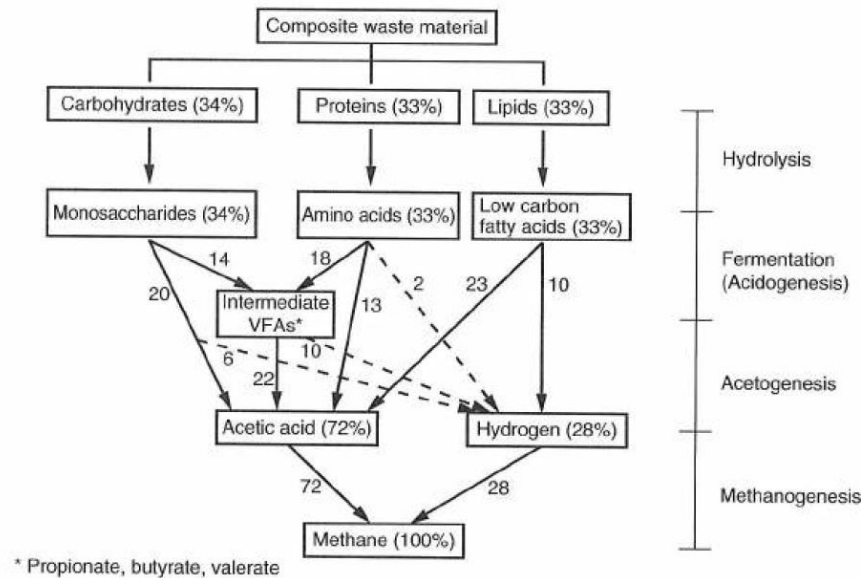


Figure 2.3 Anaerobic digestion pathway [29].

- Hydrolysis

Hydrolysis is the first step where complex particulate material is converted into soluble products. The process involves two processes: disintegration and hydrolysis both of which are extracellular. Disintegration is a non-biological step and converts composite particles into simple products which can be acted upon by hydrolytic enzymes. The components are further degraded into soluble monomers by extracellular enzymes. The final products of hydrolysis are monosaccharides, amino acids, and fatty acids. This step is often considered as the rate-limiting step in the AD process [29].

- Acidogenesis

Soluble products formed during hydrolysis steps are broken down into volatile fatty acids (VFA) namely propionic, butyric, and valeric acids along with carbon dioxide, acetate, and hydrogen. These are carried out by a group of bacteria known as acidogens. Ammonia is also produced from the degradation of amino acids [29].

- Acetogenesis

The products from acidogenesis are further broken down by acetogenic bacteria to hydrogen, carbon dioxide, and acetic acid. Acetogenic bacteria are sensitive to hydrogen and favor low pressure of hydrogen to convert all the intermediate acids into acetic acids [29].

- Methanogenesis

Methanogenesis is the final step in the AD process where the final product is methane and carbon dioxide. Methane can be formed by two different pathways as shown in Figure 2.3 either by

acetoclastic methanogens or hydrogenotrophic methanogens. Acetoclastic methanogens contributes towards 72% of methane formation by using acetic acid whereas hydrogenotrophic methanogenesis converts hydrogen and carbon dioxide to methane [29].

2.4.1 Anaerobic Digestion Assessment

In order to evaluate the performance of AD process, various laboratory test have been purposed. These tests help in understand the methane potential of substrate, or effect of substrate on methanogens or effect of substrate on AD process.

2.4.1.1 Biochemical Methane Potential Test

Biochemical methane potential test (BMP) is the popular testing method for determining the methane potential and biodegradability of organic waste. In the test, substrate are mixed with inoculum (anaerobic culture), retrieved from active digester, for 30-60 days at desired temperature of 35°C or 55°C [30]. It gives the information about methane production from different substrate and experimental results can be used during mathematical modelling [30].

Usually, BMP test requires blank, control and substrate. Blank test are carried out using inoculum only to consider the background methane generation from organic material in the inoculum, whereas control, carried out using inoculum and substrate, helps in understanding the performance of inoculum [30]. It was previously reported that inoculum should be used from active digester and as fresh as possible, since inoculum stored for longer time results in decrease in methane production and shows lag phase[31]. However, it is not convenient to use fresh inoculum and to remove the background methane production from inoculum, inoculum should be degassed for 5-7 days [32].

BMP test requires carrying out test by removing oxygen from headspace by flushing with nitrogen gas, and constant temperature with gentle mixing [33].Methane generated from the test are usually used to calculate the methane potential (methane yield) of the substrate and can be expressed as volume of methane produced from the substrate per mass of volatile solids or chemical oxygen demand (COD) added [30]. Theoretically, 1 gCOD results in 0.35 mL CH₄ at standard temperature and pressure [29].

BMP test are usually carried out in the batch test. Incubation period and organic load are the major sensitive parameter during the test. Incubation period can be related with solid retention time (SRT). SRT is time the substrate remains in the reactor. Increase or decrease in SRT results in increase or decrease in methane production volume. Thus, it was recommended that if the daily methane production over three consecutive days remains relatively small, the test could be ended [30]. Another major parameter is the organic load (OL) supplied to reactor. Organic load (OL) refers to mass of volatile solids or COD of substrate supplied to the mass of volatile solids or COD or volume of inoculum used. Both over-loading and underloading results in decrease in methane yield. Thus, OL gives the understanding of suitable concentration of substrate to be used to achieve the optimal methane yield and gives a better understanding of the extreme limit where the AD process can takes place[33].

2.4.1.2 Specific Methanogenic Activity Test

Specific Methanogenic Activity (SMA) test are batch test carried out using blank, control and substrate at different concentration or OL. SMA are generally used to understand the affect of OL and carried out with specific purpose determining the performance of methanogens at different OL. To consider the effect on methanogens only, acetate is typically used as substrate.

2.5 ADM1

Anaerobic Digestion Model No.1(ADM1) was developed by International Water Association (IWA) for the sole purpose of mathematical modeling of AD process. ADM1 model, represented as standard ADM1 model hereafter, includes the biochemical process that describes the AD pathway process (Figure 2.4) and physio-chemical process, a non-biological process used to determine the effect of physio-chemical states such as pH and liquid gas transfer. However, the model has been limited to only major AD processes (Figure 2.3) to make it simpler and easier for modification in the future as per need and does not consider some of known relevant processes during AD such as syntrophic association between microorganism (acetate oxidation), sulfide inhibition, long chain fatty acid (LCFA) inhibition, and so one [11]. But model can be further enhanced to include the relevant processes depending upon the need.

Figure 2.4 shows the process of AD implemented in standard ADM1 model. The numbers 1-8 represent the uptake process of specific compounds in standard ADM1, for example 1 represents the uptake of sugars. But Figure 2.4 does not represent process such as death of organism and physio-chemical process. The detail stoichiometry and fractions of decomposition of compounds and death of organism are presented in Appendix B.

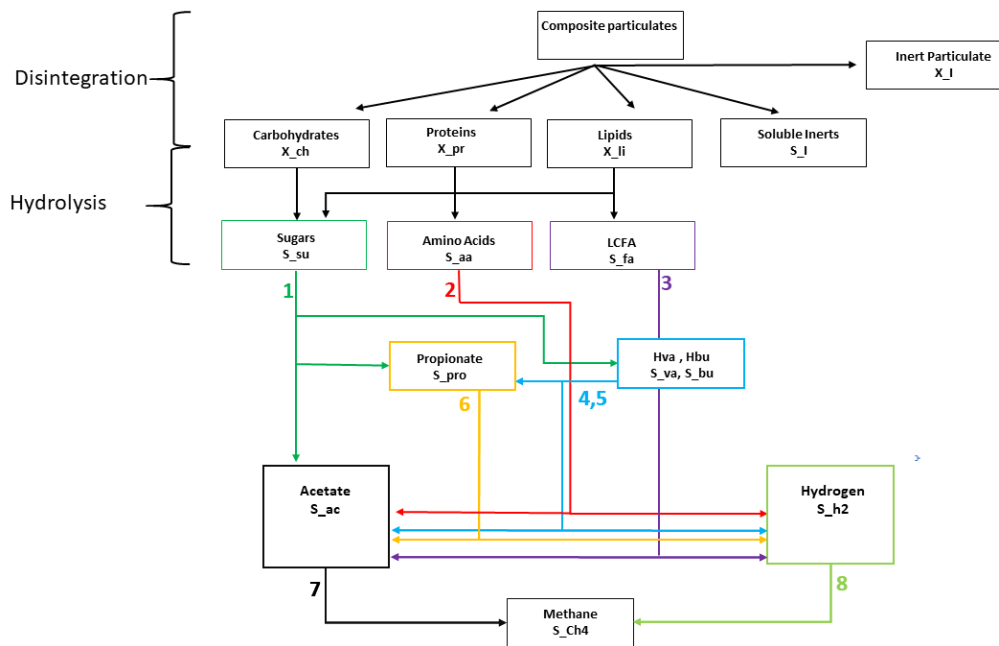


Figure 2.4 AD process included in ADM1 model

2.5.1 Growth kinetics

Standard ADM1 model implements substrate-based uptake Monod type kinetics for all the biochemical reactions [27]. Monod equation (2.1) includes substrate concentration as a limiting factor and the specific growth rate of bacteria increases strongly for low substrate concentration and slows down for higher concentration, until reaching the saturation. Monod accuracy is considered to be very high for simple culture and substrate. However, Monod equation has its own limitation and does not include inhibition by substrate itself[34].

$$\mu = \mu_{max} \frac{s}{k_s + s} \quad (2.1)$$

Where, μ_{max} = maximum specific growth rate of bacteria in d^{-1}
 μ = specific growth rate of bacteria in d^{-1}
 k_s = half saturation constant in g/L at $\frac{\mu_{max}}{2}$
 s = substrate concentration in g/L

Haldane-Andrews equation generally describes such phenomenon where specific growth rate decrease when a maximum tolerate concentration of substrate is reached [34]. Haldane-Andrews equation ((2.2) introduces the inhibition constant (K_i), where bacteria growth is reduced to 50 % of maximum specific growth, in existing Monod equation[34].

$$\mu = \mu_{max} \frac{s}{k_s + s + \frac{s^2}{k_i}} \quad (2.2)$$

2.5.2 Inhibition

Inhibition caused by hydrogen, free ammonia and pH are included in standard ADM1 and mostly uses non-competitive inhibition to model the effect of inhibitory compound, whereas it uses empirical expression to model pH inhibition[11]. Inhibition expression as expressed in by Batstone et al are represented in Figure 2.5.

Description	Equation	Used for	j ¹
(a) Non-competitive inhibition	$I = \frac{1}{1 + S_i / K_i}$	Free ammonia and hydrogen inhibition	7-12
Uncompetitive	$\rho_j = \frac{k_m \times S}{K_s + S \left(1 + \frac{K_i}{S_i}\right)}$	Not used	
Competitive	$\rho_j = \frac{k_m \times S}{K_s \left(1 + \frac{S_i}{K_i}\right) + S}$	Not used	
(b) Reduction in yield	$Y = f(S_j)$	Not used	
Increased biological decay rate	$k_{dec} = f(S_j)$	Not used	
(c) Empirical upper and lower inhibition	$I = \frac{1 + 2 \times 10^{0.5(pH_{UL} - pH_{LL})}}{1 + 10^{(pH - pH_{UL})} + 10^{(pH_{LL} - pH)}}$	pH inhibition when both high and low pH inhibition occur	5-12 ²
Empirical lower inhibition only	$I = \exp\left(-3 \left(\frac{pH - pH_{UL}}{pH_{UL} - pH_{LL}}\right)^2\right)$ $I = 1$ if $pH > pH_{UL}$	pH inhibition when only low pH inhibition occurs	5-12 ²
(d) Competitive uptake	$I = \frac{1}{1 + S_i / S}$	Butyrate and valerate competition for C ₄	8-9
(e) Secondary substrate	$I = \frac{1}{1 + K_i / S_i}$	All uptake, to inhibit uptake when S _{IN} =0	5-12

Nomenclature: K_i = inhibition parameter; ρ_j = rate for process j; S = substrate for process j; S_i = inhibitor concentration; X = biomass for process j.

Figure 2.5 Equation used to express inhibition in standard ADM1.

While using non-competitive inhibition, it was recommended to use IC₅₀ value as Ki value. IC₅₀ is concentration of inhibitory compounds which reduces the activity by 50 % [11].

2.6 Inhibitors in AD

Anaerobic digestion is a sensitive process. In AD process, the product of one step becomes the substrate for the next step as explained in chapter 2.4. Thus, any imbalance in one step can hamper the proceeding steps. On the other hand, the compounds present in APL directly inhibit the AD process [9]. Temperature and nutrients available also play a vital role in the stability of AD reactors. Thus, all mentioned parameters can affect or possibly permanently disturb the AD process.

Microorganisms present in AD are sensitive to pH and prefers an optimum pH between 6.8 to 7.6. Methanogens are the most sensitive towards change in pH and prefer an optimum neutral pH for better performance [26] whereas, acidogens and acetogens can tolerate up wide range of pH (4-8.5) [27].

VFA accumulation during AD process can inhibit the process itself. Accumulation of acids due to overloading or inhibition of methanogens results in a drop in pH which leads to disturbance of the overall process.

Total ammonium nitrogen and free ammonia are mostly released during the breakdown of nitrogen-rich compounds such as protein and urea. It was previously reported that 2000 mgNH₄/L resulted in some inhibition of methanogenic pathway and 3300 mgNH₄/L resulted in complete inhibition of AD process [35]. It was also previously reported that free ammonia of 30 mg/L inhibited the AD process by 50% in ADM1 [36].

2.6.1 Inhibitory compounds from APL

As mentioned in chapter 2.3, constituents of APL such as alcohol, ketones, aldehydes, phenolic compounds are known to inhibit the methanogens. Inhibitory effects include inhibition in microbial growth, decrease in biogas production and possibly increase in lag-phase during biogas production. Furthermore, inhibition on methanogens can also be expressed in terms of IC₅₀ values[37].

Table 2.3 Inhibitory concentration of compounds on Methanogens presented as IC₅₀ (mg/L)

Compounds	IC ₅₀ (mg/L) for methanogens	Reference
Phenolic Compounds		
Phenol	470	[38]
m-cresol	432	[38]
p-cresol	380	[38]
Ketones		
acetones	50000	[39]
Alcohol		
Methanol	22000	[39]

Ethanol	43000	[39]
---------	-------	------

Study by Ghasimi reported that 2 g/L of furfural and 2 g/L of HMF severely inhibited the methanogens, whereas 0.4 g/L showed no effects on methanogens. They also reported that concentration of furfural at 0.8g/L and HMF at 0.8 g/L resulted in a slight increase in lag phase, however, final methane production was similar to that of control (sludge with only acetate as carbon source) [40]. Consistently, Silvie also found that furfural at 2g/L inhibits the methanogens, and 1g/L of furfural showed an increase in lag phase with final methane production to be same as control. However, the same studied reported that a significant effect on methane production was seen at 0.5 g/L of HMF, and 1g/L severely affected the methane production [41].

Threshold value of 1.5 g/L and 2 g/L of phenol was reported to inhibit the methanogenic activity completely during the anaerobic digestion [10]. Similarly Olgun-lora reported that methanogenic activity was completely inhibited at a concentration of 2.5 g/L of phenol and inhibited methanogens by 50% at 0.47 g/L [38]. They also reported acclimated sludge was inhibited completely at concentration of phenol at 7.8 g/ [38].

It was previously reported that presence of 2 g/L of furfural and 3 g/L of HMF in combination lowered the methane production when compared with adding individually [42] expressing that presence of several inhibitory compounds together may produce synergy effect by reducing the threshold value for inhibition compared to inhibition occurred by those compounds separately [43]. Increase in inhibition was mostly observed by increase in lag phase.

However, all of these inhibitory compounds are observed to degrade in AD process. Phenol are known to produce benzoate, as intermediate product, before degrading completely to acetate [44]. Similarly, previous studies have reported that furfural and HMF also produce acetate as a final product during anaerobic digestion [43].

2.7 APL integrated AD process

Integration of various technology aims at utilizing the resource at best and focus on high operation efficiency. Integration of pyrolysis with AD would help in increasing the overall efficiency of the process as APL would be converted into energy in form of biomethane (Figure 2.6) [3]. Only few studies have been carried out for using pyrolysis integrated AD process.

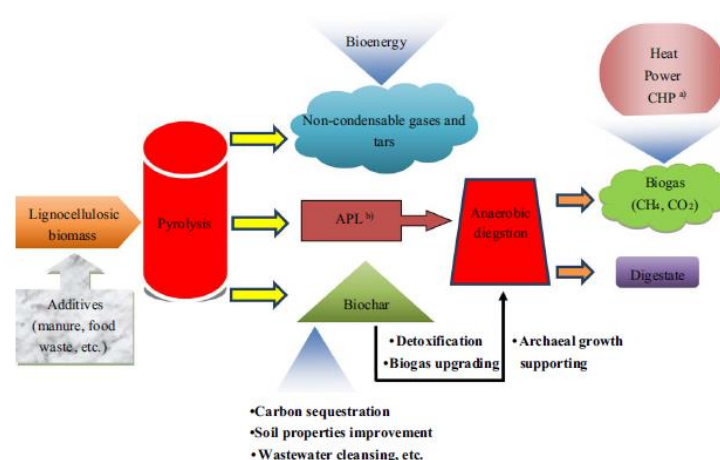


Figure 2.6 Pyrolysis of biomass in pyrolysis process and integration of pyrolysis product in AD process [3].

Torri and Fabbri suggested the use of adapted inoculum and addition of biochar would make use of APL efficient. Methane yield from digestion of APL using unadapted, adapted inoculum, and adapted inoculum along with addition of biochar was 20% , 37% and 60% of theoretical methane yield respectively[16].

Yu et al. carried out swine manure co-digestion with APL (diluted at 5, 50 and 100 times with distilled water namely A5, A50 and A100) found that digestion with diluted APL favored the methane production, which surpassed the control. Digestion with A5 showed continuous low level of methane production in comparison with control. They suggested that lower APL concentration stimulate the microbial activity which in turn exhibited higher capacity of methanogenesis [10].

Different study carried out by Hubner and Mumme using APL from pyrolysis of digestate at different temperature 330°C, 430°C and 530°C found that methane yield from APL at 330°C (199 mL/gCOD) was higher than the methane yield from APL at 530°C (129 mL/gCOD) and concluded that methane yield decreases with increase in pyrolysis temperature[21].

2.8 Phenol

Phenol is one of the product during pyrolysis of lignin[45]. Usually, lignin decomposition during pyrolysis takes at range of 180- 900 °C [3] and decomposes slowly in comparison to cellulose and hemicellulose.

Phenol (C₆H₅OH) are also commonly known as carboic acid and are known to be weak acid in its ionized form [44]. They are white crystalline solid that are soluble in organic solvents[44]. Phenol is known to damage microbial cells by inactivation of essential enzymatic systems[43]. However, microorganism has ability to grow and adapt even in presence of toxic compounds such as phenol as well [38].

Number of microorganisms are known to grow using Phenol as a sole carbon and energy sources. *Acinebacter Sps*, *Alcaligenes eutrophus*, *Nocardioideess*, *Pseudomonas fluorescens*, *Pseudomonas putida* are some of bacteria that are known to degrade phenol aerobically, whereas *Paracoccus denitrificans* and *Desulfobacterium phenolicum sp.* are known to degrade anaerobically [46].

Under mesophilic conditions, researchers proposed that phenol is first converted in benzoate. Benzoate is further dearomatized into cyclohexane carboxylic acid, which goes under beta-oxidation to form VFA's and acetate. However, experiments carried out resulted in formation of only acetate during anaerobic degradation of benzoate indicating no production of intermediate VFA's formation [47].

2.9 Furfural

Pyrolysis of cellulose and hemicellulose both forms furfural and is a product of dehydration of sugars. Depending upon the source (biomass) and pyrolysis temperature, its concentration in APL can vary[48].

Furfural (C₅H₄O₂) is also known as 2- furaldehyde and are soluble in organic solvents. Furfural acts as a germicides and higher concentration of furfural inhibits the cell growth and fermentation process as well[49]. Previous studies found that furfural induces DNA damages also [43].

Desulfovibrio sp., *Desulfovibrio sp* strain f-1, *Pseudomonas putida* S12, *Pseudomonas putida* KT2440 are the some species of bacteria which are known to degrade furfural anaerobically as a sole source of carbon and energy [50].

Degradation of furfural in anaerobic digestion yield acetate as a product and have furoic acid as an intermediate product [49]. Moreover, microbes have capacity to reduce the toxic compounds to their corresponding alcohol and can be oxidized back again [51] as illustrate by Figure 2.7. The stoichiometric reaction during decomposition of furfural is given by equation (2.3 [49]).

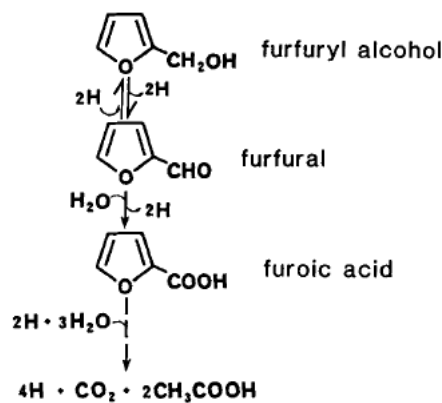


Figure 2.7 Degradation pathway of furfural [51].

2.10HMF

HMF and furfural both are commonly part of furanic compounds. Both HMF and furfural are product of pyrolysis of cellulose and hemicellulose resulted due to dehydration of sugars[48]. The decomposition of cellulose and hemicellulose takes place at temperature range of 200-380°C [3]. Hence, presence of both of the furanic compounds can be found in treatment carried out at lower range of temperature as well 200-400°C[21].

HMF or 5-HMF (actually 5-HMF, however represented as HMF throughout the thesis) stands for hydroxymethylfurfural. HMF (C₆H₆O₃) are highly soluble in water and organic solvents as well [48]. As furfural, HMF are known to inhibit cell growth and also have known to induce DNA damages [43].

Number of species of bacteria have been known to degrade the HMF as a sole source of carbon and energy. However, there are several species of bacteria such as *Pseudomonas putida* S12, *Pseudomonas putida* KT2440 capable of using both HMF and furfural for metabolism [50]. It was also found that degradation of HMF takes place after degradation of furfural as some species of bacteria prefer furfural over HMF during AD process [8].

The degradation pathway of HMF into acetate during anaerobic digestion follows nearly same path as furfural. HMF degradation results in intermediate product, furoic acid, which is also the intermediate product during the degradation of furfural (Figure 2.8).

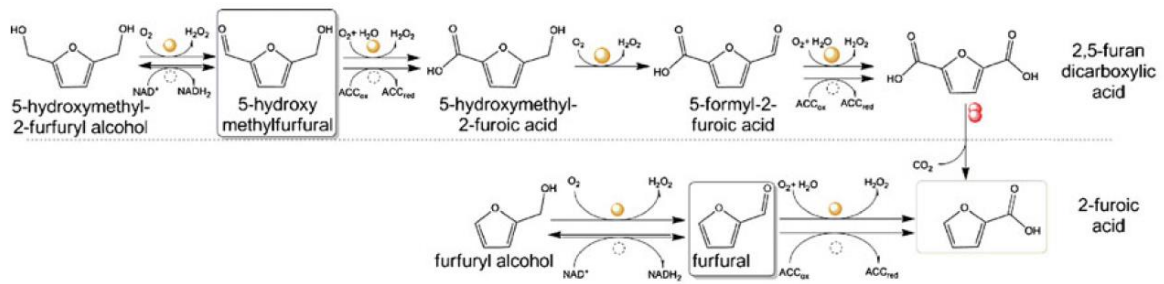


Figure 2.8 Degradation pathway of HMF showing formation of same intermediate product as in furfural degradation [50].

Furfural and HMF are also both known to inhibit its own cell growth if present in higher concentration. It was previously found that when the concentration of furfural and HMF were doubled, concentration of microorganism degrading these compounds decreased by 30% [52].

2.11 Possible treatment of APL for reduced toxicity

Number of methods (like overliming, addition of activated carbon, bleaching [27], and air stripping [9]) has been tested to reduce the toxicity of APL. Among all the methods tested, overliming was suggested to be the most effective to reduce the concentration of inhibitors in APL [27]. Zhou reported that BMP test carried out for raw APL, and APL treated by bleaching, and activated carbon did not improve the biogas yield however, APL treated by calcium hydroxide (overliming) increased the biogas yield [27].

APL overliming was carried out by addition of calcium hydroxide (11g) to raw APL (100 ml). The mixture was cooled down to room temperature and centrifuged to extract the supernatant. They reported that overliming treatment partially or completely removed majority of toxic compounds in comparison to other methods tested, without significantly changing the VFA's of the APL [27]. By using the APL treated by overliming, Zhou carried out batch test of APL at organic loading of 14.58 gCOD/L (3% of raw APL) without showing any lag-phase and inhibition. They reported that batch test and continuous AD of overlimed APL can tolerate loading of 3% to 18% without showing any significant inhibition [27].

3 Materials and Methods

To understand the anaerobic digestability of APL, batch scale tests were performed using Automatic Methane Potential Testing System II (AMPTS II, Bioprocess Control® Sweden AD, Lund, Sweden 2017) and 100 mL plastic medical syringes. APL was also co-digested with HS waste to understand the effects of APL during co-digestion. Modelling and simulation of APL was carried out in Aquasim 2.1 using the IWA Anaerobic Digestion Model no.1 (ADM1).

This sub-chapter presents the details about the materials, reactors, analytical and experimental methods used and implementation of APL in ADM1 model using Aquasim 2.1.

3.1 Analytical Methods

pH values were measured by a Beckman 390 pH-meter. The pH-meter was calibrated using two buffer solutions of pH 4.0 and 7.0. Samples were at room temperature and mixed using a magnetic stirrer while measuring the pH.

Total and soluble COD, ammonium nitrogen and alkalinity was measured using commercial kits as per US standard 5220D, 53 and 208[53] and Spectroquant®Pharo 300 UV/VIS spectrophotometer (Darmstadt, Germany). Samples were diluted as per the range of commercial kits. For all analyses except total COD (tCOD), the diluted sample was filtered through 0.45 µm GxF multi-layered acrodisc PSF syringe filter.

Gas compositions were determined by gas chromatography (SRI Instruments, model 8610 C) following standard procedure Norsk Standard NS-EN6974-4, using Helium as carrier gas.

Concentrations of C, H, N and S were determined using Vario El Cube Elemental Analyser (Elementar Anlaysensysteme GmbH, Hanau, Germany) [54]. Analyses were carried out by LabTek NMBU.

VFA concentrations were determined by gas chromatography (HP 6890, serial C), using helium as a carrier gas.

3.2 Material Characterization

3.2.1 Inoculum

Inoculum was provided by Lindum AD plant in Drammen, Norway, a mesophilic process with an installed thermal hydrolysis step prior to AD. The plant treats sewage sludge from surrounding municipalities (about 90% of total VS) and food waste from industry. The inoculum was collected from the effluent stream of the reactor and had a pH of 7.97, TS of 16.78 g/L, VS of 13.14 g/L, Total ammonium nitrogen (TAN) was 486 mg/L, Total Chemical Oxygen Demand (tCOD) of 37.25 gCOD/L and Soluble Chemical Oxygen Demand (sCOD) of 28 gCOD/L. Inoculum contained 28.9%, 4.53%, 0.6% and 4.533% (w/w) of carbon, nitrogen, hydrogen and sulphur.

To reduce biogas production from the inoculum, it was left for degassing at 30°C for 5 days before starting the experiment.

3.2.2 APL

APL was provided by Scanship AS. The origin was pyrolysis of commercial softwood pellets (Norway spruce and Scots pine 60/40 per volume, Hallingdal Trepellets AS) at 600°C, using the Biogreen® technology. The pyrolysis liquid was condensed from syngas cooled to 5-8°C, and the APL provided was the top phase decanted after settling by gravity for two weeks in a cool environment.

COD and VFA concentration of APL is shown in Table 3.1 and Table 3.2 are investigated by laboratory analysis.

Table 3.1 Results from Laboratory analysis of APL

Sample	tCOD (g/L)	sCOD (g/L)	pH	VFA (g/L)
APL	456	428	2.46	84.66

Table 3.2 VFA concentration in APL from laboratory analysis

Sample	Acetic acid (g/L)	Propionic acid (g/L)	Butyric acid (g/L)	Total (g/L)
APL	75.466	5.5	3.7	84.66

3.2.3 Food/sludge Co-substrate

The sludge co-substrate, which will further in the text be named hydrolyzed sludge (HS), came from the influent stream to the AD tanks, after the thermal hydrolysis step and had a pH of 6.615, alkalinity of 1.19 g/L, Total Ammonium Nitrogen (TAN) of 0.905 g/L, Total solids (TS) of 86.273 g/L and Volatile solids (VS) of 53.669 g/L. HS contained 3.06% of Carbon, 3% of Nitrogen, 0.35% of Sulfur and 4.9% of Hydrogen. The results from the laboratory analysis are presented in Table 3.3.

Table 3.3 Relevant parameters measured for HS from laboratory analysis

Analysis	Substrate
TCOD (g/L)	99
SCOD (g/L)	19.45
Acetic acid (g/L)	1.58
Propionic acid (g/L)	0.43
Butyric acid (g/L)	0.5
Isobutyric acid (g/L)	0.23
Isovaleric acid (g/L)	0.42

3.3 Experimental Approach

This subchapter explains briefly about the bio-methane potential tests carried out using AMPTS II setup and Syringe setup at different organic loads.

3.3.1 AMPTS II Test

Anaerobic biogas potential tests were performed in AMPTS II (Figure 3.1). AMPTS II gives a real time automated measurement of methane production (NmL, resolution 9 NmL) during anaerobic digestion. The system can analyze 15 samples simultaneously.



Figure 3.1 AMPTS II general setup showing water-bath, scrubbing unit and control unit (from left to right)[55].

Each sample, according to compositions listed in Table 3.5, was added to a 500 mL reactor with a cap equipped with a motorized stirrer. Mixing was programmed for 60 s every hour with a motor adjustment speed of 50%, equivalent to 100 rpm, to imitate a small anaerobic digester with intermittent mixing. All reactors were submerged in a water bath maintained at 35°C.

To remove CO₂ and H₂S and measure produced CH₄, the produced gas was passed through pipes to a scrubbing reactor. The scrubbing reactors (100mL) contained 80 mL of 3 M sodium hydroxide (NaOH) and a 0.4% thymolphthalein solution as pH indicator. The solution has an absorption efficiency of >98% [55]. Methane then passes to the measuring cell. The gas is then measured by a gas flow measuring device and the data is recorded by the Bioprocess Control® software.

The system was flushed with pure nitrogen gas for 5-7 min to ensure anaerobic conditions before start-up of the experiment. Samples were run in triplicates.

Two sets of experiment were conducted on AMPTS II using fresh and stored inoculum. The first set was carried out using inoculum degassed for 5 days at 30 °C and using different organic loads in gCOD of substrate per litre of inoculum.

Table 3.4 Organic loading of AMPTS II tested for digestion of APL and co-digestion of APL and HS using fresh inoculum

AMPTS II	Sample	Innoculum	Substrate		OL (gCOD/L)
			HS (mL)	APL (mL)	
Reactor 1	Blank	300			0
Reactor 2	Control	300	37.1		12.24
Reactor 3	APL-2.4	300		1.58	2.40
Reactor 4	co-digestion	300	29.68	0.32	10.28
Reactor 5	APL-1.2	300		0.79	1.20

Second run was carried out for same organic load using same inoculum degassed for 54 days at 30°C.

Table 3.5 Organic loading of AMPTS II tested for mono-digestion of APL and co-digestion of APL and HS using stored inoculum

AMPTS II	Sample	Inoculum (mL)	Substrate		OL (gCOD/Li)
			HS (mL)	APL (mL)	
Reactor 1	Blank-s	200			0
Reactor 2	Control-s	200	4.8		2.4
Reactor 3	Co-digestion-s	200	4.4	0.1	2.4
Reactor 4	APL-2.4-s	200		1.1	2.4
Reactor 5	APL-1.2-s	200		0.5	1.2

3.3.2 Syringe Test

Plastic medical syringes of 100 ml were used as anaerobic reactors for the BMP test as described elsewhere [56]. The test was carried out using different organic loadings (Table 3.6). The required amount of inoculum and substrate were kept in the syringe (Figure 3.2) and a rubber stopper was used to prevent any leakage and maintain anaerobic conditions. Before starting the test, the mixture was shaken thoroughly and hung on a rack (Figure 3.2). Triplicates were run for each loading. The syringes were kept inside an incubator maintaining a temperature of 35 °C.



Figure 3.2 Medical plastic syringes with inoculum and APL inside the incubator.

Biogas generated was recorded everyday using the mark levels on the syringe. An interconnected gas valve (Mininert® syringe valve) was used to transfer the accumulated biogas to a different syringe for determining the gas composition. Biogas volume was recalculated to Normal volume (0 °C and 1 atm), NmL. Due to low resolution (2 mL), the syringe test was used to understand the trend and effect of different organic loadings on the inoculum.

Table 3.6 Organic Load of syringe tested for APL

Reactors	Sample	Innoculum (mL)	APL (mL)	OL (gCOD/L)
1	Blank	30		
2	APL0.5	30	0.03	0.5
3	APL1	30	0.07	1
4	APL2	30	0.13	2
5	APL3	30	0.20	3

3.4 Modelling and Simulations

The goal of the modelling was to modify the ADM1 to incorporate the inhibitory compounds phenol, furfural and HMF to increase the predictability of the existing model. The developed model helps to understand inhibition effect and methane production. Specific simulation cases were carried out to understand effects of APL during AD.

3.4.1 Determination of Inhibition Constant (Ki)

Prior knowledge of parameter, inhibition constant, is required for modelling the effects of inhibition from furfural and HMF, but this knowledge is limited and to the best of the my knowledge, no known source has provided data for the Ki by the time of this writing (May 2021).

IC₅₀ is the concentration of substrate at which 50% inhibition occurs and can be used as Ki for using noncompetitive inhibition function[37], [11].

Ghasimi et al. [40] carried out the specific methanogenic activity (SMA) test to determine the maximum methane production using 1 g/L of sodium acetate with inoculum (control). The SMA test in the presence of 0.4 g/L, 0.8 g/L and 2 g/L of furfural and HMF (separately) in control was tested to determine the possible inhibition caused. The test was carried out in AMPTS II and results are shown in Table 3.7.

Table 3.7 SMA activity of control, furfural and HMF in Ghasimi et al[40]

Concentrations (g/L)	Specific Methanogenic Activity (gCOD-CH ₄ /(gVS.d))	
	Furfural	HMF
0 (Control)	0.55	0.55
0.4	0.53	0.53
0.8	0.45	0.50

2	0	0
---	---	---

The value of IC₅₀ can be determined graphically by determining the concentration where 50% of methanogenic activity was inhibited (Figure 3.3)[9].

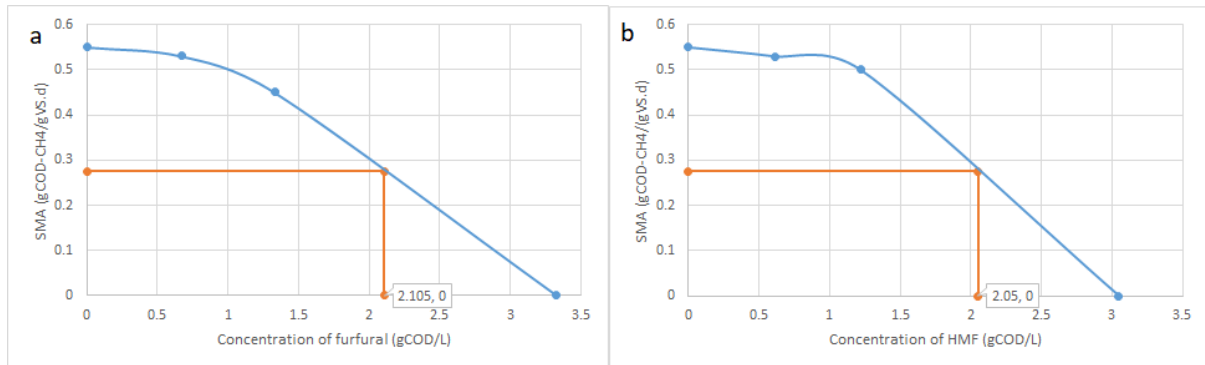


Figure 3.3 IC₅₀ value determined graphically for furfural (a) and HMF (b) for SMA activity by Ghasimi et. al [40].

3.4.2 Extended ADM1 model implementation

A schematic of extended model is shown in Figure 3.4. Number in the schematic diagram represents the process whose stoichiometry and decomposition fractions are further explained in Appendix B. Process 6a, 6b and 6c are modification made in standard ADM1 model to incorporate phenols, furfural and HMF kinetics and biochemical reactions, respectively. All of these combined represents the extended model of ADM1.

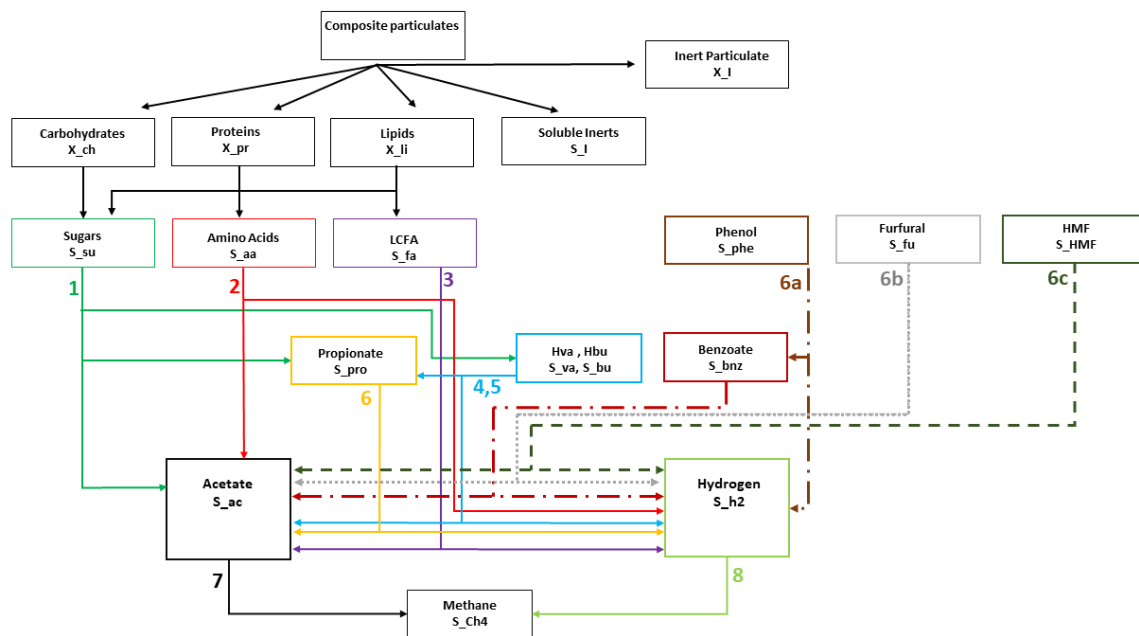


Figure 3.4 Brief schematic diagram of extended ADM1 model which includes phenol, furfural and HMF

Simulation of the batch tests was performed by modifying the standard ADM1 to a batch reactor. Initial biomass concentration of microorganisms was adjusted by factor of 0.6 ($X_{ini}=0.6$).

3.4.2.1 Implementation of phenol

In order to incorporate phenol and its degradation, modifications was made in the standard ADM1. The uptake of phenol was modelled by using Monod type kinetic equation (equation 3.1).

$$\text{Uptake}_{\text{phe}} = K_{m_{\text{phe}}} \times X_{\text{phe}} \times \frac{S_{\text{phe}}}{S_{\text{phe}} + K_{s_{\text{phe}}}} \times I_{\text{ph}_{\text{bac}}} \times I_{\text{NH}_{\text{limit}}} \quad (3.1)$$

$\text{Uptake}_{\text{phe}}$ is the uptake rate of phenol expressed in $\text{kgCOD}_s/\text{m}^3\text{d}^{-1}$. Related parameters for equation 3.1 and its value are described in Table 3.8 and detail stoichiometry is given in Appendix B. $I_{\text{ph}_{\text{bac}}}$ and $I_{\text{NH}_{\text{limit}}}$ were used as in standard ADM1 model and S_{phe} is the soluble phenol concentration in $\text{kgCOD}_s/\text{m}^3$. $I_{\text{ph}_{\text{bac}}}$ is inhibition caused by pH on the microorganism and $I_{\text{NH}_{\text{limit}}}$ is the inhibition due to lack of inorganic nitrogen.

X_{phe} is the concentration of phenol degraders in $\text{kgCOD}_x/\text{m}^3$. However, initial biomass concentration of phenol degrader was unknown, thus a factor $X_{\text{ini_in}}$ was used to adjust the startup biomass concentration used in extended ADM1 model (equation 3.2). The startup biomass concentration was assumed to be $0.35 \text{ kgCOD}/\text{m}^3$.

$$X_{\text{phe}} = 0.35 \times X_{\text{ini_in}} \quad (3.2)$$

The endogenous decay of phenol degrading bacteria were represented as first order kinetics (equation 3.3) and dead biomass were maintained as composite particulate material as in standard ADM1 model.

$$\text{Decay}_{\text{phe}} = K_{\text{dec}_{\text{phe}}} \times X_{\text{phe}} \quad (3.3)$$

Inhibition due to phenol on acetoclastic methanogens was implemented as non-competitive inhibition (equation 3.4) as described by Batstone et. al [11].

$$I_{\text{phe}} = \frac{1}{1 + \frac{S_{\text{phe}}}{K_{i_{\text{ac},\text{phe}}}}} \quad (3.4)$$

As, phenol is a weak acid and both phenol and benzoate contribute towards change in pH. The charge balance equation used in standard ADM1 model was extended to include the contributions from phenol and benzoate. The extended charge balance used is given in equation (3.5).

$$S_{\text{H}^+} - S_{\text{OH}^-} = S_{\text{HCO}_3^-} + \frac{S_{\text{ac}^-}}{64} + \frac{S_{\text{pro}^-}}{112} + \frac{S_{\text{bu}^-}}{160} + \frac{S_{\text{va}^-}}{208} + \frac{S_{\text{phe}^-}}{224} + \frac{S_{\text{bnz}^-}}{240} + S_{\text{An}^+} - S_{\text{cat}^+} - S_{\text{NH}_4^+} \quad (3.5)$$

Where S_{phe^-} and S_{bnz^-} are phenol and benzoate ion concentration and implemented in ADM1 as described by Batstone et al [11].

$$S_{\text{phe}^-} - \frac{K_{a,\text{phe}} \times S_{\text{phe}}}{K_{a,\text{phe}} + S_{\text{H}^+}} = 0 \quad (3.6)$$

Where $K_{a,phe}$ is phenolic acid dissociation constant and is implemented as in equation (3.7).

$$K_{a,phe} = 10^{-pK_{a,phe}} \quad (3.7)$$

Where $pK_{a,phe}$ is the phenolic acid strength.

Similarly for benzoate ion concentration was implemented as equation 3.8.

$$S_{bnz} = \frac{K_{a,bnz} \times S_{bnz}}{K_{a,bnz} + S_{H^+}} \quad (3.8)$$

Where $K_{a,bnz}$ is benzoic acid dissociation constant and is implemented as shown in equation 3.9

$$K_{a,bnz} = 10^{-pK_{a,bnz}} \quad (3.9)$$

Where $pK_{a,bnz}$ is the benzoic acid strength.

The uptake of benzoate was model by using Monod type kinetic equation as in equation 3.10

$$\text{Uptake}_{bnz} = K_{m,bnz} \times X_{bnz} \times \frac{S_{bnz}}{S_{bnz} + K_{S,bnz}} \times I_{ph_{bac}} \times I_{NH_{limit}} \times I_{H_2,bnz} \quad (3.10)$$

Uptake_{bnz} is the uptake rate of benzoate expressed in $\text{kgCOD}_s/\text{m}^3\text{d}^{-1}$. Related parameters for equation 3.10 and its value are described in Table 3.8 and detail stoichiometry is given in Appendix B. S_{bnz} is the soluble benzoate concentration expressed in kgCOD/m^3 . $I_{ph_{bac}}$ and $I_{NH_{limit}}$ were used as in standard ADM1 model. $I_{H_2,bnz}$ is the inhibition caused by free hydrogen on benzoate degrading organism and modelled as non-competitive inhibition equation [47].

$$I_{h_2,bnz} = \frac{1}{1 + \frac{S_{H_2}}{K_{i,bnz,H_2}}} \quad (3.11)$$

The endogenous decay of benzoate degrading bacteria were represented as first order kinetics and dead biomass were maintained as composite particulate material as in standard ADM1 model.

$$\text{Decay}_{bnz} = K_{dec,bnz} \times X_{bnz} \quad (3.12)$$

To adjust the initial biomass concentration of benzoate degrader, a factor X_ini_in (value of 0.6) was used to adjust the biomass concentration in extended ADM1 model. X_{bnz} , initial concentration of benzoate degrader was assumed to be $0.4 \text{ kgCOD}/\text{m}^3$.

To incorporate all the processes mentioned in equation 3.1-3.12 in standard ADM1 model, parameters and variables in those equation were added in the standard ADM1 model. Added parameters and its description are shown in Table 3.8 and Appendix B.

Table 3.8 Kinetic parameters defined in ADM1 model for degradation of phenol into acetate.

Parameters	Description	Units	Value	Source
C_phe	Carbon content of phenol	Kmole C/kgCOD	0.0319	[47]
f_bnz_phe	Yield of benzoate from phenol degradation	-	0.87	[47]
f_h2_phe	Yield of hydrogen from phenol degradation	-	0.13	[47]
Km_phe	Maximum uptake rate for phenol degradation organism	d ⁻¹	15	[47]
Ks_phe	Half saturation constant for phenol uptake	kgCOD _s /m ³	30	[47]
Kdec_phe	Decay rate for phenol degrading organism	d ⁻¹	0.02	[47]
Y_phe	Yield of biomass on uptake of phenol	kgCOD _x /kgCOD _s	0.01	[47]
KI_ac_phe	Inhibition constant due to phenol on methanogens	kgCOD/m ³	1.12	[38]
C_bnz	Carbon content of benzoate	Kmole C/kgCOD	0.034	[47]
f_ac_bnz	Yield of acetate from benzoate degradation	-	0.51	[47]
f_h2_bnz	Yield of hydrogen from benzoate degradation	-	0.49	
Km_bnz	Maximum uptake rate for benzoate degradation organism	d ⁻¹	8	[47]
Ks_bnz	Half saturation constant for benzoate uptake	kgCOD _s /m ³	15.5	[47]
Kdec_xbnz	Decay rate for benzoate degrading organism	d ⁻¹	0.02	[47]
Y_bnz	Yield of biomass on uptake of benzoate	kgCOD _x /kgCOD _s	0.0135	[47]

KI_bnz_h2	Inhibition constant for benzoate by hydrogen	kgCOD/m ³	9.5e-5	[57]
pKa_bnz	Acid Dissociation constant for benzoate	-	4.2	[58]
pKa_phe	Acid Dissociation constant for phenols	-	10	[59]
X_phe	Phenol degraders	kgCOD _x /m ³	0.35	Assumed
X_bnz	Benzoate degraders	kgCOD _x /m ³	0.4	Assumed

3.4.2.2 Implementation of furfural

Conversion of furfural to acetate was modelled as Monod type kinetic equation for implementing in standard ADM1 model (equation 3.13).

$$\text{Uptake}_{fu} = K_{m_{fu}} \times X_{fu} \times \frac{S_{fu}}{S_{fu} + K_{S_{fu}}} \times I_{ph_{bac}} \times I_{NH_{limit}} \quad (3.13)$$

S_{fu} is the soluble furfural concentration in kgCOD_s/m³ and Uptake_{fu} is uptake rate of soluble furfural expressed in kgCOD_s/m³d⁻¹. $I_{ph_{bac}}$ and $I_{NH_{limit}}$ are implemented as described by Batstone et al. [11]. Detail stoichiometry is given in Appendix B and its value are presented in Table 3.9.

The decay of furfural degrading microorganism was modelled as first order kinetic equations.

$$\text{Decay}_{fu} = K_{dec_{fu}} \times X_{fu} \quad (3.14)$$

X_{fu} is the concentration of microorganism in kgCOD_x/m³. The initial biomass concentration of furfural degrader was adjusted by using X_{ini_in} (value of 0.6) as in equation 3.2

Inhibition due to furfural on methanogens was modelled using non-competitive inhibition function as described by Batstone et. al [11].

$$I_{fu} = \frac{1}{1 + \frac{S_{fu}}{K_{i_{ac, fu}}}} \quad (3.15)$$

$K_{i_{ac, fu}}$ is the inhibitory concentration which would reduce the methanogenic activity by 50% expressed in kgCOD/m³.

All the process were implemented in standard ADM1 model which are shown in equation 3.13-3.15. Parameters and variable that were introduced in standard ADM1 model are described in Table 3.9 and Appendix B .

Table 3.9 Kinetic parameters added in ADM1 for degradation of furfural into acetate.

Parameters	Description	Unit	Value	Source
C_fu	Carbon content of furfural	Kmole C/kgCOD	5/160	
f_ac_fu	Yield of acetate from furfural degradation	-	0.8	[49]
f_h2_fu	Yield of hydrogen from furfural degradation	-	0.2	[49]
Km_fu	Maximum uptake rate for furfural degradation organism	d ⁻¹	10	[60]
Ks_fu	Half saturation constant for furfural uptake	kgCOD _s /m ³	10	[60]
Kdec_fu	Decay rate for furfural degrading organism	d ⁻¹	0.02	Assumed
Y_fu	Yield of biomass on uptake of furfural	kgCOD _x /kgCOD _s	0.08	[49]
KI_ac_fu	Inhibition constant for acetate degrader by furfural	kgCOD _s /m ³	2.105	
X_fu	Furfural degraders	kgCOD _x /m ³	0.2	Assumed

3.4.2.3 Implementation of HMF

HMF was implemented in same manner as that for furfural. The degradation of HMF to acetate was modelled by Monod type kinetic equation as shown in equation 3.16

$$\text{Uptake}_{\text{HMF}} = K_{\text{mHMF}} \times X_{\text{HMF}} \times \frac{S_{\text{HMF}}}{S_{\text{HMF}} + K_{\text{S}_{\text{HMF}}}} \times I_{\text{ph}_{\text{bac}}} \times I_{\text{NH}_{\text{limit}}} \quad (3.16)$$

Uptake_{HMF} is the reaction/uptake rate of HMF expressed in kgCOD_s/m³d⁻¹ and S_{HMF} is the soluble concentration of HMF in kgCOD_s/m³. I_{ph_{bac}} and I_{NH_{limit}} is implemented as for phenol and furfural degradation.

The decay of HMF degrader was modelled as first order kinetics equation.

$$\text{Decay}_{\text{HMF}} = K_{\text{dec}_{\text{HMF}}} \times X_{\text{HMF}} \quad (3.17)$$

X_{HMF} is the concentration of HMF degrading organism adjusted with a factor of X_{ini_in} (value of 0.6) as in equation 3.2 and expressed as kgCOD_x/m³.

Inhibition caused by HMF on methanogens was modelled as non-competitive inhibition as described by Batstone et. al [11].

$$I_{\text{HMF}} = \frac{1}{1 + \frac{S_{\text{HMF}}}{K_{i_{\text{ac,HMF}}}}} \quad (3.18)$$

$K_{i_{\text{ac,HMF}}}$ is the inhibitory concentration of HMF which reduce the methanogenic activity by 50%.

Parameters and variable in equation 3.16-3.18 was introduced and described in Table 3.10. The biochemical reaction and rate of equation are also added (Appendix B).

Table 3.10 Kinetic parameter added in ADM1 for HMF degradation

Parameters	Description	Unit	Value	Source
C_HMF	Carbon content of HMF	Kmole C/kgCOD	5/160	
f_ac_HMF	Yield of acetate from HMF degradation	-	0.88	[60]
f_h2_HMF	Yield of hydrogen from HMF degradation	-	0.12	[60]
Km_HMF	Maximum uptake rate for HMF degradation organism	d ⁻¹	10	[60]
Ks_HMF	Half saturation constant for HMF uptake	kgCOD _s /m ³	10	[60]
Kdec_HMF	Decay rate for HMF degrading organism	d ⁻¹	0.01	[60]
Y_HMF	Yield of biomass on uptake of HMF	kgCOD _x /kgCOD _s	0.1	[60]
KI_ac_HMF	Inhibition constant for acetate degrader by HMF	kgCOD _s /m ³	2.05	
X_HMF	HMF degraders	kgCOD _x /m ³	0.3	Assumed

3.4.2.4 Modification on acetoclastic methanogens

In order to incorporate the inhibition by phenol, furfural and HMF on methanogens, modification was made to standard ADM1 model (equation 3.19) to model the effect of phenol, furfural and HMF inhibition (equation 3.20).

Standard ADM1 Model (original)

$$\text{Uptake}_{\text{ac}} = K_{m_{\text{ac}}} \times X_{\text{ac}} \times \frac{S_{\text{ac}}}{S_{\text{ac}} + K_{S_{\text{ac}}}} \times I_{\text{ph}_{\text{bac}}} \times I_{\text{NH}_{\text{limit}}} \times I_{\text{ac, NH}_3} \quad (3.19)$$

Extended Model

$$\text{Uptake}_{ac} = K_{m_{ac}} \times X_{ac} \times \frac{S_{ac}}{S_{ac} + K_{S_{ac}}} \times I_4 \quad (3.20)$$

Where, I_5 is the total inhibition on acetoclastic methanogens

$$I_4 = I_{ph_{bac}} \times I_{NH_{limit}} \times I_{ac, NH_3} \times I_{phe} \times I_{fu} \times I_{HMF} \quad (3.21)$$

3.4.3 Simulation cases

To better understand the implemented extended model, a number of simulations were run on different cases. Sim-1 to Sim-10 uses the extended model to predict APL1.2 and APL2.4 mentioned in chapter 3.4.4.

Table 3.11 List of simulation for this thesis.

Simulation Number	Description	Reference experimental Results from AMPTS II with fresh inoculum (first run)
Standard ADM1	Standard ADM1 without any modification	
Sim-1	Simulation of Blank	Simulation to adjust the inoculum methane production compared with B-1
Sim-2	Simulation of APL with organic load of 1.2 gCOD/L (APL 1.2) with X_{ini} and X_{ini_in} equals to 0.6	Compared with experimental results from APL-1.2-3 (AMPTS II with fresh inoculum)
Sim-3	Simulation of Sim-2 with different concentration of S_{phe} , S_{fu} , S_{HMF}	
Sim-4	Simulation of Sim-2 with different inhibition constant for furfural, phenol and HMF	
Sim-5	Simulation of Sim-2 with $X_{ini}=0.6$ and $X_{ini_in}=0.1$	

Sim-6	Simulation of APL with organic load of 2.4 gCOD/L (APL2.4) with X _{ini} and X _{ini_in} equals to 0.6	Compared with experimental results from APL-2.4-1 (AMPTS II with fresh inoculum)
Sim-7	Simulation of Sim-6 with different concentration of S _{phe} , S _{fu} , S _{HMF}	
Sim-8	Simulation of Sim-6 with change K _i for furfural and HMF	
Sim-9	Simulation of Sim-8 with X _{ini} =0.6 and X _{ini_in} =0.1	
Sim-10	Use of Haldane growth kinetics instead of Monod growth kinetics for Sim-8	

3.4.4 Inputs for ADM1

Instead of removing the amount of methane produced from the blank from all the results from AMPTS II, simulated result from blank was used as initial condition for all the simulations carried out as it makes it easier for the APL2.4 simulation where it was producing less methane than blank itself initially. Thus, implementation of APL1.2 and APL2.4 would use the composition of blank (inoculum in chapter 3.2.1) and its constituent composition (Table 3.12) for simulation.

Table 3.12 APL composition implemented in ADM1

APL Composition		Reference
Parameters	Value	
tCOD(g/L)	456	Chapter 3.2.2
sCOD(g/L)	428	Chapter 3.2.2
VFA(g/L)	81.16	Chapter 3.2.2
Acetic (g/L)	75.83333	Chapter 3.2.2
Propionic(g/L)	5.333333	Chapter 3.2.2
Phenol(g/L)	25	[10]
Furfural(g/L)	10	[16]
HMF(g/L)	7	[16]

As exact information on concentration of phenols, furfural and HMF were not known for APL, the concentration for these compounds were extracted from the previous studies of pyrolysis of birch bark carried out at 600°C and is discussed in chapter 5.6. For concentration of phenols, overall concentration of phenolic compounds from literature review was used as studies suggest that phenols have similar kinetics as for a mixture of phenolic compounds[38].

Table 3.13 Inputs used for simulation of blank, standard ADM1, Sim-2 (APL1.2) and Sim-6 (APL2.4)

Parameters	Description	Blank	Standard ADM1	APL1.2	APL2.4
tCOD	Total COD (kgCOD/m ³)		1.2008	1.2008	2.4016
sCOD	Soluble COD (kgCOD/m ³)			1.127067	2.254133
X_C	Particulate Composites (kgCOD/m ³)	2	0.966536	0.730302	1.460604
X_I	Particulate Inert (kgCOD/m ³)	5		0.007377	0.014754
S_ac	Soluble acetate (kgCOD/m ³)		0.213007	0.213007	0.426015
S_pro	Soluble propionate (kgCOD/m ³)		0.021256	0.021256	0.042513
S_phe	soluble phenol (kgCOD/m ³)			0.156879	0.313759
S_fu	soluble furfural (kgCOD/m ³)			0.043889	0.087778
S_HMF	soluble HMF (kgCOD/m ³)			0.028089	0.056178
S_I	souble inert (kgCOD/m ³)	0.025	0.025	0.025	0.025
S_IN	souble inorganic nitrogen (M)	3.673	3.673	3.673	3.673

For APL used, only VFA's could be measured from our laboratory and accounts for only 17% of tCOD (Table 3.12). Even though, phenol, furfural and HMF concentration were extracted from literature review, nearly 50% of COD of APL was unknown most of which were soluble COD (refer to Table 3.12). However, for simulation in ADM1 unknown COD was used as X_C as microorganism need to adapt to the composition of APL and would take time to use the soluble components to from more easily degradable monomers [10].

4 Results

This chapter summarizes the results from the experiments (chapter 4.1) and simulations of implementation of APL in the ADM1 using Aquasim (chapter 4.2).

4.1 Experimental results

The results from the batch test on AMPTS II using fresh inoculum and stored inoculum along with the syringe test are presented in this chapter. The batch tests were run using organic loads mentioned in chapter 3.3.1 for AMPTS II and chapter 3.3.2 for the syringe tests.

4.1.1 AMPTS II using fresh inoculum

Results from the batch test of APL and its co-digestion with HS is presented in this sub-chapter.

- Methane Production trend

The methane production from running the five tests with three parallels was measured for 54 days (Figure 4.1). However, only two results from blank i.e with only inoculum (blank-1 and blank-2), one from control (with HS as substrate) at the organic load of 12.24 gCOD/L (control-3), two from APL with an organic load of 2.4 gCOD/L (APL-2.4-1 and APL-2.4-2), two results from co-digestion of APL with HS at an organic load of 10.28 gCOD/L with COD ratio of 95:5 gCOD_{HS}/gCOD_{APL} (co-digestion 2 and co-digestion-3) and two results from APL with an organic load of 2.4 gCOD/L (APL-1.2-1 and APL-1.2-3) are presented. Results from the rest of the batch test were not detected by AMPTS II due to technical issues.

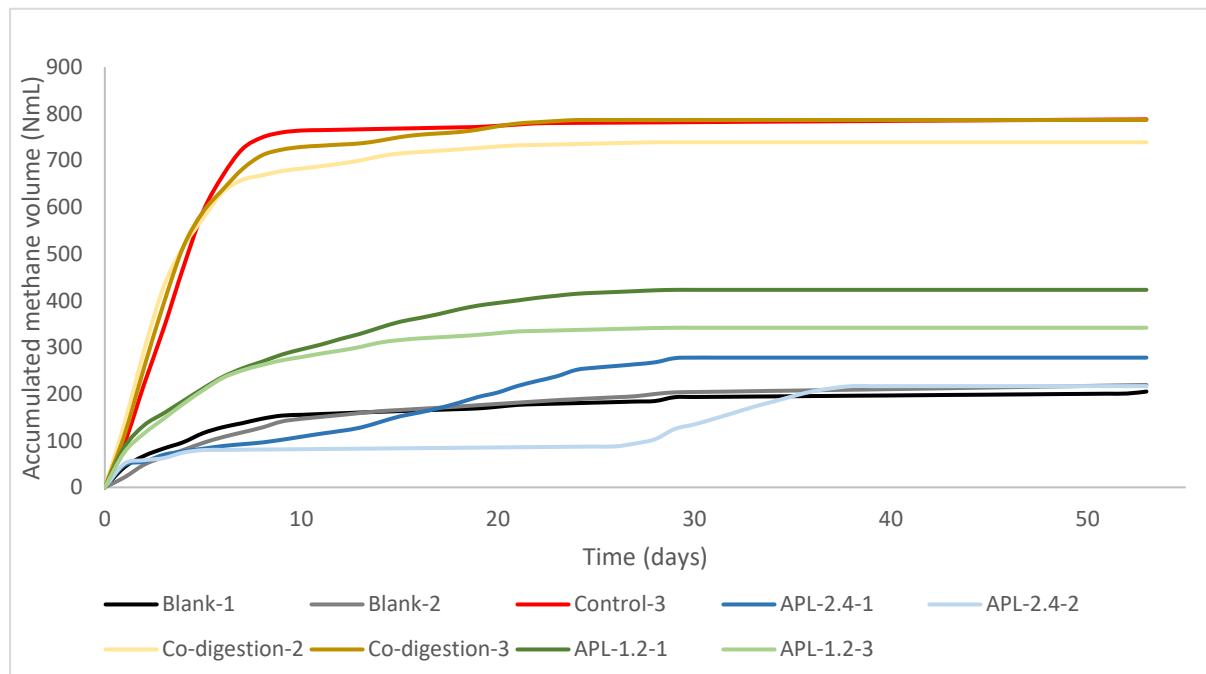


Figure 4.1 Accumulated methane production (NmL) from batch test of APL (APL1.2 and APL2.4), HS (control), and co-digestion of APL with HS (Co-digestion) from AMPTS II using fresh inoculum at different organic loads which are referred as 1.2 and 2.4 at end of text APL for load of 1.2 and 2.4 gCOD/L respectively.

Methane production from the blank and control started within a few hours suggesting that the inoculum was ready to digest the acetic acids and organic matter present in HS. Both tests nearly reached their final volume around day 10, after which it remained almost the same, reaching a final volume of 209 NmL, 219 NmL, and 788 NmL for blank-1, blank-2, and control-3. Co-digestion of APL and HS also showed a similar trend in methane production as the control, producing nearly the same amount of methane even though it had a lower organic load.

Similarly, batch test with lower organic load showed no lag phase and showed higher methane production rate till day 10 for both parallels. APL-1.2-3 showed slow but progressive methane production after day 10 and reached its final volume after day 20. A similar trend was observed for APL-1.2-1 and accumulated methane production almost same after day 25.

In contrast, APL with higher organic load showed a lag phase of 10 days for APL-2.4-1 and nearly 28 days for APL-2.4-2. Both tests showed lower methane production than APL1.2 and produced 68 NmL and 2 NmL more than blank, respectively.

- Methane Yield

The methane yield from the AMPTS II with fresh inoculum is shown in Figure 4.2 and calculated using the procedure presented in Appendix C. The batch test with co-digestion of APL and HS improved the methane yield by 8 % and 15 % for co-digestion-2 and co-digestion-3 when compared with control. Much lower methane yield was observed for APL2.4, at 88 NmL/gCOD and 3.67 NmL/gCOD for APL-2.4-1 and APL-2.4-2. A higher yield was observed for APL1.2. The yield was far higher than the theoretical methane yield at 579 NmL/gCOD for APL-1.2-1 and 343.79 NmL/gCOD for APL-1.2-3.

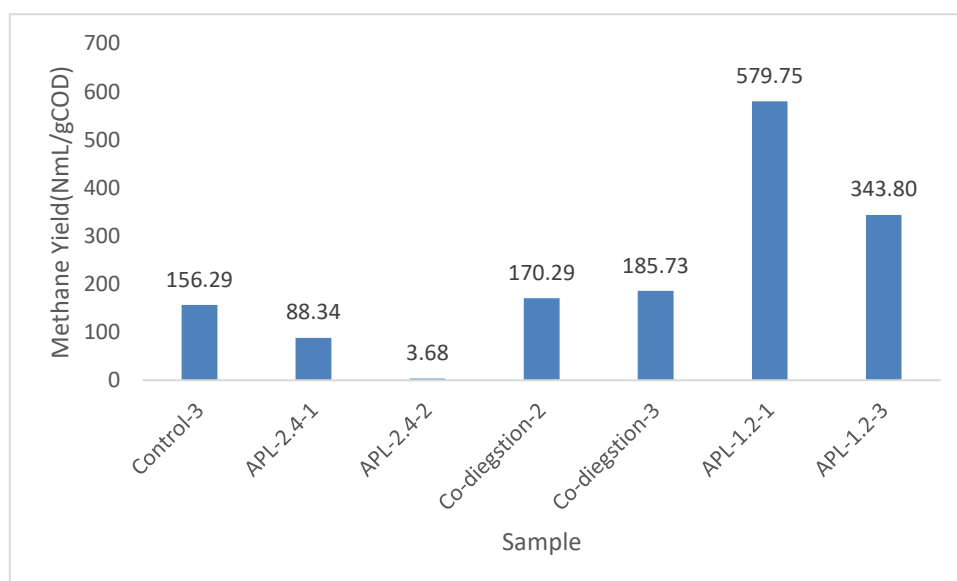


Figure 4.2 Methane yield obtained for batch test carried out in AMPTS II using fresh inoculum.

- pH

The pH of the inoculum was 7.97 before the startup of the experiment. The pH was stabilized for all the tests and was measured in the range of 8.02-8.18.

4.1.2 Syringe Test

- Cumulative biogas production

Cumulative biogas production from the syringe test for different organic loads (Table 3.6) during the 23 days of the test is shown in Figure 4.3.

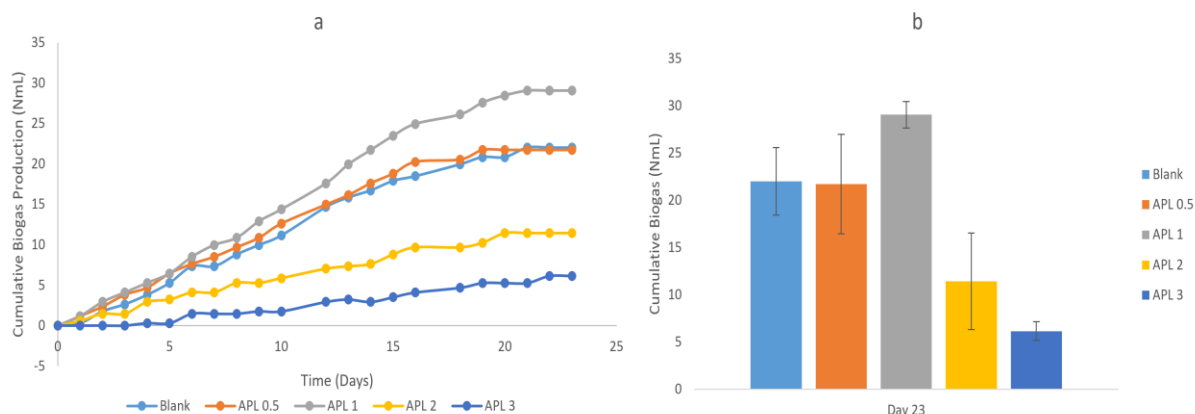


Figure 4.3 Cumulative biogas production 1a: trend of biogas production from syringe test, 1b: standard deviation on the final biogas production for different samples.

Biogas production from Blank, APL0.5 and APL1 showed a similar trend with gradual production without showing any immediate increase on day 1. However, APL1 and APL0.5 gave a little boost in daily biogas production from day 3 when compared with Blank. APL1 produced 7 NmL more than Blank. Even though APL0.5 boosted the daily biogas production, the final volume was the same as for Blank (22 NmL \pm 4). The standard deviation of APL0.5 and APL1 was 5 NmL and 1 NmL than average.

With an increasing organic load of APL, the biogas production decreased gradually, and the final biogas production was 50% and 72% lower than Blank for APL2 and APL3.

- Biogas Composition

The biogas composition was measured at day 24 and shown in Figure 4.4. Lower methane concentration was observed for APL3, at 23.76% \pm 4.71. Even though lower biogas production was observed for APL2 in Figure 4.3, a higher methane concentration (73.76% \pm 4.67) was measured.

APL0.5 and APL1 showed higher methane concentration at 78.42% \pm 2.13 and 78.83% \pm 5.

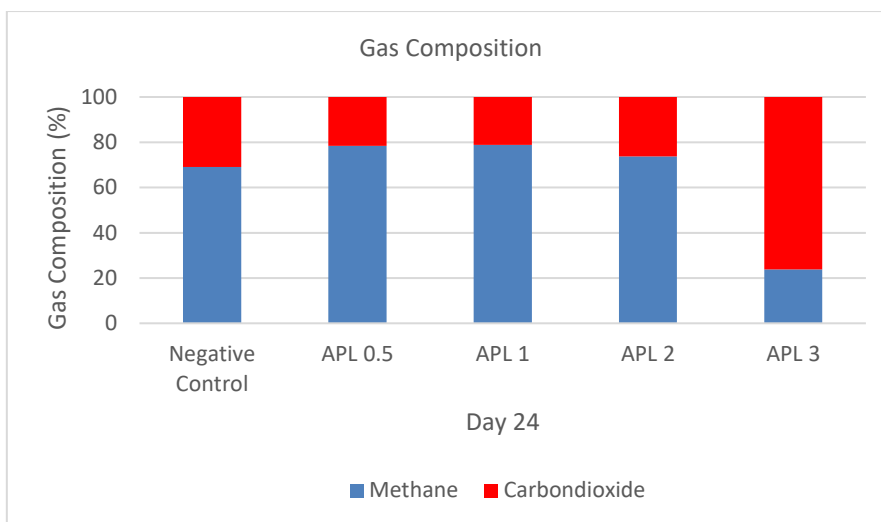


Figure 4.4 Gas composition from syringe test of APL at different organic loads.

Methane yield from APL1 was about 230 NmL/gCOD. For APL2 and APL3 the methane yield was not calculated as its methane formation was less than the blank.

4.1.3 Inoculum

Inoculum COD measured at different times is shown in Figure 4.5. The detailed calculation steps for calculating COD from CHNS-concentrations are shown in Appendix C. We can see that the inoculum COD was decreasing from initial COD measurement at 31st January.

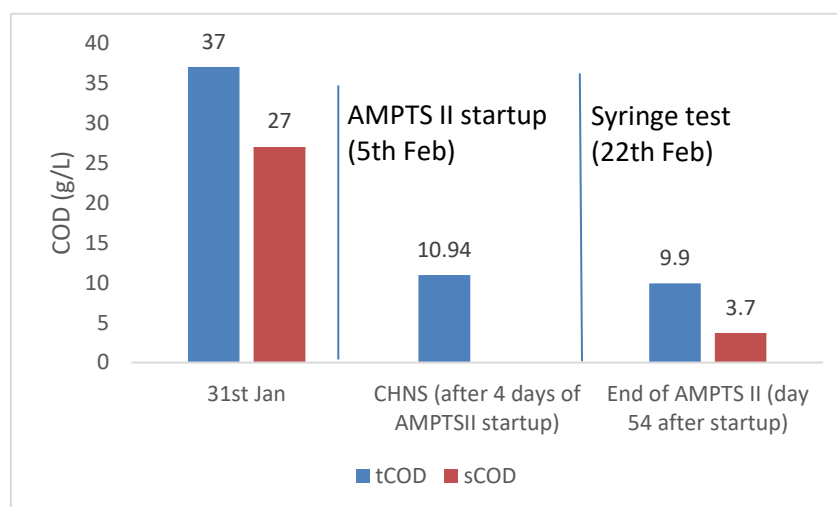


Figure 4.5 COD of inoculum over different time period and showing dates for startup of AMPTS II and syringe test.

4.1.4 AMPTS II using stored inoculum

Results from the batch test of APL and its co-digestion with HS using stored inoculum is presented in this sub-chapter.

- Methane production trend

Average of methane production rate of all the test are shown in Figure 4.6. Control-s (batch test of HS) showed methane production of 119 NmL \pm 3.8. Co-digestion of APL and HS (Co-

diegston-s) followed a similar trend as in Figure 4.1 and showed highest methane production for all the tests carried out, at $138 \text{ NmL} \pm 6$.

Batch test with higher load (APL2.4-s) initially produced biogas at the beginning but showed no methane production throughout the test after day 1. The final methane volume was $29 \text{ NmL} \pm 4$ which was 14 NmL lower than blank-s. Blank-s (only inoculum) showed gradually increase in methane volume after day 1.

Batch test with lower organic load of APL (APL1.2-s) followed the similar trend as blank-s and showed slow and gradual increase in methane production. The final methane volume settled at around $45 \text{ NmL} \pm 10.1$.

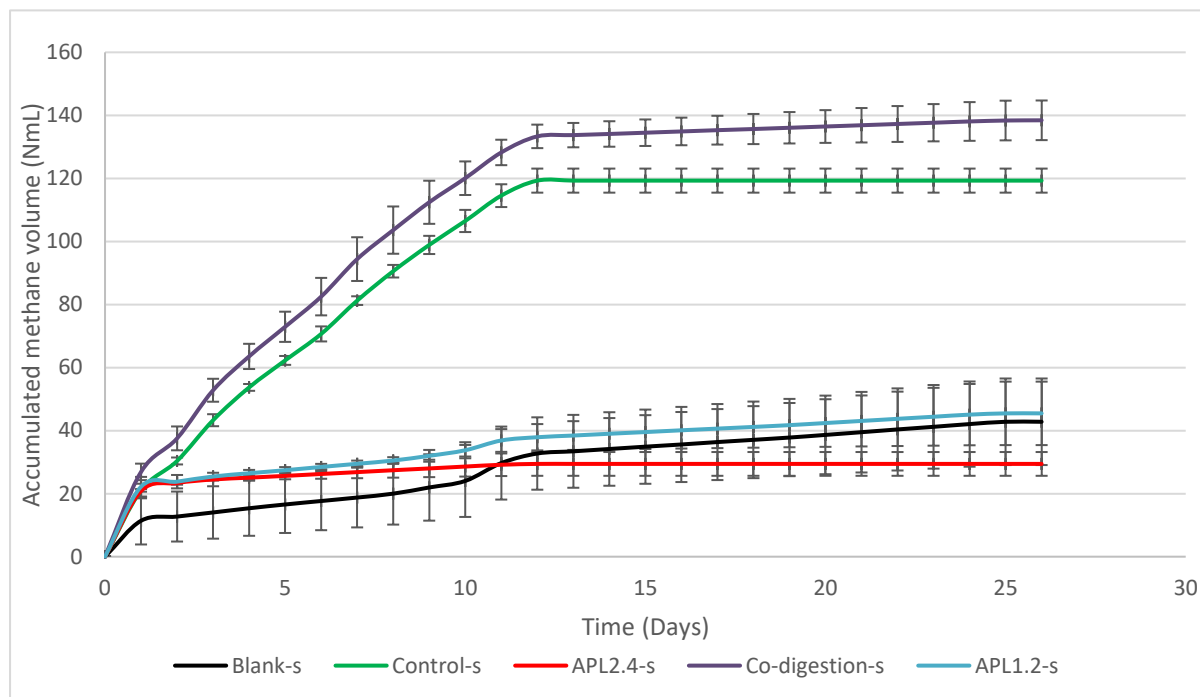


Figure 4.6 Accumulated methane formation during batch test of APL (APL1.2-s and APL2.4-s), HS (control-s) and co-digestion of APL and HS (Co-digestion) from AMPTS II using stored inoculum at different organic load referred as 1.2 and 2.4 at the end of text APL for organic load of 1.2 and 2.4 gCOD/L.

- Methane yield

Methane yield during batch test using stored inoculum using AMPTS II is shown in Figure 4.7. Similar to methane yield using fresh inoculum, batch test for HS (Control-s) was $160.9 \pm 8.9 \text{ NmL/gCOD}$. An improved methane yield was observed by co-digesting APL with HS. The final methane yield was $198.7 \pm 13.5 \text{ NmL/gCOD}$ which is 23 % higher than the control-s.

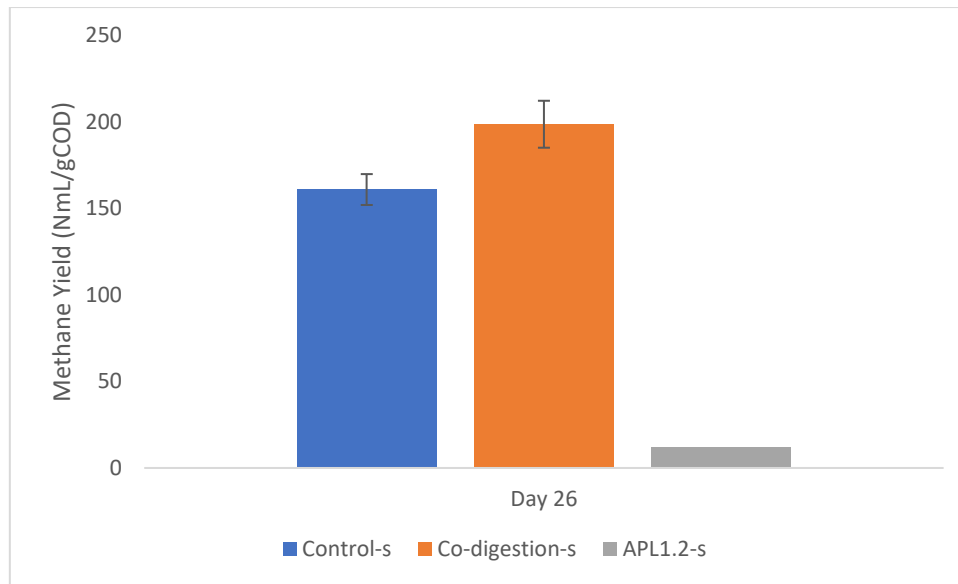


Figure 4.7 Calculated methane yield for batch test of APL, HS and Co-digestion of APL and HS using stored inoculum.

However, much lower methane yield was observed for APL1.2-s. Its final methane yield was 11.7 NmL/gCOD. Methane yield of APL2.4-s was not calculated as its methane production was lower than the blank-s.

4.2 Simulation result

This chapter presents the results from the simulation of different cases mentioned in chapter 3.4.3.

4.2.1 Simulation of Inoculum (Sim-1)

Simulation by modelling the inoculum with inputs mentioned in Table 3.13 is assessed in this subchapter. Simulated results were compared with experimental results from AMPTS II using fresh inoculum until 35 days, as the methane production remained almost the same after the mentioned time period. The simulated results showed a good agreement with the experimental results. The daily methane production rate and accumulated methane from simulation followed the same trend as in AMPTS II (Figure 4.8).

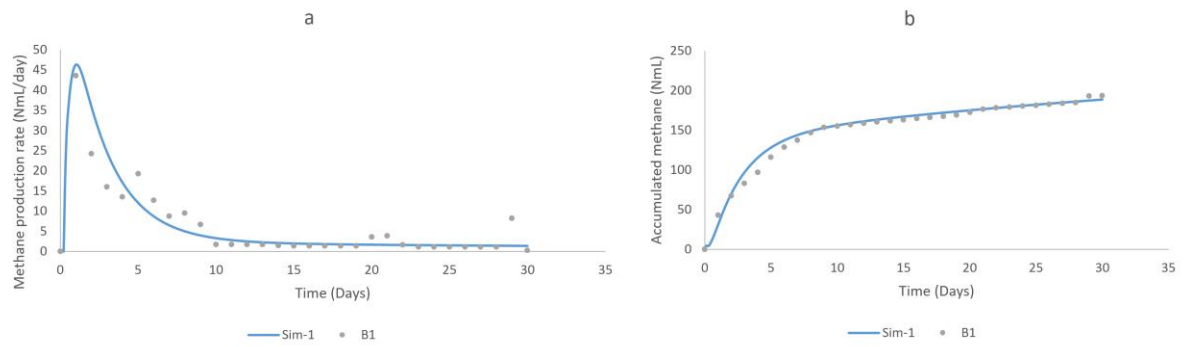


Figure 4.8 a: Simulated daily methane production rate for inoculum (Blank) and b: accumulated methane for inoculum compared with Blank-1 (B1) results from AMPTS II using fresh inoculum (dots)

The methane production starts to decrease after day 1 (Figure 4.8), indicating that all the substrate in the inoculum was used, which was also consistent with the reactor biomass simulation that showed decrease in biomass concentration after day 4, suggesting that the methane production after day 10 is due to endogenous decay (Figure 4.9). Even though the propionate degrader seems to be stable, the decay rate is very slow since we consider the decay of biomass in ADM1 first order. The decay rate increases with an increase in initial biomass concentration.

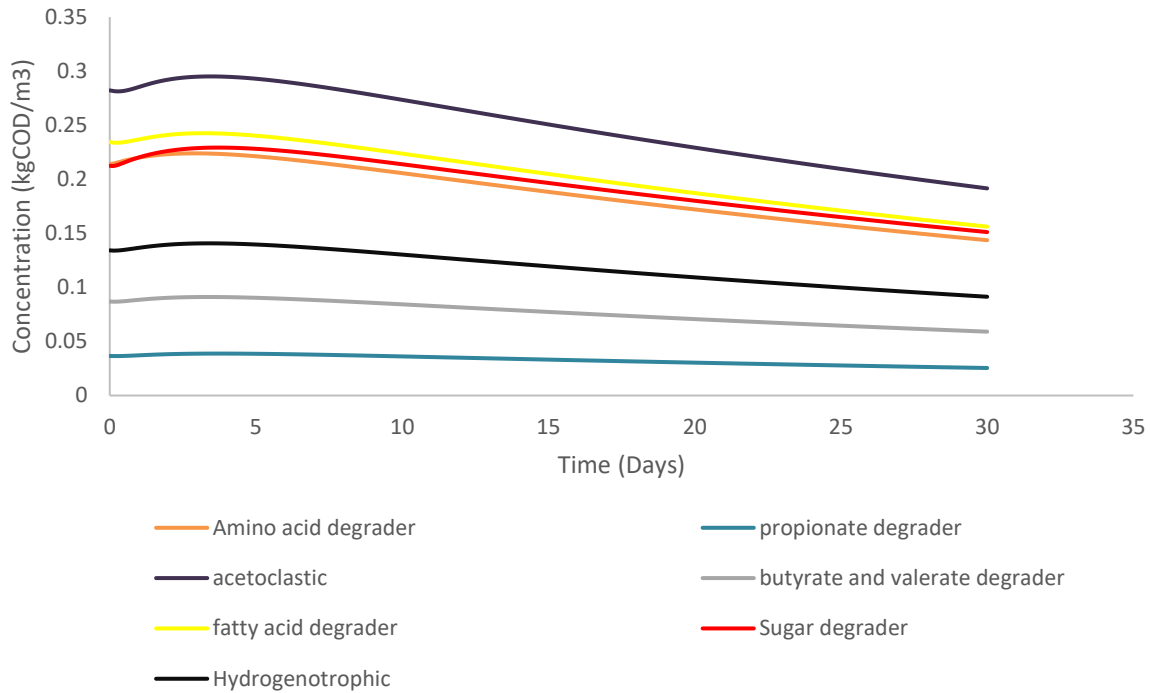


Figure 4.9 Simulated reactor biomass for inoculum for Simulation of inoculum.

Figure 4.10 b shows the inhibition by free ammonia on methanogens and simulated pH for the inoculum. Experimental data for pH is presented for day 35, but it was measured at day 56 (Figure 4.10 a). The simulated pH was lower than the experimental pH with a difference of 0.5.

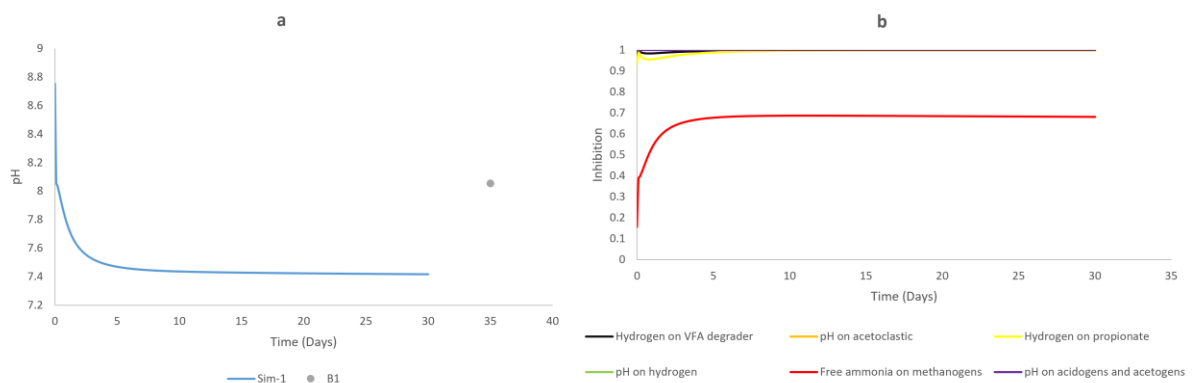


Figure 4.10 a: simulated pH for inoculum compared with experimental pH measurement of reactor Blank-1 represented as B1 from AMPTS II using fresh inoculum. b: simulated inhibition on inoculum (1=no inhibition and 0=complete inhibition)

4.2.2 Simulation of APL1.2

This subchapter presents the simulation from standard ADM1, Simulation case 2 (Simulation for APL 1.2 (Lower organic load of APL at 1.2 gCOD/L)), Simulation case 3 (Simulation of case 2 with change in concentration of phenol, furfural and HMF), simulation case 4 (Simulation of case 2 with changed inhibition constant for phenol, furfural and HMF), and Simulation case 5 (Simulation of case 2 with change in startup biomass concentration) and compared with experimental result (APL-1.2-3) from AMPTS II using fresh inoculum. Inputs for ADM1 were used from Table 3.13 (further inputs are provided in Appendix C) and includes input for blank (inoculum) as well.

4.2.2.1 Simulation of APL1.2 (Sim-2)

The simulation of APL1.2 (Sim-2) shows a good fit to the experimental results. In comparison, standard ADM1 showed nearly the same results as APL1.2 (Figure 4.11). Standard ADM1 showed slightly higher maximum methane production rate than Sim-2.

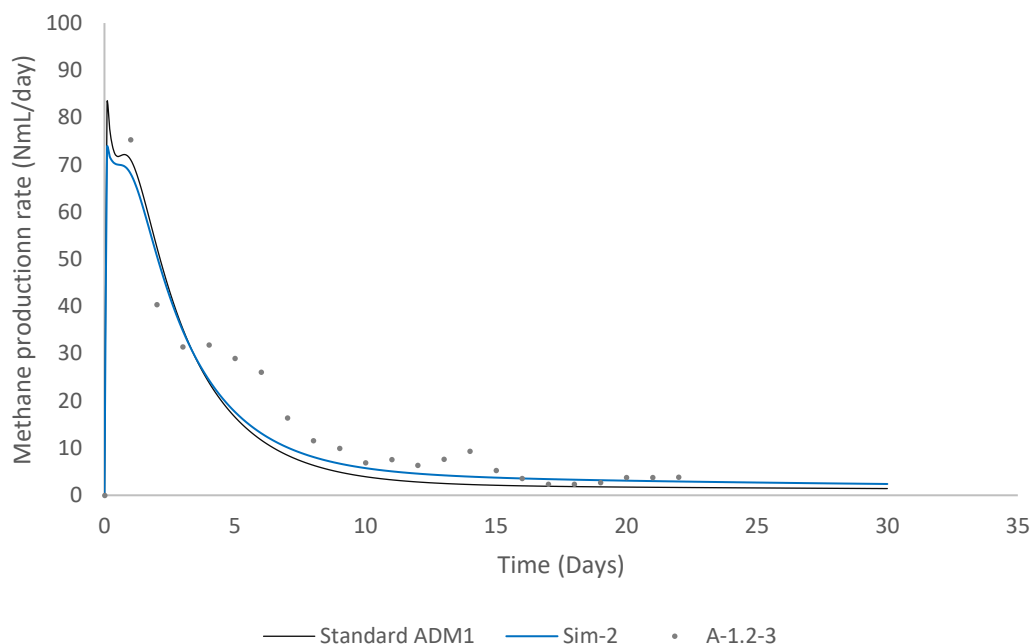


Figure 4.11 Simulated methane production rate of standard ADM1 (Black line) and Simulation of APL1.2 (blue line) compared with experimental results from AMPTS II using fresh inoculum (grey dots).

Similar inhibition from free ammonia on methanogens was observed for both Sim-2 and Sim-1 (Figure 4.12 a). However, with the extended model, inhibition from inhibitory compounds (phenol, furfural and HMF) was also observed at the beginning, decreasing gradually over a simulation period where nearly no inhibition was observed at the end (Figure 4.12 b). For a better understanding of the effects of inhibitory compounds, simulation results for different cases shown in results from here onwards would only show inhibition from inhibitory compounds as the inhibition from free ammonia would be same.

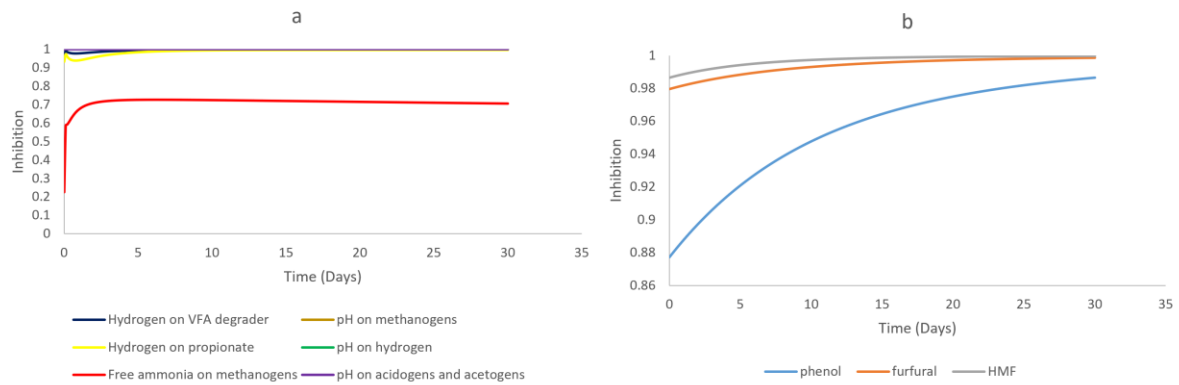


Figure 4.12 Simulated inhibition on methanogens a: inhibition by hydrogen, free ammonia and pH b: inhibition by phenol, furfural and HMF.

The decrease in inhibition from inhibitory compounds was due to the decrease in concentration overtime (Figure 4.13). We assumed that inhibitory compounds would be degraded by microorganism within the simulated time resulting in gradual decrease in inhibition by these compounds (Figure 4.12). With degradation of phenol, its intermittent product benzoate concentration increases which can be seen to decrease gradually after day 10. With decrease in these compounds gradually over time, acetate is produced which converts to methane which can be seen by observing (Figure 4.11) where at around day 10, methane production from extended model is little higher than standard ADM1 model.

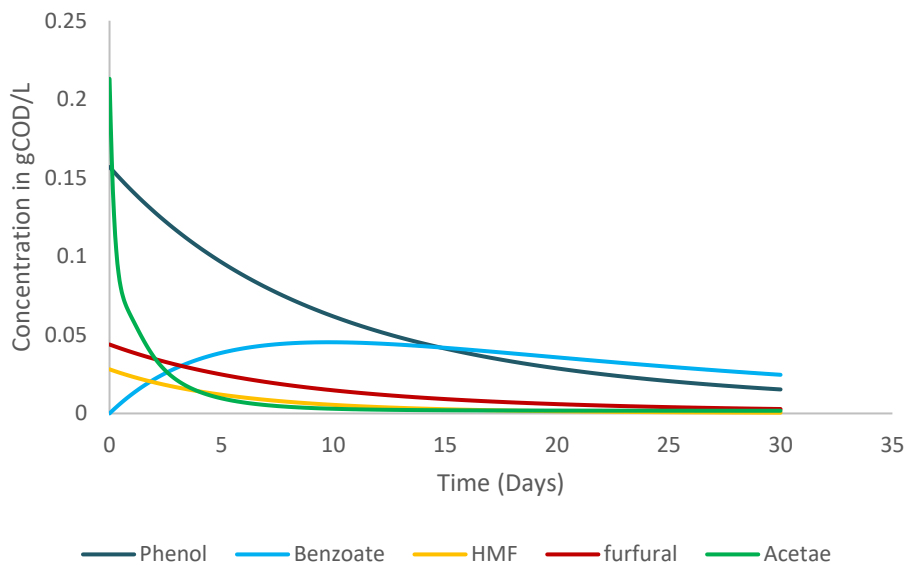


Figure 4.13 Concentration of phenol, furfural, HMF, benzoate and acetate in reactor during Sim-2 (Simulation of APL1.2)

4.2.2.2 Simulation of APL1.2 with change in concentration of inhibitory compounds (Sim-3)

Since the exact concentration of phenol, furfural and HMF was unknown for APL and were extracted from the literature review (Table 3.13), simulation was performed by changing the concentration to see its effect on daily methane production rate. The concentrations used in the simulations are listed in Table 4.1 and detailed inputs for ADM1 model in Aquasim are given

in Appendix C. Simulated results are compared with experimental data (APL-1.2-3) from AMPTS II using fresh inoculum.

Table 4.1 Different concentration for phenol, furfural and HMF used for Sim-3 and shows concentration of these compounds used in Sim-2

	SIM-2	SIM-3 a	SIM-3 b	SIM-3c
Phenol (g/L)	25	25	5	40
Furfural (g/L)	10	25	5	40
HMF (g/L)	7	25	5	40

The simulations performed with changed concentrations showed similar trend as Sim-2. However, by increasing the concentration of phenol, furfural and HMF (inhibitory compounds) in Sim-3c, a slight decrease in maximum methane production rate was observed (Figure 4.14) without showing any significant impact on the trend.

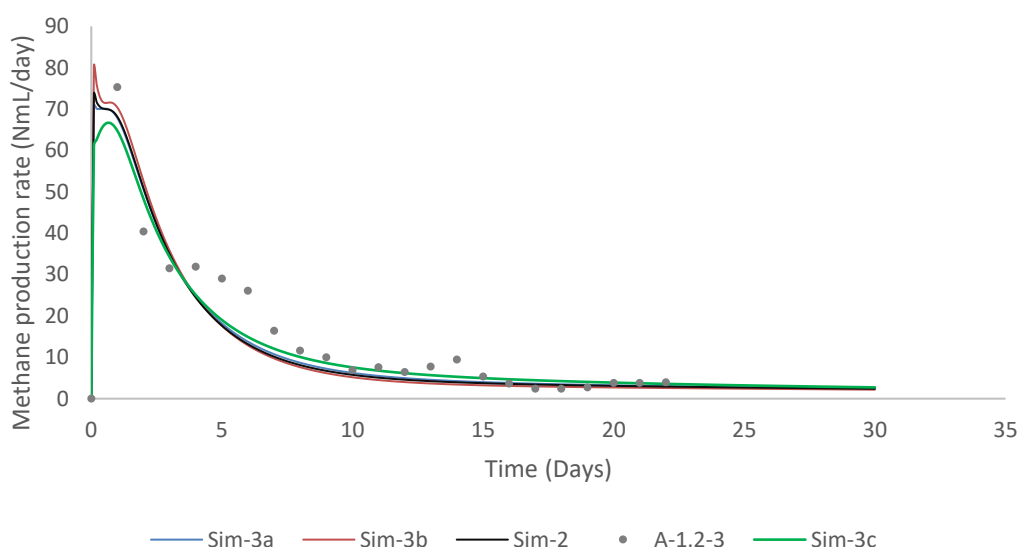


Figure 4.14 Simulated daily methane production at different concentration of inhibitory compounds (Sim-3a represented by blue line, Sim-3b represented by orange line, and Sim-3c represented by green line) along with Simulation of APL1.2 and experimental results from AMPTS II using fresh inoculum (dots).

The simulated results of the methane production rate depended on the inhibition of the methanogens. With increasing concentration of the modelled inhibitors, the inhibition also increased, as seen in Figure 4.15. However, higher inhibition was not observed for all the cases and inhibition increased by 0.05, 0.1 and 0.05 for furfural, phenol and HMF in Sim-3c when compared with Sim-2.

Inhibition by the inhibitory compounds are seen to be decreasing overtime gradually, as this simulation also assume inhibitory compounds decreases over simulated time period as in Sim-2.

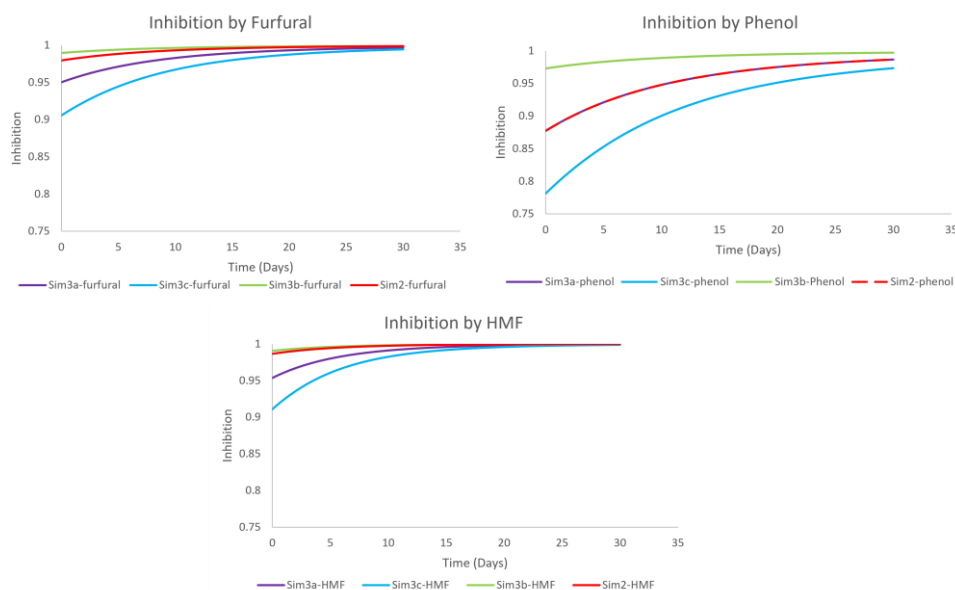


Figure 4.15 Simulated inhibition caused by furfural (top left), phenol (top right) and HMF (bottom) for Sim-3a (Purple line), Sim-3b (Green line), Sim-3c (Blue line) and Sim-2 (Red line) were the simulation carried out for varying concentration of inhibitors; Sim-3c had the highest concentration and Sim-3b had the lowest concentration.

4.2.2.3 Simulation of APL1.2 with change in inhibition constant (Sim-4)

Simulation (Sim-2) was re-simulated with changed inhibition constant (Table 4.2) to evaluate the effect on methane production rate.

Table 4.2 Inhibition constant used for Sim-4.

	SIM-2	SIM-4a	SIM-4b	SIM-4c
KI_fu (kgCOD/m ³)	2.105	0.842	0.2105	0.10525
KI_HMF (kgCOD/m ³)	2.05	0.82	0.205	0.1025
KI_phe (kgCOD/m ³)	1.12	0.448	0.112	0.056

Change in the trend of the methane production rate was observed by changing the inhibition constant of the compounds (Figure 4.16). Sim-4a showed a comparatively better fit than Sim-2, whereas Sim-4c, using the lowest inhibition constant, showed the highest deviation. Maximum methane production rate of Sim-4c was nearly half of Sim-2 and methane production rate was at a range of 40-30 NmL/day from day 1 to day 5 whereas other simulation cases reached a maximum peak and started to decrease gradually. Sim-4c indicated inhibition on methanogens was higher from day 1 to day 5 and inhibition decreased after day 5.

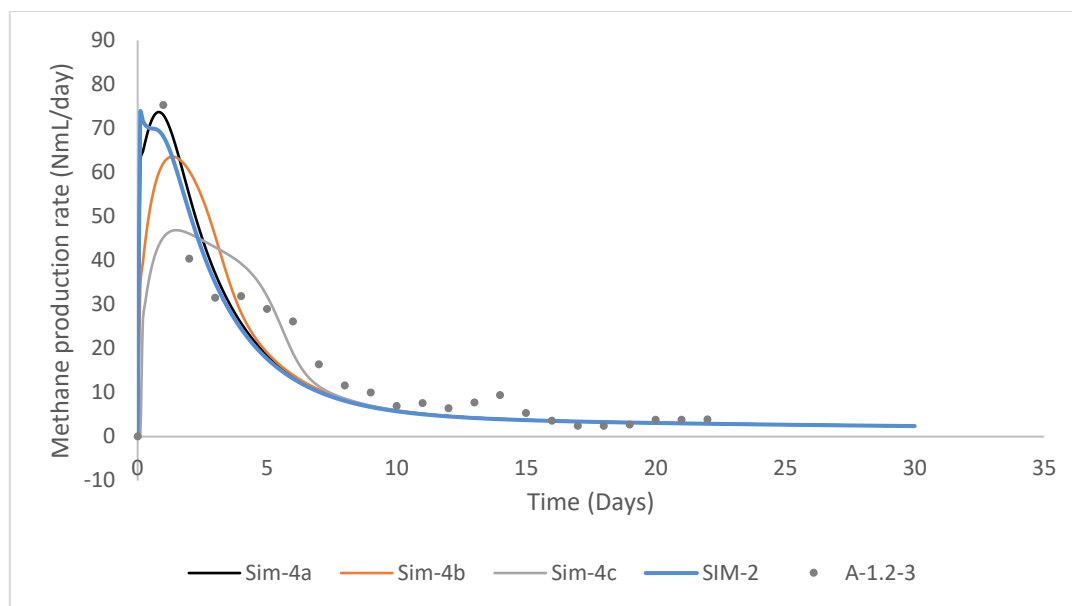


Figure 4.16 Simulated methane production rate with changed inhibition constant for phenol, furfural and HMF (Sim-4a, Sim-4b and Sim-4c) compared with Sim-2 and experimental results from AMPTS II using fresh inoculum (dots).

Similarly, by decreasing the inhibition constant for the compounds, the inhibition on methanogens also increased (Figure 4.17). Sim-4c showed high degree of inhibition on methanogens whereas the least was observed for Sim-2.

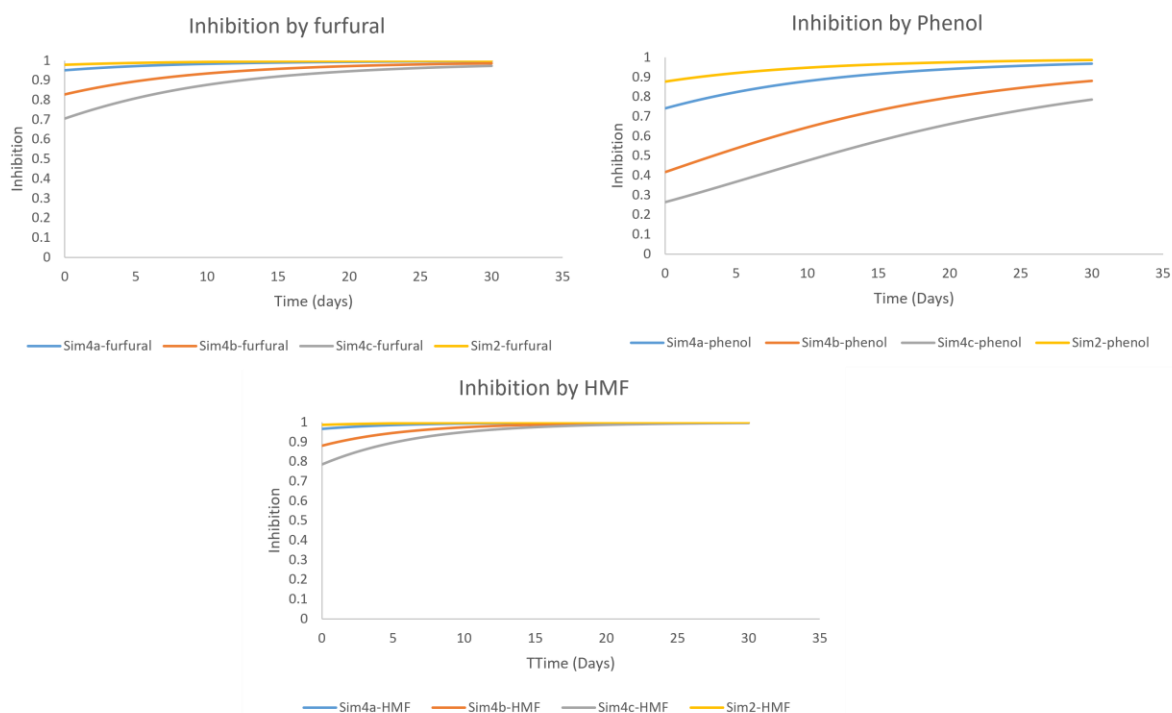


Figure 4.17 Simulated inhibition caused by furfural (top left), phenol (top right) and HMF (bottom) for Sim-4a (blue line), Sim-4b (orange line), Sim-4c (grey line) and Sim-2 represented by yellow line (simulation carried out using varying inhibition constant; Sim-4c had lowest inhibition constant and Sim-2 had highest inhibition constant).

4.2.2.4 Simulation of APL1.2 with low startup concentration of inhibitory compounds degrading biomass (Sim-5)

By reducing the startup concentration of biomass in the batch test for Sim-2, a comparatively better fit was observed (Figure 4.18) as the compounds degrade slowly. The maximum methane production rate was reached in day 1 and no initial methane formation was observed at the beginning.

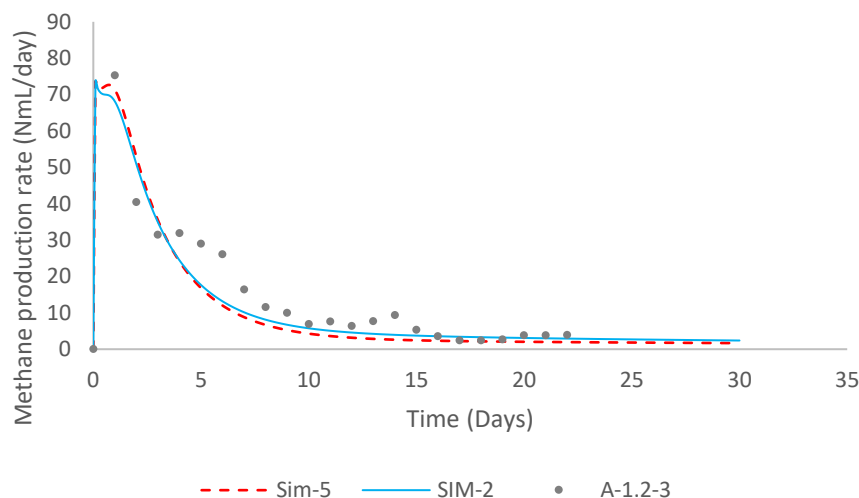


Figure 4.18 Simulated methane production with low degradation of the inhibitors (blue dashed line) and simulated methane production with nearly complete degradation (blue line). Experimental data is shown as grey dots.

Using the inputs for Sim-5, methanogens were inhibited more than in Sim-2 (I₄ in chapter 3.4.2.4). Overall inhibition on methanogens was higher and remained stable at around 0.62, however it decreased for Sim-2 because of degradation of inhibitory compounds.

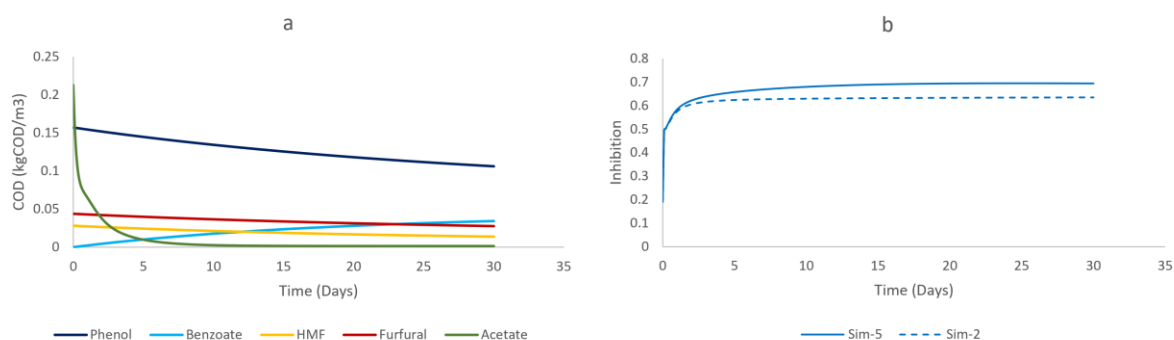


Figure 4.19 a: Simulated concentration of inhibitors (left) and b: simulated overall inhibition on methanogens (right) for lower degradation (sim-5) compared with Sim-2 (Simulation of APL1.2 with high startup concentration of inhibitory compounds degrading biomass).

4.2.3 Simulation of APL2.4

This subchapter presents the simulation from standard ADM1, Simulation case 6 (Simulation for APL 2.4 (higher organic load of APL at 2.4 gCOD/L)), Simulation case 7 (Simulation of case 6 with change in concentration of phenol, furfural and HMF), simulation 8 (Simulation of case 6 with changed inhibition constant for phenol, furfural and HMF), and Simulation case 9 (Simulation of case 8 with change in startup biomass concentration) and compared with

experimental result (APL-2.4-1) from AMPTS II using fresh inoculum. Inputs for ADM1 were used from Table 3.13 (further inputs are provided in Appendix C) and includes input for blank (inoculum) as well.

4.2.3.1 Simulation of APL2.4 (Sim-6)

Simulation of APL2.4 (chapter 3.4.4) showed poor agreement with the experimental results. Standard ADM1 poorly predicted methane production rate (Figure 4.20). Standard ADM1 and APL2.4 (Sim-6) predicted 77 NmL/day and 57 NmL/day more than the maximum methane produced during the experiment.

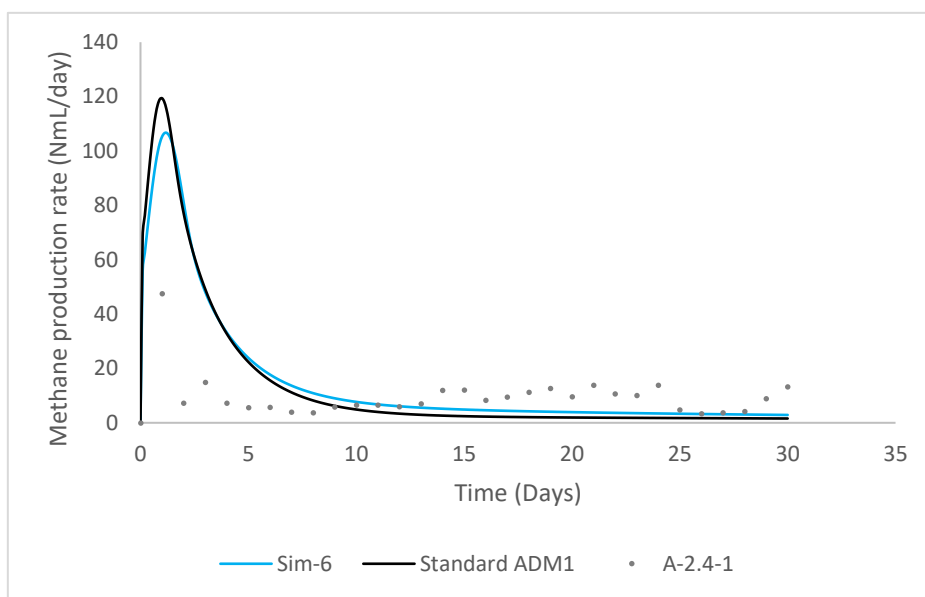


Figure 4.20 Simulated methane production rate for standard ADM1(Black line) and Simulation of APL2.4 represented as Sim-6 (Blue line) compared with experimental results from AMPTS II using fresh inoculum (gray dots).

The predicted pH was lower than the experimental results and the difference was around 0.6 (Figure 4.21). Lower inhibition was predicted by the implemented model which can also be validated from higher methane production rate for the simulated case.

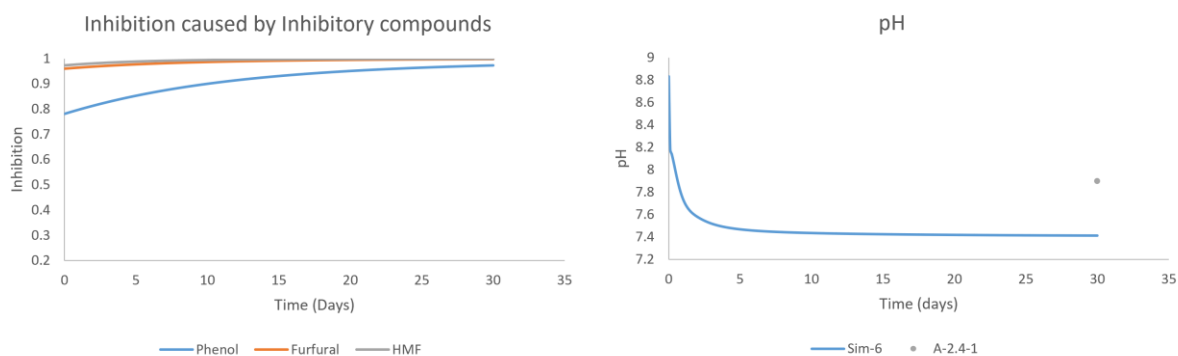


Figure 4.21 Predicted inhibition by inhibitory compounds (left) and simulated pH vs experimental pH (right).

The decrease in inhibition observed in Figure 4.21 can be explained by the decrease in concentration of those compounds. The concentration at the end of day 30 was low, thus there was little inhibition.

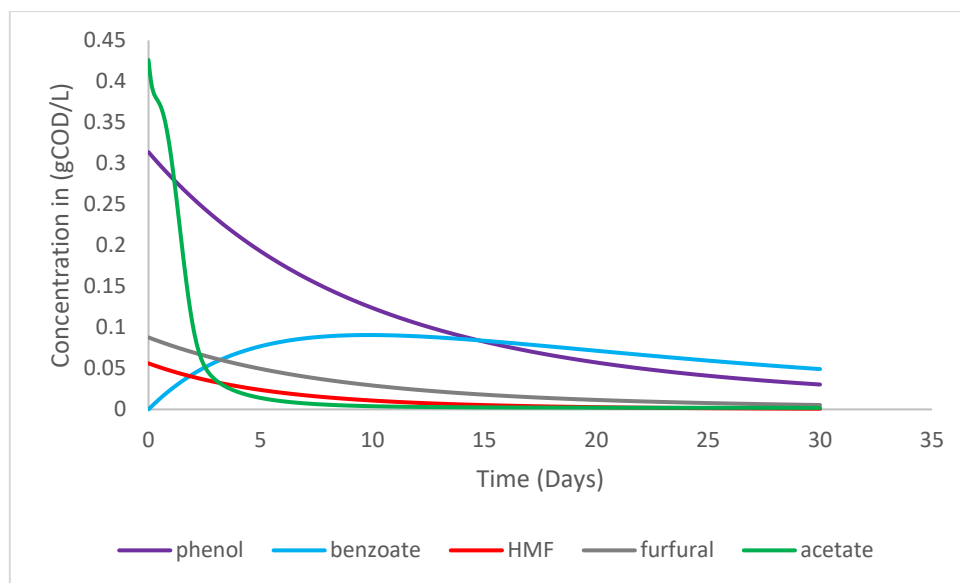


Figure 4.22 Concentration of inhibitory compounds and acetate (green line) during simulation of APL2.4 (Sim-6)

4.2.3.2 Simulation of APL2.4 with change in concentration of inhibitory compounds (Sim-7)

In the same manner as Sim-3 (simulation of APL1.2 with change in concentration of inhibitory compounds), the concentration of inhibitory compounds was changed (Sim-7). The detailed inputs for ADM1 are in Appendix C and concentration of inhibitory compounds used are in Table 4.3.

Table 4.3 Different concentration of inhibitory compounds used for Sim-7.

	SIM-6	SIM-7a	SIM-7b	SIM-7c
Phenol (g/L)	25	25	5	40
Furfural (g/L)	10	25	5	40
HMF (g/L)	7	25	5	40

The simulations showed an increase in maximum methane production rate for Sim-7b whereas the lowest maximum methane production rate was observed for Sim-7c. Sim-7a showed a slight decrease compared to Sim-6. The attributed maximum methane production rate for Sim-7b was due to an increase in X_C as the rest of unknown COD was presented as composite particulate (Appendix C). The effect of changing concentration of inhibitors and the use of X_C was much more prominent in Sim-7 than Sim-3.

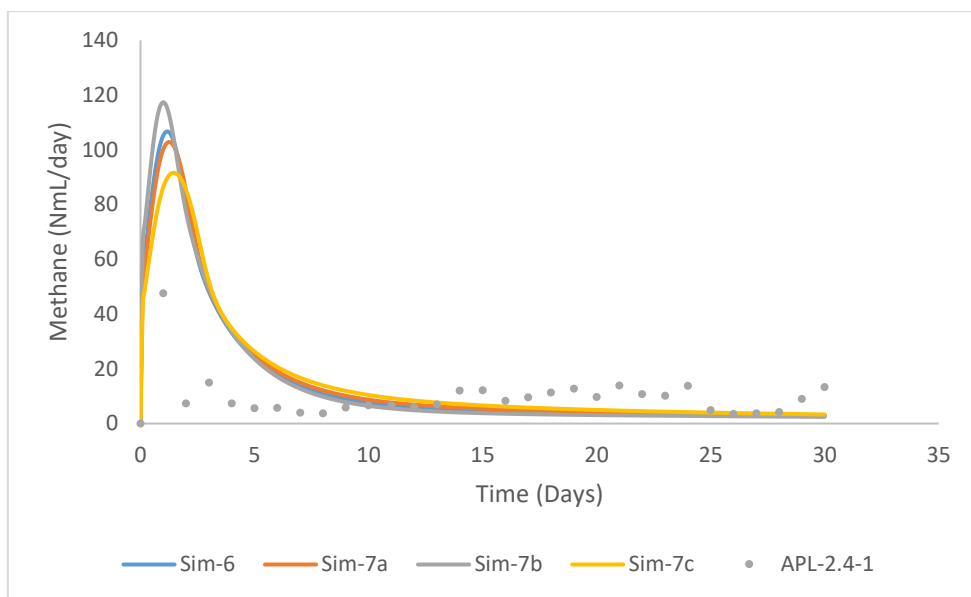


Figure 4.23 Comparison of methane production rate by changing the concentration of inhibitors.

The inhibition by these compounds also increases with increasing the concentration, in order of Sim-7c>Sim-7a>Sim-6>Sim-7b (Figure 4.24), Sim-7c using the highest inhibitors concentration and Sim-7b using the lowest, can be seen in methane production rate in Figure 4.23. The inhibition from phenol was the same for Sim-6 and Sim-7a as both simulations had same concentration of phenol.

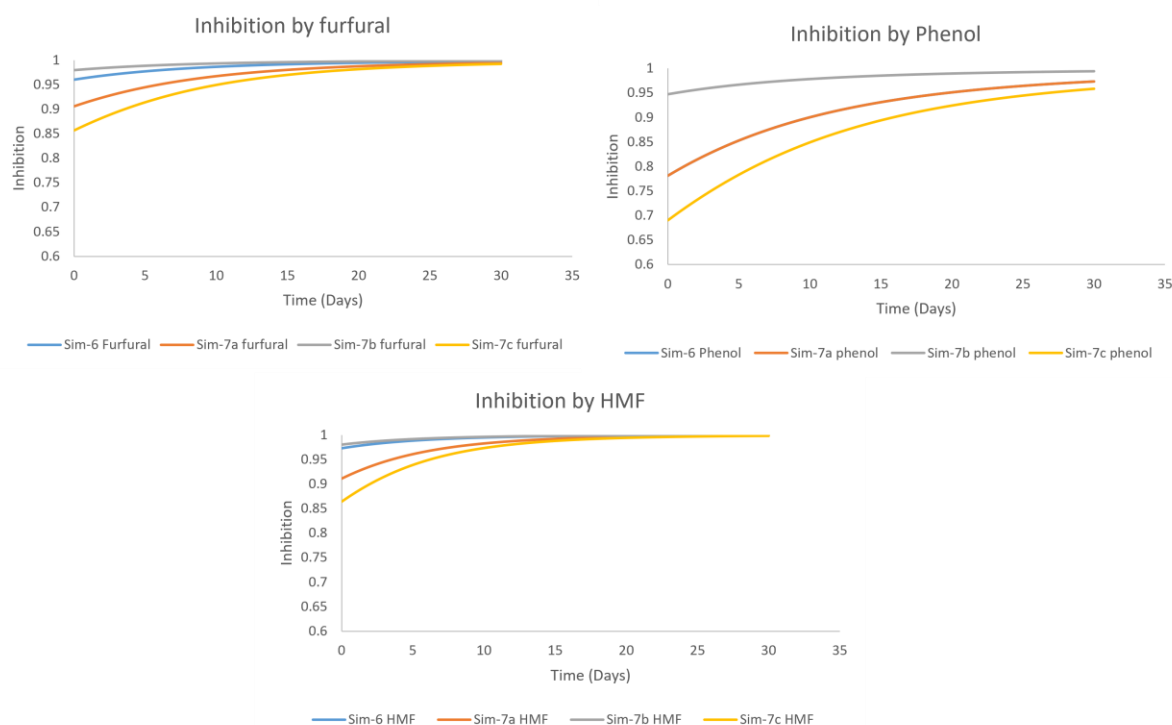


Figure 4.24 Simulated inhibition by furfural (top left), phenol (top right), and HMF (bottom) for Sim-6, Sim-7a, Sim-7b and Sim-7c (simulations carried out varying concentration of inhibitors; Sim-7c with high concentration, and Sim-7b using low concentration).

4.2.3.3 Simulation of APL2.4 with change in inhibition constant (Sim-8)

In the same manner as for Sim-4, Sim-6 was varied by changing the inhibition constant only. The changed inhibition constant with simulation number is shown in Table 4.4 .

Table 4.4 Changed inhibition constant for Simulation 7.

	SIM-6	SIM-8a	SIM-8b	SIM-8c
KI_fu (kgCOD/m ³)	2.105	0.842	0.2105	0.10525
KI_HMF(kgCOD/m ³)	2.05	0.82	0.205	0.1025
KI_phe (kgCOD/m ³)	1.12	0.448	0.112	0.056

By decreasing the inhibition constant for the inhibitory compounds, we observe change in the trend of methane production rate, Figure 4.25. Maximum methane production rate decreased drastically. Sim-8c showed the highest inhibition as it had the lowest inhibition constant and the predicted value was even lower than the maximum methane production rate found in experiments.

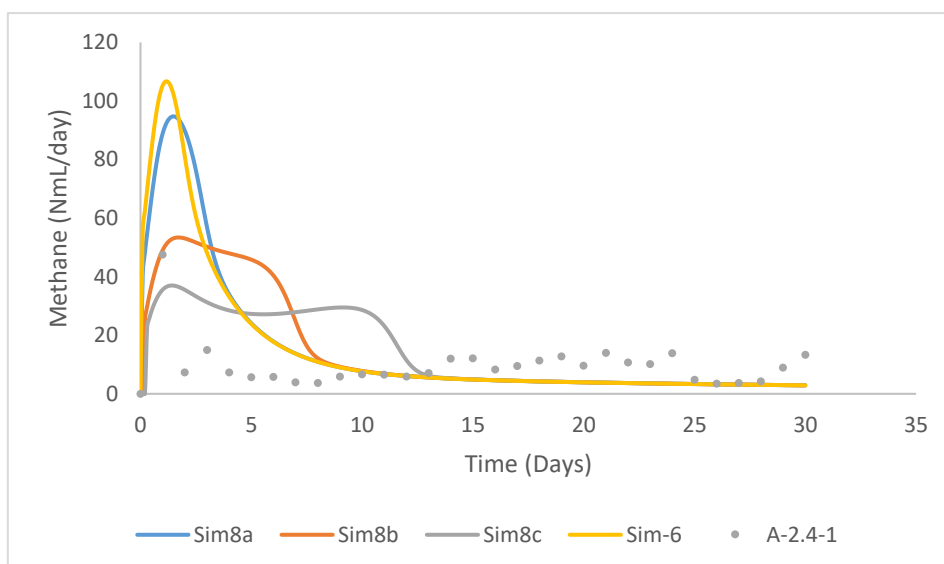


Figure 4.25 Methane production rate for changed inhibition constant in Sim-8a (blue line), Sim-8b (orange line), Sim-8c (grey line) compared with Sim-6 (yellow line) and experimental results from AMPTS II using fresh inoculum (grey dots).

Decreased methane production was primarily influenced by increased inhibition which we see in Figure 4.26. Phenol inhibits more than furfural and HMF, because of the higher concentration and lower inhibition constant used for phenol.

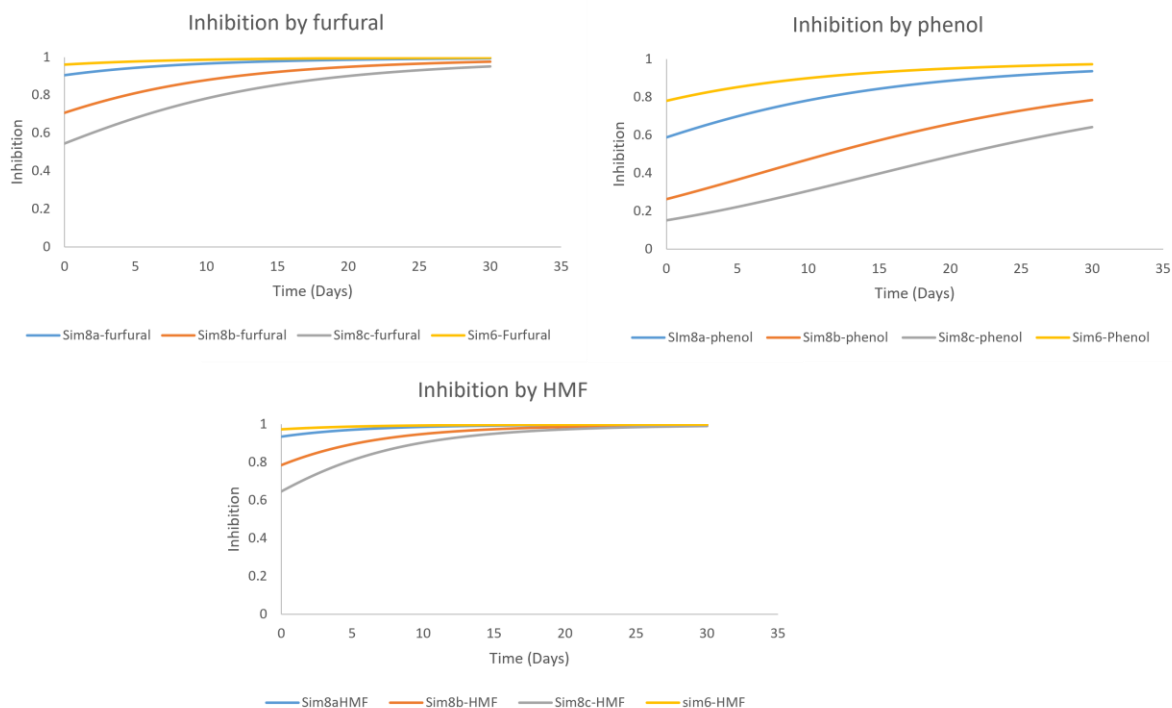


Figure 4.26 Simulated inhibition by Furfural (top right), Phenol (top right), and HMF (bottom) for Sim-8a (blue line), Sim-8b (orange line), Sim-8c(grey line)) and Sim-6 (yellow line) for change in inhibition constant; Sim-8c having lowest and Sim-6 having highest inhibition constant value.

4.2.3.4 Simulation of APL2.4 with low startup concentration of inhibitory compounds degrading biomass (Sim-9)

Simulation case 8a, 8b and 8c were further simulated to see the effect of degradation of inhibitory compounds. For running the simulation, X_{ini_in} was changed to 0.1 in order to see the effects of low startup concentration of biomass. Simulated cases with changed parameters were presented as Sim-9a, Sim-9b and Sim-9c respectively.

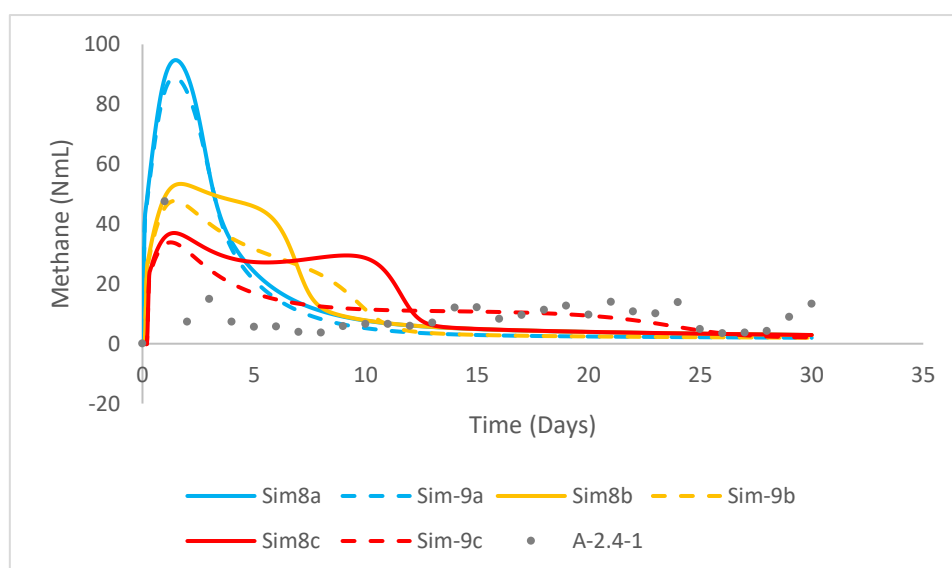


Figure 4.27 Simulated methane production rate with change in startup concentration of biomass which degrades inhibitory compounds. Simulated cases with mentioned changes

(Sim-9a, Sim-9b and Sim-9c) are presented in dotted line whereas their respective simulation with higher startup concentration is presented as line

Change in daily methane production rate was observed for simulated cases (Figure 4.27). Simulation showed comparatively lower methane production rate. Simulated case Sim-9c showed lower methane production rate for longer period of time and followed the trend of the experimental results. The decrease in methane production rate can be explained by increase in inhibition by methanogens for longer duration of time (Figure 4.28).

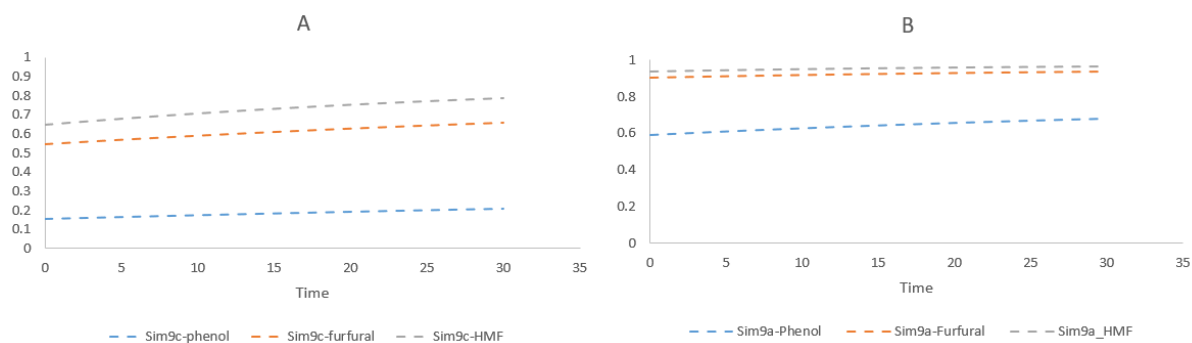


Figure 4.28 A: Inhibition on methanogens due to phenol, furfural and HMF during Sim-9c B: Inhibition on methanogens due to phenol, furfural and HMF during Sim-9a

Further, looking into the concentration of inhibitory compounds along with acetate, it can be seen that higher concentration of acetate accumulation can be seen until day 5 after which it starts to decrease gradually (Figure 4.29). It can also be seen in the Figure 4.27 where, methane is produced gradually until day 20 and starts to decrease.

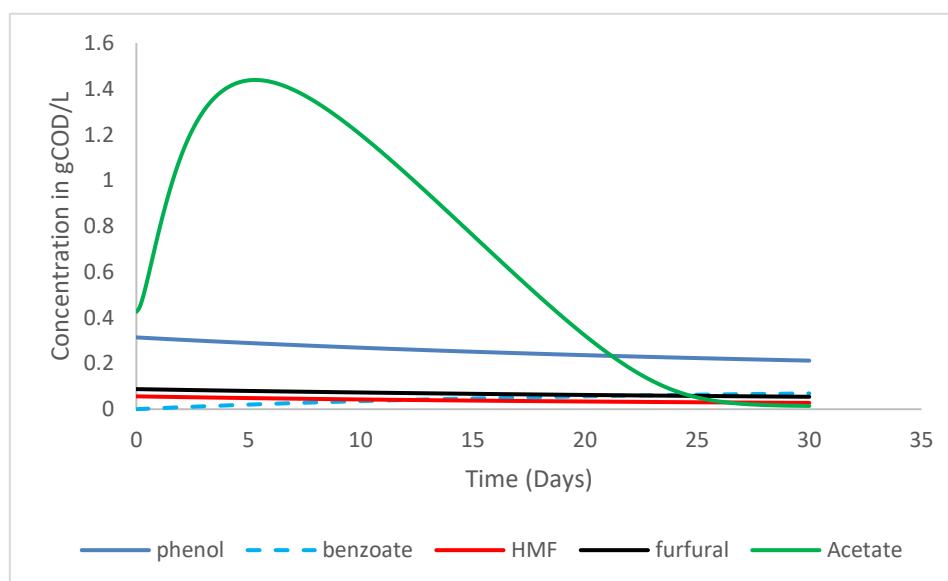


Figure 4.29 Concentration of inhibitory compounds present in reactor during Sim-9c

Acetate conversion seen in Figure 4.29 was mainly due to acetoclastic methanogens as seen in Figure 4.30. It can be observed that the acetoclastic methanogens were growing slowly over the simulation period.

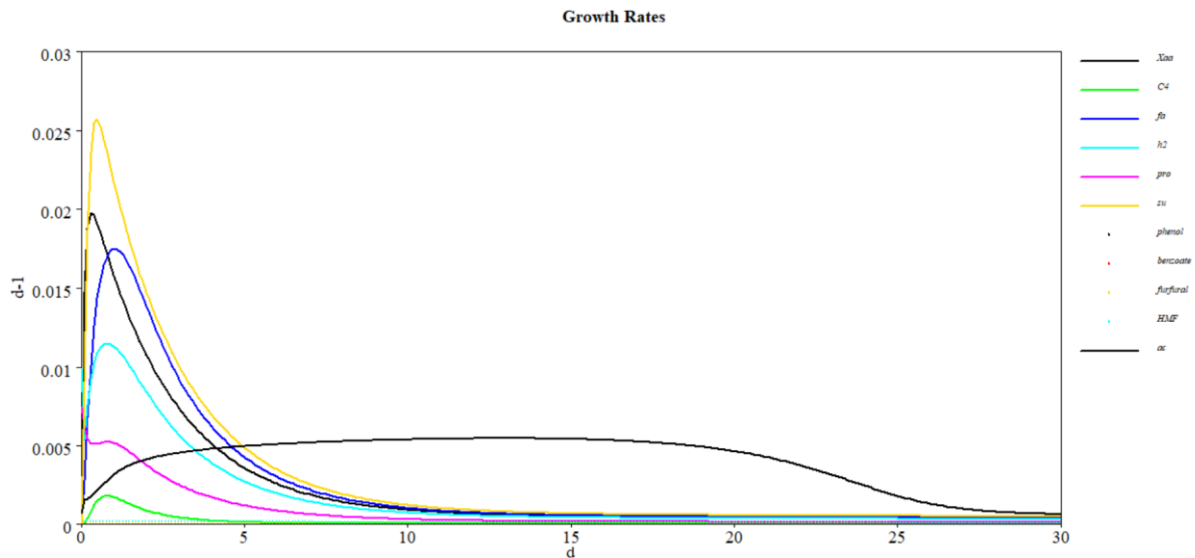


Figure 4.30 Growth rate of different microorganism present in reactor during simulation of sim-9c (APL2.4 with low startup concentration of biomass and lowest inhibition constant) where acetoclastic methanogens are represented by ac (black line)

4.2.4 Comparative simulation using Monod and Haldane growth kinetics

To better understand the kinetics to be used in the simulation, Monod type growth kinetics used in Sim-8 (APL2.4) for inhibitory compounds was changed to Haldane growth kinetics (equation 2.3). However, limited information is available for inhibition constant (K_i) in Haldane equation used for determining the growth limiting concentration of biomass degrading inhibitory compounds. Thus, as per recommendation from a author, K_i inhibitory concentration for methanogens from particular compounds is used as K_i growth limiting concentration of that particular inhibitory compound degrading microorganism. Details of Haldane equation used with K_i is presented in Table 4.5.

Table 4.5 Haldane equation implementation in ADM1

Compounds	Haldane type growth kinetics used	K_i value used
Phenol	$\mu = \mu_{max} \frac{S_{phenol}}{k_s + S_{phenol} + \frac{S_{phenol}^2}{k_i}}$	$k_i = Ki_{ac_phe}$ Or Ki_phe used in Sim-8
HMF	$\mu = \mu_{max} \frac{S_{HMF}}{k_s + S_{HMF} + \frac{S_{HMF}^2}{k_i}}$	$k_i = Ki_{ac_HMF}$ Or Ki_HMF used in Sim-8
Furfural	$\mu = \mu_{max} \frac{S_{furfural}}{k_s + S_{furfural} + \frac{S_{furfural}^2}{k_i}}$	$k_i = Ki_{ac_fu}$ Or Ki_fu used in Sim-8

As in Sim-8, K_i value for furfural, HMF and phenol was changed and its value are presented in Table 4.6. K_i value used in Sim-8a and Sim-10a are same to understand the effect of using different type of kinetics equation. Similarly, Sim10-b and Sim-10c uses same K_i value as used in Sim-8b and Sim-8c.

Table 4.6 Variation of Ki value in Haldane equation

	Sim-6	Sim-10a	Sim-10b	Sim-10c
KI_fu (kgCOD/m ³)	2.105	0.842	0.2105	0.10525
KI_HMF(kgCOD/m ³)	2.05	0.82	0.205	0.1025
KI_phe (kgCOD/m ³)	1.12	0.448	0.112	0.056

By changing the Monod type growth kinetics to Haldane, nearly similar methane production rate was observed showing no effect on it (Figure 4.31). Even, by using higher inhibition constant for Sim-10c, methane production rate was same as Sim-8c which used Monod-type growth kinetics.

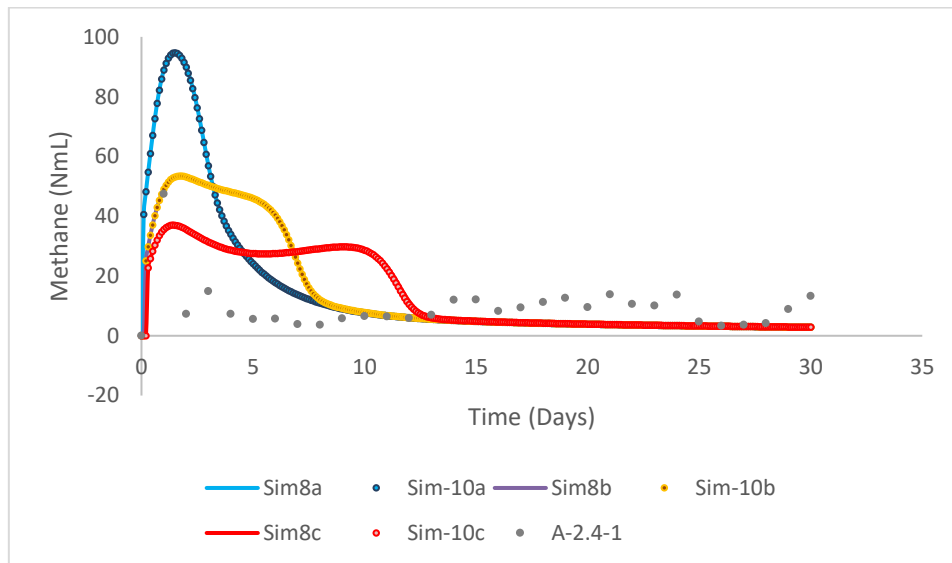


Figure 4.31 Methane production rate by using Monod equation (solid line) vs methane production rate by using Haldane equation (dotted line) for different values of inhibition constant

5 Discussion

5.1 Co-digestion of APL and HS

The results obtained from the experiments explained in chapter 4.1.1 showed increase in methane yield during co-digestion of APL and HS. The methane yield increased by 8% and 15% for parallels and higher than the digestion of HS (Control) only. Similarly, Yu previously reported that addition of APL during co-digestion of swine manure increased the methane yield. They also reported an optimum concentration of APL to add – this increased methane yield by 23% during co-digestion and the highest concentration inhibited the methane production [10]. The authors suggested that the addition of APL improved the methanogenic activity [10].

Constituents of APL have also shown similar results. Experiments conducted with addition of low concentration of furfural during sodium acetate digestion have shown to increase the methane yield [40], [41]. Similar results were also obtained by adding low concentrations of HMF [40], [41].

Researchers have pointed out that trace elements present in APL could enhance the microorganisms resistance towards TAN [10], while some have suggested that the constituents of APL at low strength acts as an additional carbon source enhancing methanogenesis [41]. Decisive conclusions on actual mechanisms are not known to date and the improvements on methanogenesis has only been shown experimentally. Thus, the topic needs further research to shed light on the underlying mechanism which stimulate the microbial community.

5.2 Effect of OL on methane yield from APL

Syringe tests are manual tests which always have a possibility of error that could propagate throughout the test period. Even though all sources of error previously found [61] were considered during the experiment, results from the syringe test would only be used for verification of the trend observed in AMPTS II with fresh inoculum and to have brief idea of the effect of different OL.

A decrease in methane production is observed by increasing the OL of APL for both the AMPTS II test and the syringe test. APL during syringe batch test at concentration up to 1 gCOD/L had no significant impact on methane production whereas 2 and 3 gCOD/L inhibited the methane production process (Figure 4.3). Seyedi et al. also found that higher concentration of APL (2 gCOD/L and 4 gCOD/L) inhibited methane production [9].

5.2.1 Effect of higher OL in batch tests

The longer lag phase we experienced during the higher loading of APL 2.4 (Figure 4.1) could be possible because of inhibition towards the methanogens and a shift in the microbial community as the pH of the reactors were stable at range of 8.02-8.18 (chapter 4.1.1) indicating there was no sharp decrease in pH which would inhibit the anaerobic digestion process. For the batch tests with higher load of APL, Zhou reported a major shift in microbial community from acetoclastic methanogens to hydrogenotrophic methanogens [27]. Hydrogenotrophic methanogens along with syntrophic acetate oxidizing bacteria (SAOB) were also abundant during co-digestion of higher concentration of APL with swine manure [10]. This indicates a complete shift in microbial community both during anaerobic digestion of APL with co-

substrate and with APL only. Both SAOB and hydrogenotrophic methanogens are known for slow metabolic processes and methane yield is comparatively low [36]. This could be a probable reason behind the low methane yield during the batch test of APL2.4 in AMPTS II (chapter 4.1.1).

This can also be verified through the biogas composition from the syringe test (Figure 4.4), where it showed that APL3 had very low methane content, which indicates that methanogenesis had not started yet. However, APL2 showed higher methane content indicating that methanogenesis started at day 24, similar to APL2.4 from AMPTSII (Figure 4.1) where the detector recorded methane from day 25.

5.2.2 Effect of lower OL on batch test

Methane yield from APL1.2 was unexpectedly higher than the theoretical methane yield. One of parallel showed 579 NmL/gCOD. One of possible reason could be from the unaccounted methane production from inoculum itself by addition of APL. Inoculum used during the experiment was effluent from the reactor and even after 5 days of degassing, it still had some COD which led to production of methane gas during initial days as seen in chapter 4.2.1. As discussed in chapter 5.1, APL are known to increase the methanogenesis rate during co-digestion. Furthermore, CHNS analysis carried out (Chapter 4.1.3) helped in calculating the C/N molar ratio to be 7.43 for inoculum (Appendix C) and APL are known to have high C/N ratio[16]. There could be possible inhibition by high nitrogen content in inoculum itself during the test (Blank) and addition of APL acted as additional carbon source, thus producing methane (which was unaccounted during Blank/inoculum). As, it is difficult to pin-point on one possible cause, parallel of APL1.2 showing higher yield was not used for simulations purpose. Furthermore, simulation showed inhibition from free ammonia (product of TAN disassociation) by addition of APL slightly reduced the inhibition by free ammonia when compared with inoculum only. The difference was not huge; hence, it was hard to conclude the C/N ratio resulted in higher methane yield for the parallel.

Even though, higher methane yield was observed for one of the parallels of APL1.2 (chapter 4.1.1) similar trend of biogas production was seen for APL1 during syringe test which was performed after 18 days of startup of AMPTS II (chapter 4.1.2). Batch test of blank during syringe test showed gradual increase in biogas production indicating methane produced was due to endogenous decay. Each test reveals that APL with OL upto 1 gCOD/L shows the similar trend and produces methane. Methane yield for APL1.2 from syringe test and AMPTS II was 343 NmL/gCOD and 230 NmL/gCOD, thus, it is not decisive to conclude methane yield for APL1.2.

5.3 Effect of inoculum storage on methane yield during batch test of APL

Co-digestion of APL and HS and digestion of HS (control) was little affected by storage of inoculum, which was stored for 54 days. Final methane yield of Co-digestion of HS and APL was 198.7 NmL/gCOD which is 23% higher than the Control. Studies found that storage at lower temperature would induce longer lag phase whereas inoculum stored at ambient temperature till 1 month showed no effect on final methane production [32]. HS is readily degradable substrate and neither lag phase nor decrease in methane yield was observed and final methane yield was as nearly same as test carried out using fresh inoculum (156.2 NmL/gCOD) and 160.9 NmL/gCOD using stored inoculum. Co-digestion of APL and HS

(20:80 on COD basis) showed increased in methane yield (discussed in chapter 5.1) which further supports the improved methane yield by addition of APL as a co-substrate.

However, significant difference was observed for both APL1.2 and APL2.4 during batch test using AMPTS II using stored inoculum. Lower methane production was the noticeable change (Figure 4.6). Change in microbial community and relatively fewer microorganism might be reason for reduced methane production during test. It was found that relative abundance of specific organism and overall community composition changed after 2 months of storage [31]. APL contains wide range of compounds which are still unidentified, thus, diverse group of microorganisms could speed up the degradation process [16].

5.4 Possible overcome of inhibition and microbial adaption

Numerous studies have been carried out to overcome possible inhibition during anaerobic digestion of APL using different methods such as over liming (addition of lime in APL), using activated carbon and air stripping. One of study found that over liming was much more effective for removing the inhibitory compounds than rest of method and improves the biogas production[27]. While use of biochar produced during pyrolysis contradicts as some suggest its use enhanced the methane yield [16] while some showed no impact on methane yield with its addition [26], [27] .

Another major method for enhancing the possible yield from the APL could be through possible microbial adaption. It was previously found that adaption of microbial community to APL for extensive time period increases the methane yield (Chapter 2.7). It has also been reported that adapted microbial community could also sustain higher concentration of phenolic compounds without showing significant inhibition [38].

Nevertheless, it can be said that to some extent use of overliming to reduce the concentration of inhibitory compounds and use of adapted microbial community could enhance the methane yield and increases its capacity to tolerate the APL.

5.5 Comparison of Standard ADM1 model and Extended model

Standard ADM1 was designed with specific purpose for application of AD process and has options to extend its existing model to fit best for different substrate. However, it is not a best idea to use it for complex substrate and needs modification. Presence of limited option for degradation process, inhibition kinetics and necessity to use unknown compounds in APL as X_C (Composite particulates), acts as a constraint. Standard ADM1 model used for both cases (APL1.2 and APL2.4) showed high methane production rate during initial days of simulation which was in some agreement with APL1.2, however, completely predicted wrong for APL2.4. Thus, standard ADM1 limits its possibility of simulating for cases of APL with high OL without modification.

On other hand, modifications made in ADM1 (extended model) also did not show proper agreement with experimental results initially, however, it showed the flexibility towards changing various parameters of APL to show good agreement with experimental results.

5.6 Necessity for properly defining the APL during simulation

Little information about the constituent of APL was known for performing the simulation. Exact concentration of compounds present in APL were unknown. Due to limitation of equipment available for detecting these compounds and complexity during measurement,

concentration of inhibitory compounds implemented in extended ADM1 had to be used from the literature review. Still, limited information was available on literature regarding constituents of APL during pyrolysis at higher temperature.

Simulation using extended model, specially APL1.2 (Figure 4.14) showed little effect of changing the concentration of inhibitory compounds. With minimum concentration of inhibitory compounds used (Sim-3b), its inhibition towards the methanogens reduced, thus increasing the methane production rate. Even, higher concentration of inhibitory compounds used (Sim-3c) showed little effect on methane production rate and would not induce huge inhibition (Figure 4.15). Hence, indicating minimum effect of change in concentration can be seen in APL1.2 as OL and volume of APL used were low.

However, its effect during simulation of APL2.4 (Figure 4.23) was higher. High OL and high concentration of these compounds resulted in high inhibition (Figure 4.24) which can be translate into a low methane production rate in Sim-7c.

Possibility of such concentration of these compounds used in both Sim-3c and Sim-7c is minimum. So far, in literature review, no information regarding such high concentration of these compounds were observed. But, exact concentration of these compounds would increase the predictability of model for simulating APL with higher OL.

5.7 Effect of inhibition constant (Ki)

Methane production rate was highly sensitive towards inhibition constant. With change in inhibition constant, higher degree of inhibition was observed for both simulations carried out (APL1.2 and APL2.4).

Even though, lowest inhibition constant showed better fit to experimental result (Sim-8b and Sim-8c) for APL2.4, it might not be good to use these inhibition constants for phenol, furfural and HMF. Inhibition constant value for HMF and furfural were obtained from the previous research work and thus, those value are used for showing the effect of inhibition constant on methane production rate.

However, for phenols, as mentioned in chapter 3.4.4, concentration of phenolic compounds (as phenol) was used along with kinetics and inhibition constant for phenol during the simulation. But, it would be much more accurate to evaluate simulation using the inhibition caused by mixture of phenolic compounds. However, there is limited information on inhibition constant by mixture of phenolic compounds. Thus, simulations were performed using the inhibition constant of phenol only. Looking at the inhibition constant of several phenolic compounds, they have even lower inhibition constant such as p-cresol (380 mg/L) and 3,4-dimethylphenol (320 mg/L) which are all known to be present in APL [9]. Hence, there is probability that inhibition could be low or even lower than simulated in Sim-8 (0.448 gCOD/L) if inhibition caused by phenolic mixture is to be considered.

Use of low inhibition constant in simulation of APL2.4 resulted in higher inhibition and lower methane production rate. The methane produced was mainly from the acetoclastic methanogens. However, as described in chapter 5.2.1, during higher OL, presence of acetoclastic methanogens were negligible. Simulation results were obtained by use of non-competitive inhibition function which would not completely inhibits the methanogenesis process i.e $I \neq 0$ that could be avoided by using empirical inhibition function as suggested by Bergland et al. [36].

Nevertheless, inhibition constant is very important parameter while simulating the APL. It is important to determine the inhibition constant for phenolic mixture (combination of phenolic compounds present in APL sample).

5.8 Degradation of inhibitory compounds

Simulation of APL1.2 and APL2.4 with incomplete degradation showed impact on methane production rate. As, the inhibitory compounds remained in the reactors for long time, inhibition on methanogens were also observed for longer duration. Previous studies have shown that phenol, furfural and HMF are known to degrade either partially or completely [38], [41]. However, for our studies exact concentration of these compounds were unknown.

Simulation performed with partial degradation of inhibitory compounds showed better agreement for APL2.4 (Sim-9c). Even though, inhibition constant used in Sim-9 c was not feasible, it can be justified that there are a lot of unknown compounds in APL that have potential to inhibit the methanogenesis. Compounds such as chlorinated alkenes and alkanes, nitros and nitriles are known to severely inhibit the methanogenesis even at lower concentration [39]. As discussed in chapter 5.2.1, higher loading of APL could inhibit the methanogenesis process. Thus, there is possibility that inhibition seen in Sim-8c could also be observed if further inhibitory compounds such as ketones, polyaromatic hydrocarbons, esters and so on which are present in APL and known to inhibit the methanogenesis are added.

However, as mentioned in chapter 2.10, furfural is preferred over HMF for degradation. Both are carried out by same species of bacteria. But this thesis doesnot explore the option of degradation of furfural over HMF using same species of microorganism and considers the two separate species for breakdown, due to complexity. Though, it is recommended to test or explore various ways to give preference to the furfural over HMF using same species of bacteria.

5.9 Difference of using Monod and Haldane type growth kinetics

Furfural and HMF were found to inhibit the growth of microorganism degrading these compounds. However, simulation performed using Monod and Haldane equation showed similar trend in methane production rate indicating use of Haldane equation does not impact a lot on the simulation results. The concentration of inhibitory compounds subjected during test and simulation were small and thus, no impact of use of Haldane equation was observed. But, simulation with higher concentration of these compounds and use of Haldane equation could show better results than use of Monod type equation as Haldane growth kinetics consider inhibition due to substrate itself.

6 Conclusion

Co-digestion of APL and HS, and digestion of APL was tested in batch at 35°C using AMPTS II and syringe test. The methane yield of digestion of HS was 160 and 156 NmL/gCOD by using stored and fresh inoculum. It was clear that co-digestion of APL with HS increases the methane yield and was not affected by the storage of inoculum for 2 months. Addition of APL in range of (5-20% of COD) during digestion with HS increased the methane yield in range of 8-23% indicating APL can be used as co-substrate in anaerobic digestion.

However, storage time of inoculum was found important during digestion of APL. Longer storage time resulted in less methane yield for all the organic load indicating fresh and diverse inoculum should be used. Digestion of APL was also found to be sensitive towards the OL. Higher OL greater than 2 gCOD/L resulted in inhibition of the AD process as it produced methane lower than the inoculum itself and was same for both fresh and stored inoculum. But, digestion of APL with lower OL showed good results using fresh inoculum. The methane yield was 343 NmL/gCOD for one of parallel from AMPTS II and 230 NmL/gCOD from syringe test. There was huge difference found in yield of the APL1.2, thus, it is hard to conclude methane yield for it.

Simulation performed using standard ADM1 model was not able to predict methane production rate accurately. In comparison, extended ADM1 model showed good agreement with the experimental data and showed higher flexibility towards predicting the methane production at different organic load. Simulation of APL1.2 (organic load of 1.2 gCOD/L) showed relatively low sensitivity towards concentration of inhibitors and startup concentration of biomass indicating simulation of APL with lower organic load would be predicted by extended ADM1 model.

Inhibition constant was found to be the most sensitive parameter for both simulation. With change in inhibition constant, methane production rate also changed. Concentration of inhibitors, startup concentration, and inhibition constant showed effect on the methane production rate. Use of low inhibition constant and low startup concentration of biomass during simulation of APL2.4 resulted in good fit with experimental results indicating that with addition of further compounds present in APL, extended model could predict the trend of methane production rate.

Monod type and Haldane type growth kinetics showed same methane production rate representing simulation of APL at loading rate 1.2 and 2.4 gCOD/L is not affected.

7 Suggestion for future works

Integration of pyrolysis and anaerobic digestion is new and emerging research topic. There are possibilities that could be explored which could help in further understanding of the topic. The following suggestion for future work is suggested:

1. Co-digestion of APL and HS at higher concentration of APL to determine the optimum COD ratio of HS and APL should be tested. The mechanism behind the improvement of methane yield during co-digestion with APL could be further analysed.
2. It is recommended to carry out batch test of APL subjected to overliming.
3. Further modification for simulating the APL could be done by testing different inhibition function, that may results in complete inhibition of acetoclastic methanogens at certain concentration, and addition of SAOB.
4. As APL contains hundreds of compounds, it is suggested to extend the model by implementing group of compounds like Alcohols (methanol, ethanol, ethylene), ketones (acetone), esters, sugars (glucose, fructose) which are present in APL. For example, sugars could be implemented in extended model. Sugars like glucose, fructose, D- mannose are found in APL which could be implemented as explained by Vibeke et. al.
5. It is recommended to carry out experiments (batch test) to determine the kinetics and inhibition constant for groups of inhibitory compounds as explained by Olguin-Lora et. al. [38]. For example, constituent of phenolic compounds present in APL could be replicated into synthetic phenolic mixture and can be tested at different concentration to determine the inhibition constant.

References

- [1] “Key World Energy Statistics 2020,” p. 81.
- [2] S. Pang, “Advances in thermochemical conversion of woody biomass to energy, fuels and chemicals,” *Biotechnol. Adv.*, vol. 37, no. 4, pp. 589–597, Jul. 2019, doi: 10.1016/j.biotechadv.2018.11.004.
- [3] Q. Feng and Y. Lin, “Integrated processes of anaerobic digestion and pyrolysis for higher bioenergy recovery from lignocellulosic biomass: A brief review,” *Renew. Sustain. Energy Rev.*, vol. 77, pp. 1272–1287, Sep. 2017, doi: 10.1016/j.rser.2017.03.022.
- [4] F. R. Amin *et al.*, “Pretreatment methods of lignocellulosic biomass for anaerobic digestion,” *AMB Express*, vol. 7, no. 1, p. 72, Dec. 2017, doi: 10.1186/s13568-017-0375-4.
- [5] L. Zhang, C. (Charles) Xu, and P. Champagne, “Overview of recent advances in thermo-chemical conversion of biomass,” *Energy Convers. Manag.*, vol. 51, no. 5, pp. 969–982, May 2010, doi: 10.1016/j.enconman.2009.11.038.
- [6] D. Kim, “Physico-Chemical Conversion of Lignocellulose: Inhibitor Effects and Detoxification Strategies: A Mini Review,” *Molecules*, vol. 23, no. 2, p. 309, Feb. 2018, doi: 10.3390/molecules23020309.
- [7] D. Fabbri and C. Torri, “Linking pyrolysis and anaerobic digestion (Py-AD) for the conversion of lignocellulosic biomass,” *Curr. Opin. Biotechnol.*, vol. 38, pp. 167–173, Apr. 2016, doi: 10.1016/j.copbio.2016.02.004.
- [8] N. Ghimire, R. Bakke, and W. H. Bergland, “Liquefaction of lignocellulosic biomass for methane production: A review,” *Bioresour. Technol.*, vol. 332, p. 125068, Jul. 2021, doi: 10.1016/j.biortech.2021.125068.
- [9] S. Seyedi, K. Venkiteshwaran, and D. Zitomer, “Toxicity of Various Pyrolysis Liquids From Biosolids on Methane Production Yield,” *Front. Energy Res.*, vol. 7, p. 5, Feb. 2019, doi: 10.3389/fenrg.2019.00005.
- [10] X. Yu, C. Zhang, L. Qiu, Y. Yao, G. Sun, and X. Guo, “Anaerobic digestion of swine manure using aqueous pyrolysis liquid as an additive,” *Renew. Energy*, vol. 147, pp. 2484–2493, Mar. 2020, doi: 10.1016/j.renene.2019.10.096.
- [11] D. J. Batstone *et al.*, “The IWA Anaerobic Digestion Model No 1 (ADM1),” *Water Sci. Technol.*, vol. 45, no. 10, pp. 65–73, May 2002, doi: 10.2166/wst.2002.0292.
- [12] V. Dhyani and T. Bhaskar, “A comprehensive review on the pyrolysis of lignocellulosic biomass,” *Renew. Energy*, vol. 129, pp. 695–716, Dec. 2018, doi: 10.1016/j.renene.2017.04.035.
- [13] F. Xu and Y. Li, “Biomass Digestion,” in *Encyclopedia of Sustainable Technologies*, Elsevier, 2017, pp. 197–204. doi: 10.1016/B978-0-12-409548-9.10108-3.
- [14] Z. E. Zadeh, A. Abdulkhani, O. Aboelazayem, and B. Saha, “Recent Insights into Lignocellulosic Biomass Pyrolysis: A Critical Review on Pretreatment, Characterization, and Products Upgrading,” *Processes*, vol. 8, no. 7, 2020, doi: 10.3390/pr8070799.

- [15] M. Pecchi and M. Baratieri, "Coupling anaerobic digestion with gasification, pyrolysis or hydrothermal carbonization: A review," *Renew. Sustain. Energy Rev.*, vol. 105, pp. 462–475, May 2019, doi: 10.1016/j.rser.2019.02.003.
- [16] C. Torri and D. Fabbri, "Biochar enables anaerobic digestion of aqueous phase from intermediate pyrolysis of biomass," *Bioresour. Technol.*, vol. 172, pp. 335–341, Nov. 2014, doi: 10.1016/j.biortech.2014.09.021.
- [17] S. Rasi *et al.*, "Cascade processing of softwood bark with hot water extraction, pyrolysis and anaerobic digestion," *Bioresour. Technol.*, vol. 292, p. 121893, Nov. 2019, doi: 10.1016/j.biortech.2019.121893.
- [18] I. Fonts, G. Gea, M. Azuara, J. Ábrego, and J. Arauzo, "Sewage sludge pyrolysis for liquid production: A review," *Renew. Sustain. Energy Rev.*, vol. 16, no. 5, pp. 2781–2805, Jun. 2012, doi: 10.1016/j.rser.2012.02.070.
- [19] P. J. McNamara, J. D. Koch, Z. Liu, and D. H. Zitomer, "Pyrolysis of Dried Wastewater Biosolids Can Be Energy Positive," *Water Environ. Res.*, vol. 88, no. 9, pp. 804–810, Sep. 2016, doi: 10.2175/106143016X14609975747441.
- [20] I. Fonts, E. Kuoppala, and A. Oasmaa, "Physicochemical Properties of Product Liquid from Pyrolysis of Sewage Sludge," *Energy Fuels*, vol. 23, no. 8, pp. 4121–4128, Aug. 2009, doi: 10.1021/ef900300n.
- [21] T. Hübner and J. Mumme, "Integration of pyrolysis and anaerobic digestion – Use of aqueous liquor from digestate pyrolysis for biogas production," *Bioresour. Technol.*, vol. 183, pp. 86–92, 2015, doi: <https://doi.org/10.1016/j.biortech.2015.02.037>.
- [22] S. Wang and Z. Luo, *Pyrolysis of biomass*. [Berlin] : Beijing: De Gruyter ; Science Press, 2017.
- [23] A. Demirbas, "The influence of temperature on the yields of compounds existing in bio-oils obtained from biomass samples via pyrolysis," *Fuel Process. Technol.*, vol. 88, no. 6, pp. 591–597, Jun. 2007, doi: 10.1016/j.fuproc.2007.01.010.
- [24] D. Chen, X. Chen, J. Sun, Z. Zheng, and K. Fu, "Pyrolysis polygeneration of pine nut shell: Quality of pyrolysis products and study on the preparation of activated carbon from biochar," *Bioresour. Technol.*, vol. 216, pp. 629–636, Sep. 2016, doi: 10.1016/j.biortech.2016.05.107.
- [25] G. W. Huber, S. Iborra, and A. Corma, "Synthesis of Transportation Fuels from Biomass: Chemistry, Catalysts, and Engineering," *Chem. Rev.*, vol. 106, no. 9, pp. 4044–4098, Sep. 2006, doi: 10.1021/cr068360d.
- [26] C. Wen, C. M. Moreira, L. Rehmann, and F. Berruti, "Feasibility of anaerobic digestion as a treatment for the aqueous pyrolysis condensate (APC) of birch bark," *Bioresour. Technol.*, vol. 307, p. 123199, Jul. 2020, doi: 10.1016/j.biortech.2020.123199.
- [27] H. Zhou, R. C. Brown, and Z. Wen, "Anaerobic digestion of aqueous phase from pyrolysis of biomass: Reducing toxicity and improving microbial tolerance," *Bioresour. Technol.*, vol. 292, p. 121976, Nov. 2019, doi: 10.1016/j.biortech.2019.121976.
- [28] S. Seyedi, K. Venkiteshwaran, and D. Zitomer, "Current status of biomethane production using aqueous liquid from pyrolysis and hydrothermal liquefaction of sewage sludge and similar biomass," *Rev. Environ. Sci. Biotechnol.*, vol. 20, no. 1, pp. 237–255, Mar. 2021, doi: 10.1007/s11157-020-09560-y.

- [29] G. Tchobanoglous, F. L. Burton, and H. D. Stensel, *Wastewater engineering: treatment and reuse, 5th edn. Metcalf and Eddy*. McGraw-Hill series in civil and environmental engineering. McGraw-Hill, New York, 2014.
- [30] J. Filer, H. H. Ding, and S. Chang, “Biochemical Methane Potential (BMP) Assay Method for Anaerobic Digestion Research,” *Water*, vol. 11, no. 5, 2019, doi: 10.3390/w11050921.
- [31] L. H. Hagen, V. Vivekanand, P. B. Pope, V. G. H. Eijsink, and S. J. Horn, “The effect of storage conditions on microbial community composition and biomethane potential in a biogas starter culture,” *Appl. Microbiol. Biotechnol.*, vol. 99, no. 13, pp. 5749–5761, Jul. 2015, doi: 10.1007/s00253-015-6623-0.
- [32] S. Astals, K. Koch, S. Weinrich, S. D. Hafner, S. Tait, and M. Peces, “Impact of Storage Conditions on the Methanogenic Activity of Anaerobic Digestion Inocula,” *Water*, vol. 12, no. 5, p. 1321, May 2020, doi: 10.3390/w12051321.
- [33] K. Koch, S. D. Hefner, S. Weinrich, S. Astals, and C. Holliger, “Power and limitations of biochemical methane potential (BMP) tests,” *Front. Energy Res.*, vol. 8, no. ARTICLE, p. 63, 2020.
- [34] M. Gerber and R. Span, “An analysis of available mathematical models for anaerobic digestion of organic substances for production of biogas,” *Proc. Int. Gas Union Res. Conf.*, vol. 2, pp. 1–30, 2008.
- [35] R. Rajagopal, D. Massé, and G. Singh, “A Critical Review on Inhibition of Anaerobic Digestion Process by Excess Ammonia,” *Bioresour. Technol.*, vol. 143, Jun. 2013, doi: 10.1016/j.biortech.2013.06.030.
- [36] W. Bergland, D. Botheju, C. Dinamarca, and R. Bakke, “Considering Culture Adaptations to High Ammonia Concentration in ADM,” p. 8.
- [37] D. C. Swinney, “Molecular Mechanism of Action (MMoA) in Drug Discovery,” in *Annual Reports in Medicinal Chemistry*, vol. 46, Elsevier, 2011, pp. 301–317. doi: 10.1016/B978-0-12-386009-5.00009-6.
- [38] P. Olguin-Lora, L. Puig-Grajales, and E. Razo-Flores, “Inhibition of the acetoclastic methanogenic activity by phenol and alkyl phenols,” *Environ. Technol.*, vol. 24, no. 8, pp. 999–1006, Aug. 2003, doi: 10.1080/09593330309385638.
- [39] D. J. Blum and R. E. Speece, “A database of chemical toxicity to environmental bacteria and its use in interspecies comparisons and correlations,” vol. 63, no. 3, pp. 198–207, 1991.
- [40] D. S. M. Ghasimi, K. Aboudi, M. de Kreuk, M. H. Zandvoort, and J. B. van Lier, “Impact of lignocellulosic-waste intermediates on hydrolysis and methanogenesis under thermophilic and mesophilic conditions,” *Chem. Eng. J.*, vol. 295, pp. 181–191, Jul. 2016, doi: 10.1016/j.cej.2016.03.045.
- [41] S. Pekařová, M. Dvořáčková, P. Stloukal, M. Ingr, J. Šerá, and M. Koutny, “Quantitation of the Inhibition Effect of Model Compounds Representing Plant Biomass Degradation Products on Methane Production,” *BioResources*, vol. 12, no. 2, pp. 2421–2432, Feb. 2017, doi: 10.15376/biores.12.2.2421-2432.
- [42] M. Badshah, *Evaluation of process parameters and treatments of different raw materials for biogas production*. Lund University, 2012.

- [43] F. Monlau *et al.*, “Do furanic and phenolic compounds of lignocellulosic and algae biomass hydrolyzate inhibit anaerobic mixed cultures? A comprehensive review,” *Biotechnol. Adv.*, vol. 32, no. 5, pp. 934–951, Sep. 2014, doi: 10.1016/j.biotechadv.2014.04.007.
- [44] C. I. Nair, K. Jayachandran, and S. Shashidhar, “Biodegradation of phenol,” *Afr. J. Biotechnol.*, vol. 7, no. 25, 2008.
- [45] Z. Echresh Zadeh, A. Abdulkhani, and B. Saha, “A comparative production and characterisation of fast pyrolysis bio-oil from Populus and Spruce woods,” *Energy*, vol. 214, p. 118930, Jan. 2021, doi: 10.1016/j.energy.2020.118930.
- [46] V. K. Mishra and N. Kumar, “Microbial degradation of phenol: a review,” *J Water Pollut Purif Res*, vol. 4, no. 1, pp. 17–22, 2017.
- [47] B. Fezzani and R. Ben Cheikh, “Extension of the anaerobic digestion model No. 1 (ADM1) to include phenol compounds biodegradation processes for simulating the anaerobic co-digestion of olive mill wastes at mesophilic temperature,” *J. Hazard. Mater.*, vol. 172, no. 2–3, pp. 1430–1438, Dec. 2009, doi: 10.1016/j.jhazmat.2009.08.017.
- [48] Y. Zhang, B. Han, and T. C. Ezeji, “Biotransformation of furfural and 5-hydroxymethyl furfural (HMF) by *Clostridium acetobutylicum* ATCC 824 during butanol fermentation,” *New Biotechnol.*, vol. 29, no. 3, pp. 345–351, Feb. 2012, doi: 10.1016/j.nbt.2011.09.001.
- [49] G. Brune, S. M. Schoberth, and H. Sahn, “Growth of a Strictly Anaerobic Bacterium on Furfural (2-Furaldehyde),” *Appl. Environ. Microbiol.*, vol. 46, no. 5, pp. 1187–1192, 1983, doi: 10.1128/AEM.46.5.1187-1192.1983.
- [50] N. Wierckx, F. Koopman, H. J. Ruijssenaars, and J. H. de Winde, “Microbial degradation of furanic compounds: biochemistry, genetics, and impact,” *Appl. Microbiol. Biotechnol.*, vol. 92, no. 6, pp. 1095–1105, Dec. 2011, doi: 10.1007/s00253-011-3632-5.
- [51] C. j. Rivard and karel Grohmann, “Degradation of furfural (2- furaldehyde) to methane and carbon dioxide by an anaerobic consortium,” *Appl. Biochem. Biotechnol.*, vol. 28–29, no. 1, pp. 285–295, Mar. 1991, doi: 10.1007/BF02922608.
- [52] M. T. Guarnieri, M. Ann Franden, C. W. Johnson, and G. T. Beckham, “Conversion and assimilation of furfural and 5-(hydroxymethyl)furfural by *Pseudomonas putida* KT2440,” *Metab. Eng. Commun.*, vol. 4, pp. 22–28, Jun. 2017, doi: 10.1016/j.meteno.2017.02.001.
- [53] A. Apha, “WEF (2005) Standard methods for the examination of water and wastewater,” *Am. Public Health Assoc. Am. Water Works Assoc. Water Environ. Fed.*, 2007.
- [54] “LabTek - Analyser og priser,” May 15, 2020. <https://www.nmbu.no/tjenester/laboratorietjenester/labtek/booking> (accessed May 12, 2021).
- [55] “Automatic Methane Potential Test System from BPC Instruments,” Apr. 06, 2020. https://bioprocesscontrol.com/bpc_products/automatic-methane-potential-test-system/ (accessed Apr. 20, 2021).

- [56] N. Ghimire, R. Bakke, and W. H. Bergland, "Thermophilic Methane Production from Hydrothermally Pretreated Norway Spruce (*Picea abies*)," *Appl. Sci.*, vol. 10, no. 14, p. 4989, Jul. 2020, doi: 10.3390/app10144989.
- [57] M. S. Elshahed, V. K. Bhupathiraju, N. Q. Wofford, M. A. Nanny, and M. J. McInerney, "Metabolism of Benzoate, Cyclohex-1-ene Carboxylate, and Cyclohexane Carboxylate by 'Syntrophus aciditrophicus' Strain SB in Syntrophic Association with H₂-Using Microorganisms," *Appl. Environ. Microbiol.*, vol. 67, no. 4, pp. 1728–1738, Apr. 2001, doi: 10.1128/AEM.67.4.1728-1738.2001.
- [58] "Ionization Constants of Organic Acids." <https://www2.chemistry.msu.edu/faculty/reusch/VirtTxtJml/acidity2.htm> (accessed Apr. 21, 2021).
- [59] I. Sharma and G. A. Kaminski, "Calculating pK_a values for substituted phenols and hydration energies for other compounds with the first-order Fuzzy-Border continuum solvation model," *J. Comput. Chem.*, vol. 33, no. 30, pp. 2388–2399, Nov. 2012, doi: 10.1002/jcc.23074.
- [60] B. Liu, V. A. Ngo, M. Terashima, and H. Yasui, "Anaerobic treatment of hydrothermally solubilised sugarcane bagasse and its kinetic modelling," *Bioresour. Technol.*, vol. 234, pp. 253–263, Jun. 2017, doi: 10.1016/j.biortech.2017.03.024.
- [61] K. Østgaard *et al.*, "Syringe test screening of microbial gas production activity: Cases denitrification and biogas formation," *J. Microbiol. Methods*, vol. 132, pp. 119–124, Jan. 2017, doi: 10.1016/j.mimet.2016.11.021.
- [62] "1948209.pdf." Accessed: May 04, 2021. [Online]. Available: <https://www.oecd.org/chemicalsafety/risk-assessment/1948209.pdf>

Appendices

Appendices A Master's Thesis Description

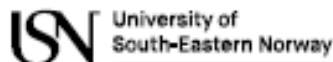
Appendix B Biochemical rate coefficient and kinetic rate equation used in extended ADM1

Appendix C Detail of Input used in Aquasim for simulating cases

Appendix D Relevant Calculations

Appendices E Experimental Results

Appendices A Master's Thesis Description



Faculty of Technology, Natural Sciences and Maritime Sciences, Campus Porsgrunn

FMH606 Master's Thesis

Title: Analysing Aqueous Pyrolysis Liquid as feed for Anaerobic digestion

USN supervisor: Wenche Hennie Bergland and Nirmal Ghimire

External partner: Gudny Øyre Flatabø at Scanship AS

Task background:

Energy and material production from lignocellulosic (wood) waste material receives increased interest as a carbon neutral economic feasible option.

The master study will be carried out to gain more knowledge related to ongoing research projects in cooperation with industry. The projects aim to integrate pyrolysis product, Aqueous Pyrolysis Liquid (APL) with anaerobic digestion (AD) to produce biogas which contributes towards resource recovery and reduce environmental pollution.

Anaerobic digestion is a method where microorganisms mineralize organic matter, generating biogas. The biogas is an energy source due to its high content of methane. Understanding the mechanisms controlling the stoichiometry and kinetics in anaerobic digestion is important to improve the usage of heat-treated products of lignocellulosic components as lignin, hemicellulose and cellulose for transport fuel production (methane from upgraded biogas).

Task description:

Evaluate anaerobic digestion (AD) of pyrolysis products APL. Tasks are:

- Evaluate content, inhibition and adaptation of APL in anaerobic digestion.
- Implement APL in ADM1.
- Anaerobic digestion batch test of the APL to evaluate the biogas potential and kinetics

The study involves:

- Literature review
- Analysing APL
- Experimental work
- Modelling and simulation

Student: Dheeraj Raya

The task is suitable for online students (not present at the campus): Yes

Practical arrangements:

-


Supervision:

As a general rule, the student is entitled to 15-20 hours of supervision. This includes necessary time for the supervisor to prepare for supervision meetings (reading material to be discussed, etc).

Signatures:

Supervisor (date and signature): 31.01.21 *Wanda Bergland*

Student (write clearly in all capitalized letters): DHEERAJ RAYA

Student (date and signature): 29th January, 2021 

Appendices

Appendix B Biochemical rate coefficient and kinetic rate equation used in extended ADM1

1 Biochemical rate coefficient and kinetic rate equation for uptake of phenol, furfural and HMF

Component --> i	1	2	3	4	5	6	6a	6a-1	6b	6c	7	8	9	10	11	12	Rate (μ , kgCOD/m ³ d)
j	S _{su}	S _{aa}	S _{fa}	S _{va}	S _{bu}	S _{pro}	S _{phe}	S _{bnz}	S _{fu}	S _{HMF}	S _{ac}	S _{h2}	S _{ch4}	S _{IC}	S _{IN}	S _I	
Disintegration																	$k_{dis} \cdot X_c$
Hydrolysis Carbohydrate	1																$k_{hyd_ch} \cdot X_{ch}$
Hydrolysis of Proteins		1															$k_{hyd_pr} \cdot X_{pr}$
Hydrolysis of Lipids	1-f _{fa_li}		f _{fa_li}														$k_{hyd_li} \cdot X_{li}$
1 Uptake of Sugar	-1				(1-Y _{su}) f _{bu_su}	(1-Y _{su}) f _{pro_su}					(1-Y _{su}) f _{ac_su}	(1-Y _{su}) f _{h2_su}		sum(C _i ^{vi} ,1) is=1-9,11-24	-(Y _{su}) N _{bac}		$km_{su} \cdot (S_{su}/(K_s+S_{su})) \cdot X_{su} \cdot I_1$
2 Uptake of Amino Acids		-1		(1-Y _{aa}) f _{va_aa}	(1-Y _{aa}) f _{bu_aa}	(1-Y _{aa}) f _{pro_aa}					(1-Y _{aa}) f _{ac_aa}	(1-Y _{aa}) f _{h2_aa}		sum(C _i ^{vi} ,2) is=1-3,11-24	N _{aa} (Y _{aa}) N _{bac}		$km_{aa} \cdot (S_{aa}/(K_s+S_{aa})) \cdot X_{aa} \cdot I_1$
3 Uptake of LCFA			-1								(1-Y _{fa}) 0.7	(1-Y _{fa}) 0.3			-(Y _{fa}) N _{bac}		$km_{fa} \cdot (S_{fa}/(K_s+S_{fa})) \cdot X_{fa} \cdot I_2$
4 Uptake of Valerate				-1		(1-Y _{c4}) 0.54					(1-Y _{c4}) 0.31	(1-Y _{c4}) 0.15			-(Y _{c4}) N _{bac}		$km_{c4} \cdot (S_{va}/(K_s+S_{va})) \cdot X_{c4} \cdot (I_1/(1+(S_{bu}/S_{va}))) \cdot I_2$
5 Uptake of Butyrate					-1						(1-Y _{c4}) 0.8	(1-Y _{c4}) 0.2			-(Y _{c4}) N _{bac}		$km_{c4} \cdot (S_{bu}/(K_s+S_{bu})) \cdot X_{c4} \cdot (I_1/(1+(S_{va}/S_{bu}))) \cdot I_2$
6 Uptake of Propionate						-1					(1-Y _{pro}) 0.57	(1-Y _{pro}) 0.43			-(Y _{pro}) N _{bac}		$km_{pro} \cdot (S_{pro}/(K_s+S_{pro})) \cdot X_{pro} \cdot I_2$
6a Uptake of Phenol							f _{bnz_phe} e ⁻¹ (1-Y _{Phe})					f _{h2_phe} (1-Y _{phe})		-sum(C _i ^{vi} ,6a) is=1-3,11-24	-(Y _{phe}) N _{bac}		$km_{phe} \cdot (S_{phe}/(K_s+S_{phe})) \cdot X_{phe} \cdot I_1$
6a-1 Uptake of Benzoate								-1			f _{ac_bnz} (1-Y _{bnz})	f _{h2_bnz} (1-Y _{bnz})		sum(C _i ^{vi} ,6a-1) is=1-3,11-24	-(Y _{bnz}) N _{bac}		$km_{bnz} \cdot (S_{bnz}/(K_s+S_{bnz})) \cdot X_{bnz} \cdot I_1 \cdot I_2$
6b Uptake of Furfural									-1		f _{ac_fu} (1-Y _{fu})	f _{h2_fu} (1-Y _{fu})		sum(C _i ^{vi} ,6b) is=1-3,11-24	-(Y _{fu}) N _{bac}		$km_{fu} \cdot (S_{fu}/(K_s+S_{fu})) \cdot X_{fu} \cdot I_1$
6c Uptake of HMF							F ¹ (1-Y _{HMF})				F ¹ (1-Y _{HMF})			sum(C _i ^{vi} ,6c) is=1-3,11-24	(Y _{HMF}) N _{bac}		$km_{HMF} \cdot (S_{HMF}/(K_s+S_{HMF})) \cdot X_{HMF} \cdot I_1$
7 Uptake of Acetate											-1		(1-Y _{ac})	-sum(C _i ^{vi} ,7) is=1-9,11-24	-(Y _{ac}) N _{bac}		$km_{ac} \cdot (S_{ac}/(K_s+S_{ac})) \cdot X_{ac} \cdot I_4$
8 Uptake of Hydrogen												-1	(1-Y _{h2})	-sum(C _i ^{vi} ,8) is=1-9,11-24	-(Y _{h2}) N _{bac}		$km_{h2} \cdot (S_{h2}/(K_s+S_{h2})) \cdot X_{h2} \cdot I_1$
9 Decay of X _{su}																	$k_{dec_X_{su}} \cdot X_{su}$
10 Decay of X _{aa}																	$k_{dec_X_{aa}} \cdot X_{aa}$
11 Decay of X _{fa}																	$k_{dec_X_{fa}} \cdot X_{fa}$
12 Decay of X _{c4}																	$k_{dec_X_{c4}} \cdot X_{c4}$
13 Decay of X _{pro}																	$k_{dec_X_{pro}} \cdot X_{pro}$
13a Decay of X _{phe}																	$k_{dec_X_{phe}} \cdot X_{phe}$
13a-1 Decay of X _{bnz}																	$k_{dec_X_{bnz}} \cdot X_{bnz}$
13b Decay of X _{fu}																	$k_{dec_X_{fu}} \cdot X_{fu}$
13c Decay of X _{HMF}																	$k_{dec_X_{HMF}} \cdot X_{HMF}$
14 Decay of X _{ac}																	$k_{dec_X_{ac}} \cdot X_{ac}$
15 Decay of X _{h2}																	$k_{dec_X_{h2}} \cdot X_{h2}$
		Monosaccharids (kgCOD/m ³)	Amino Acid (kgCOD/m ³)	LCFA (kgCOD/m ³)	Total valerate (kgCOD/m ³)	Total butyrate (kgCOD/m ³)	Total propionate (kgCOD/m ³)	Total Phenol (kgCOD/m ³)	Total Benzoate (kgCOD/m ³)	Total Furfural (kgCOD/m ³)	Total HMF (kgCOD/m ³)	Total Acetate (kgCOD/m ³)	Hydrogen gas (kgCOD/m ³)	Methane gas (kgCOD/m ³)	Inorganic carbon (kmole C/m ³)	Inorganic nitrogen (kmole C/m ³)	Soluble inerts Inhibition factors(3.7): I ₁ =L _{pH} ¹ ·NH ₄ ·lim; I ₂ =L _{pH} ¹ ·NH ₄ ·lim ¹ ·h ₂ ; I ₃ =L _{pH} ¹ ·NH ₄ ·lim ¹ ·NH ₃ ·x _{ac} ; I ₄ =L _{pH} ¹ ·SAO ¹ ·NH ₄ ·lim ¹ ·NH ₃ ·x _a e ¹ ·phe·ac ¹ ·fu·ac ¹ ·HMF·ac

Appendices

2. Biochemical rate coefficient and kinetic rate equation for decay of phenol, furfural and HMF degraders.

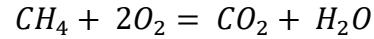
i	Component --> j	13	14	15	16	17	18	19	20	21	22a	22b	22c	22d	22	23	24	Rate (p _j , kgCOD/m ³ d)
	Disintegration	-1	f _{ch,x}	f _{pr,x}	f _{li,x}												f _{xl,x}	k _{dis} *X _c
	Hydrolysis Carbohydrate		-1															k _{hyd_ch} *X _{ch}
	Hydrolysis of Proteins			-1														k _{hyd_pr} *X _{pr}
	Hydrolysis of Lipids				-1													k _{hyd_li} *X _{li}
1	Uptake of Sugar					Y _{su}												km _{su} *(S _{su} /(K _s +S _{su}))*X _{su} *L ₁
2	Uptake of Amino Acids						Y _{aa}											km _{aa} *(S _{aa} /(K _s +S _{aa}))*X _{aa} *L ₁
3	Uptake of LCFA							Y _{fa}										km _{fa} *(S _{fa} /(K _s +S _{fa}))*X _{fa} *L ₂
4	Uptake of Valerate								Y _{c4}									km _{c4} *(S _{val} /(K _s +S _{val}))*X _{c4} (1/(1+(S _{bu} /S _{val}))) ² *L ₂
5	Uptake of Butyrate								Y _{c4}									km _{c4} *(S _{bu} /(K _s +S _{bu}))*X _{c4} (1/(1+(S _{va} /S _{bu}))) ² *L ₂
6	Uptake of Propionate									Y _{pro}								km _{pr} *(S _{pro} /(K _s +S _{pro}))*X _{pro} *L ₂
6a	Uptake of Phenol										Y _{phe}							km _{phe} *(S _{phe} /(K _s +S _{phe}))*X _{phe} *L ₁
6a	Uptake of Benzoate											Y _{bnz}						km _{bnz} *(S _{bnz} /(K _s +S _{bnz}))*X _{bnz} *L ₁ *L _{h2_bnz}
6b	Uptake of Furfural												Y _{fu}					km _{fu} *(S _{fu} /(K _s +S _{fu}))*X _{fu} *L ₁
6c	Uptake of HMF													Y _{HMF}				*L ₁
7	Uptake of Acetate														Y _{ac}			km _{ac} *(S _{ac} /(K _s +S _{ac}))*X _{ac} *L ₄
8	Uptake of Hydrogen															Y _{h2}		km _{h2} *(S _{h2} /(K _s +S _{h2}))*X _{h2} *L ₁
9	Decay of X _{su}	1				-1												k _{dec} *X _{su} *X _{su}
10	Decay of X _{aa}	1					-1											k _{dec} *X _{aa} *X _{aa}
11	Decay of X _{fa}	1						-1										k _{dec} *X _{fa} *X _{fa}
12	Decay of X _{C4}	1							-1									k _{dec} *X _{c4} *X _{c4}
13	Decay of X _{pro}	1								-1								k _{dec} *X _{pro} *X _{pro}
13a	Decay of X _{phe}	1									-1							k _{dec} *X _{phe} *X _{phe}
13a	Decay of X _{bnz}	1										-1						k _{dec} *X _{bnz} *X _{bnz}
13b	Decay of X _{fu}	1											-1					k _{dec} *X _{fu} *X _{fu}
13c	Decay of X _{HMF}	1												-1				k _{dec} *X _{HMF} *X _{HMF}
14	Decay of X _{ac}	1													-1			k _{dec} *X _{ac} *X _{ac}
15	Decay of X _{h2}	1														-1		k _{dec} *X _{h2} *X _{h2}
																		Particulate inerts Inhibition factors(3, 7): L ₁ =L _{pH} *L _{NH₄lim} ; L ₂ =L _{pH} *L _{NH₄lim} *L _{h2} ; L ₃ =L _{pH} *L _{NH₄lim} *L _{NH₃xac} ; L ₄ =L _{pH} *L _{SAO} *L _{NH₄lim} *L _{NH₃xac} *L _{phe_{ac}} *L _{fu_{ac}} *L _{HMF_{ac}}

Appendix C Detail of Input used in Aquasim for simulating cases

input for Aquasim including inoculum								
	Sim-2	Sim-3a	Sim-3b	Sim-3c	Sim-6	Sim-7a	Sim-7b	Sim-7c
X_C	2.730302	2.593621	2.884221	2.375671	3.460604	3.187242	3.768442	2.751342
X_I	4.007377	4.005996	4.008932	4.003795	4.014754	4.011992	4.017863	4.007589
S_ac	0.213007	0.213007	0.213007	0.213007	0.426015	0.426015	0.426015	0.426015
S_pro	0.021256	0.021256	0.021256	0.021256	0.042513	0.042513	0.042513	0.042513
S_phe	0.156879	0.156879	0.031376	0.251007	0.313759	0.313759	0.062752	0.502014
S_fu	0.043889	0.109722	0.021944	0.175556	0.087778	0.219444	0.043889	0.351111
S_HMF	0.028089	0.100317	0.020063	0.160508	0.056178	0.200635	0.040127	0.321016
S_I	3.675	3.675	3.675	3.675	3.675	3.675	3.675	3.675
S_IN	0.025	0.025	0.025	0.025	0.025	0.025	0.025	0.025

Appendix D Relevant Calculations

1. Methane Yield



COD per mole of methane is equivalent to 64gO₂/mole of methane.

At STP,

Pressure = 1 atm

Temperature = 273 K

Volume of methane present in 1 mole of methane is calculated by

$$PV = nRT$$

The volume of methane per mole = 22400 mL

$$\text{Methane Yield} = \frac{\text{Volume of Methane produced by sample (NmL)} - \text{Volume of methane produced by blank (NmL)}}{\text{Total concentration of sample in gCOD}}$$

The average methane production from blank is shown below:

	Volume (NmL)	Average (NmL)
Blank 1	209.00	214.15
Blank 2	219.30	

The calculated methane yield for AMPTS II using fresh inoculum (first run) is given below:

	Methane (NmL)	gCOD	Yield (NmL/gCOD)	Biodegradability (%)
Control 3	788.2	3.6729	156.2933921	44.57
APL 2.4 1	277.8	0.72048	88.34388186	25.24
APL 2.4 2	216.8	0.72048	3.678103487	1.04
Co-digestion 2	739.9	3.082639	170.55192	48.57
Co-digestion 3	786.7	3.082639	185.7337171	53.06

Appendices

APL 1.2 1	423	0.36024	579.7523873	165.42
APL 1.2 3	338	0.36024	343.7985787	98.22

The calculated methane yield for AMPTS II using stored inoculum(first run) is given below:

Reactor	Total Volume	Volume	gCOD	Yield	Biodegradability(%)
Blank-s	43	-	-	-	-
Control-s	119.3	76.5	0.4752	160.9848485	45.99
Co-digestion-s	138	96	0.4812	198.739263	56.78
APL2.4-s	29	-	-	-	-
APL1.2-s	45	3	0.228	11.69590643	3.34

2. Determination of COD from CHNS analysis.

The CHNS analysis results are:

Sample	N	C	S	H	dry weight (a) in (g)	wet weight b in (g)	weight after 105 (c) in (g)	Moisture Content
	%	%	%	%				
I1	4	27.5	0.6	4.5	79.27	119.174	80.0615	98.01648957
I2	4.6	29.3	0.6	4.6	91.382	130.74	91.9848	98.46841811
I3	5	29.9	0.6	4.5	51.5345	91.286	52.1666	98.40987133
average	4.533333	28.9	0.6	4.533333				98.29825967

Moisture Content was calculated by (%) = $\frac{(b-a)-(c-a)}{(b-a)} * 100 \%$

1 g of wet sample contained 0.982982 g of water.

Mass of H₂ in 0.982982 g of water = $\frac{MW_{H_2}}{MW_{H_2O}} * 0.982982 \text{ g} = 0.11000433$

Total carbon, nitrogen and sulfur content was adjusted for 0.017018 g.

Appendices

TS of sample was 16.604 gTS/L, VS was 13gVS/L and Ash of 3.604g/L. Oxygen was back calculated as rest of mass by subtracting sum of C,H,N,S and Ash to total mass(i.e. in this 1g).

Expression for COD was used based on OECD guideline [62].

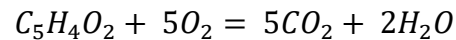
	C	H	N	S	O	Ash
Molar mass (g/mol)	12.011	1.008	14.0067	32.065	15.999	
Mass ratios of (total 0,017018 g) dry inoculum	0.004913	0.000770666	0.000770667	0.000102		
Mass ratio of (total 1g) of wet inoculum	0.0049	0.1108	0.000771	0.00000002	0.8799	0.0036
Number of moles	0.000409042	0.109895829	5.50213E-05	5.40777E-10	0.05499952	
Expression:	$C_{mol} * 2 * O_{Mm} + (H_{mol} - 3 * N_{mol}) / 2 * O_{Mm} + S_{mol} * 3 * O_{mm} - O_{mol} * O_{Mm}$					
Oxygen demand	0.013088517	0.877791257		2.59557E-08	0.87993732	
					0.01094248	10.94247973

C/N Molar ratio = Number of moles of C/ Number of moles of N = 7.43

3. COD calculation of inhibitory compounds

Furfural

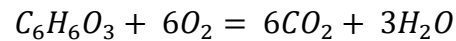
Molecular weight of furfural = 96.08 g /mole



$$\text{COD of furfural} = \frac{5 \times 32}{96.08} = 1.66 \frac{gCOD}{g \text{ furfural}}$$

HMF

Molecular weight of HMF = 126.11 g /mole



$$\text{COD of HMF} = \frac{6 \times 32}{126.11} = 1.52 \frac{gCOD}{g \text{ HMF}}$$

4. Carbon Content

The carbon content for furfural used in the ADM1 was calculated as:

$$C_{furfural} = \frac{\text{Kmole of carbon in furfural}}{\text{Kg COD of furfural}}$$

This gives the carbon content of furfural as

$$C_{furfural} = \frac{5 \text{ Kmole carbon}}{160 \text{ KgCOD}}$$

Similarly, the carbon content for HMF used in the ADM1 was calculated as:

$$C_{HMF} = \frac{\text{Kmole of carbon in HMF}}{\text{Kg COD of HMF}}$$

This gives the carbon content of HMF as

$$C_{furfural} = \frac{6 \text{ Kmole carbon}}{192 \text{ KgCOD}}$$

Appendices E Experimental Results

[Experimental Results from AMPTS II using fresh inoculum](#)

[Experimental Results from AMPTS II using stored inoculum](#)

[Experimental Results from Syringe test](#)